JET PROPULSION

Journal of the
AMERICAN ROCKET SOCIETY

Rocketry . . . . Jet Propulsion Sciences . . . . Astronautics

VOLUME 25 JUNE 1955 NUMBER 6

ARS SUMMER MEETING BOSTON, MASS., JUNE 22–23 SEE PAGE 298

Scope of JET PROPULSION

JET PROPULSION, the Journal of the American Rocket Society, is devoted to the advancement of the field of jet propulsion through the publication of original papers disclosing new knowledge and new developments. The term "jet propulsion" as used herein is understood to embrace all engines that develop thrust by rearward discharge of a jet through a nozzle or duct; and thus it includes systems utilizing atmospheric air and underwater systems, as well as rocket engines. JET PROPULSION is open to contributions, either fundamental or applied, dealing with specialized aspects of jet and rocket propulsion, such as fuels and propellants, combustion, heat transfer, high temperature materials, mechanical design analyses, flight mechanics of jet-propelled vehicles, astronautics, and so forth. JET PROPULSION endeavors, also, to keep its subscribers informed of the affairs of the Society and of outstanding events in the rocket and jet propulsion field.

Limitation of Responsibility

Statements and opinions expressed in JET PROPULSION are to be understood as the individual expressions of the authors and do not necessarily reflect the views of the Editors or the Society.

Subscription Rates

One year (twelve monthly issues)	$10.00
Foreign countries, additional postage add	.50
Single copies	1.75
Special issues, single copies	2.50
Back numbers	2.00

Change of Address

Notices of change of address should be sent to the Secretary of the Society at least 30 days prior to the date of publication.

Information for Authors

Preparation of Manuscripts

Manuscripts must be double spaced on one side of paper only with wide margins to allow for instructions to printer. Submit two copies: original and first carbon. Include a 100–200 word abstract of paper. The title of the paper should be brief to simplify indexing. The author's name should be given without title, degree, or honor. A footnote on the first page should indicate the author's position and affiliation. Include only essential illustrations, tables, and mathematics. References should be grouped at the end of the manuscript; footnotes are reserved for comments on the text. Use American Standard symbols and abbreviations published by the American Standards Association. Greek letters should be identified clearly for the printer. References should be given as follows: For Journal Articles: Title, Authors, Journal, Volume, Year, Page Numbers. For Books: Title, Author, Publisher, City, Edition, Year, Page Numbers. Line drawings must be made with India ink on white paper or tracing cloth. Lettering on drawings should be large enough to permit reduction to standard one-column width, except for unusually complex drawings where such reduction would be prohibitive. Photographs should be clear, glossy prints. Legends must accompany each illustration submitted and should be listed in order on a separate sheet of paper.

Security Clearance

Manuscripts must be accompanied by written assurance as to security clearance in the event the subject matter of the manuscript is considered to lie in a classified area. Alternatively, written assurance that clearance is unnecessary should be submitted. Full responsibility for obtaining authoritative clearance rests with the author.

Submission of Manuscripts

Manuscripts should be submitted in duplicate to the Editor-in-Chief, Martin Summerfield, Professor of Aeronautical Engineering, Princeton University, Princeton, N. J.

Manuscripts Presented at ARS Meetings

A manuscript submitted to the ARS Program Chairman and accepted for presentation at a national meeting will automatically be referred to the Editors for consideration for publication in JET PROPULSION, unless a contrary request is made by the author.

To Order Reprints

Prices for reprints will be sent to the author with the galley proof, and orders should accompany the corrected galley when it is returned to the Assistant Editor.

JET PROPULSION

Journal of the

AMERICAN ROCKET SOCIETY

JET PROPULSION, the Journal of the American Rocket Society, published monthly by the American Rocket Society at 20th and Northampton Streets, Easton, Pa., U.S.A. The Editorial Office is located at 500 5th Ave., New York 36, N. Y. Price $1.75 per copy, $10.00 per year: Entered as second-class matter at the Post Office at Easton, Pa., under the Act of March 3, 1879.

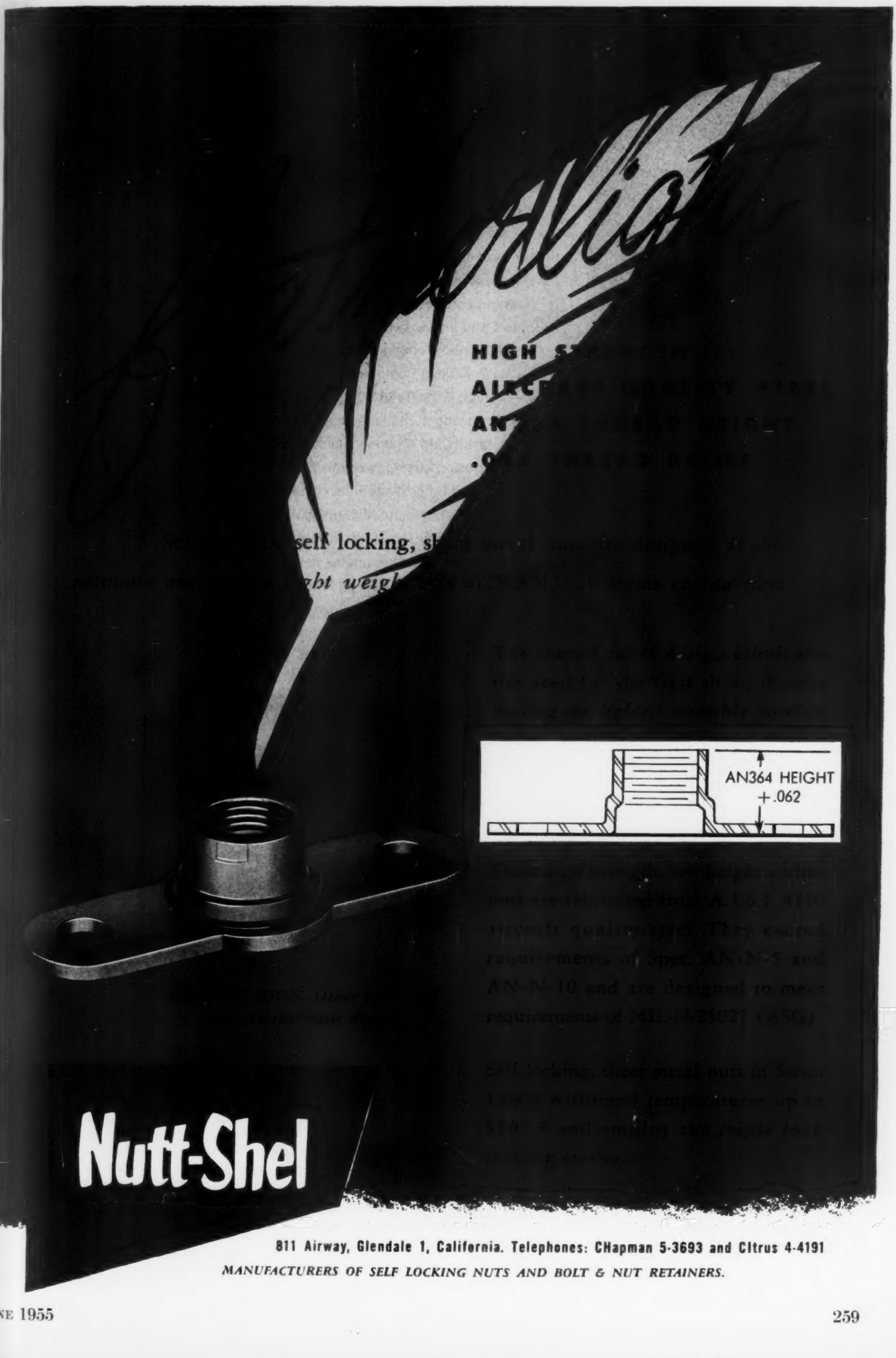
AN364 HEIGHT
+.062
Nutt-Shel
811 Airway, Glendale 1, California. Telephones: CHapman 5-3693 and CItrus 4-4191
MANUFACTURERS OF SELF LOCKING NUTS AND BOLT & NUT RETAINERS.

Admiral has built COMMUNICATIONS for a sky-ful of planes
Standard communications equipment for nearly all military aircraft is the famed AN/ARC-27. This complex all-channel transmitter-receiver can be tuned to 1,750 VHF and UHF channels. Containing 56 tubes and upwards of 3,000 parts, this unit is being produced in vast quantities to keep pace with America's expanding air power. Approximately one out of every three transceivers completed to date has come out of Admiral plants.
This particular assignment provides ample evidence of Admiral's ability to produce in quantity...and to maintain the strictest quality standards. Production capacity has now been further augmented by means of the new automation equipment, designed and built by Admiral's own engineering staff. Address inquiries to:
Admiral®
CORPORATION
Government Laboratories Division
Chicago 47, Illinois
LOOK TO Admiral FOR
RESEARCH • DEVELOPMENT • PRODUCTION
in the fields of:
COMMUNICATIONS, UHF and VHF, air-borne and ground.
MILITARY TELEVISION, receiving and transmitting, air-borne and ground.
RADAR, air-borne, ship and ground.
RADIAC • MISSILE GUIDANCE • TELEMETERING • DISTANCE MEASURING • TEST EQUIPMENT • CODERS and DECODERS
Admiral
Send for Brochure
...complete digest of Admiral's experience, equipment and facilities.
ENGINEERS! The wide scope of work in progress at Admiral creates challenging opportunities in the field of your choice. Write Director of Engineering and Research, Admiral Corporation, Chicago 47, Ill.

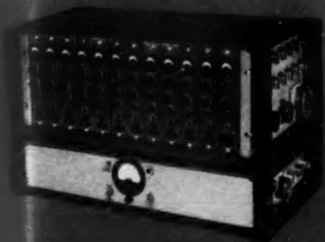

NAL MODULATOR

TOMATIC CALIBRATOR

GE-TIME GENERATOR

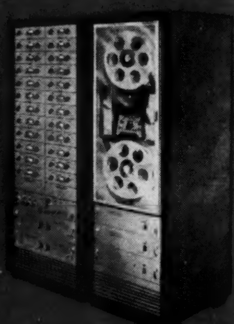

YBACK
IPMENT

SIGNAL MODULATOR

Contains up to 12 plug-in modulators per case for amplifying and "coding" signal input voltages to a form adapted to precision magnetic-tape recording. Each channel accommodates either: (a) direct-recording input unit, (b) combination compound-modulation/frequency-modulation (CM/FM) modulator or (c) pulse-duration modulator (PDM). Separate power supply provides all voltages for 12 modulators plus AM carrier for CM recording.

Power . . . 115 volts, single-phase, 50/60/400 cps; 250 watts.

Size . . . (a) 12-channel modulator case: 7⅝ x 22 x 11¾"; 53 pounds.
(b) power supply: 4⅛ x 22 x 11¾"; 50 pounds.

AUTOMATIC CALIBRATOR

Provides "in-flight" calibration for both bridge-type and self-generating transducers and for thermocouples. Signals supplied to 12 data channels simultaneously; two units used for 24-channel system. Zero check plus two positive and two negative calibration values provided for bridges and thermocouples; zero check and two amplitude levels for vibration pickups. Calibration of 12 channels completed in one second under automatic cycling control. Manual control permits calibration at chosen periods.

Power . . . 115 volts, single-phase, 50/60/400 cps; 75 watts.

Size . . . 4¼ x 22 x 11¾"; 45 pounds.

RANGE-TIME GENERATOR

Provides visual display of tuning-fork-controlled time at the recording equipment and at the remote control station. Also provides binary-coded-decimal time signal for recording on the magnetic tape and for use as a master time signal to control or operate counters, solenoids, etc. Slightly over 27 hours . . . 99,999 seconds . . . can be accumulated and indicated.

Power . . . 115 volts, single-phase, 50/60/400 cps; 100 watts.

Size . . . 4¼ x 22 x 11¾"; 35 pounds.

PLAYBACK EQUIPMENT

Standard rack-mounted playback equipment can be operated in the laboratory or trailer-mounted for field use. One cabinet houses tape-transport assembly and equalizing preamplifiers. (Servo-operated flutter-correction equipment available for compensated playback.) Second cabinet houses demodulation electronics for recovering original signals. Interchangeable demodulators, matched to the modulation technique used in recording, may be inserted into each channel drawer. Resulting signals can drive galvanometers, oscilloscopes, chart recorders . . . or automatic digital-conversion devices, such as the CEC MilliSADIC.

Power . . . 2400 watts for typical 24 data-channel system.

Consolidated's experienced Field Engineers and its Systems Division are ready now to show how DataTape can serve you. Write today to Pasadena or to any CEC local office for Bulletin CEC 1561-X2

Consolidated Engineering
Corporation

ELECTRONIC INSTRUMENTS FOR MEASUREMENT AND CONTROL

300 North Sierra Madre Villa, Pasadena 15, California

Sales and Service Offices Located in: *Albuquerque, Atlanta, Boston, Buffalo, Chicago, Dallas, Detroit, New York, Pasadena, Philadelphia, San Francisco, Seattle, Washington, D. C.*

JUNE 1955

VOLUME 25 NUMBER 6

JET PROPULSION
Journal of the
AMERICAN ROCKET SOCIETY

Editor-in-Chief
MARTIN SUMMERFIELD

The Influence of Turbulence on Flame Propagation Rates[1]

RAY E. BOLZ[2] and HENRY BURLAGE, JR.[3]

Case Institute of Technology, Cleveland, Ohio

A technique for the experimental study of laminar and turbulent flame propagation is presented. The method consists of igniting, by a single spark discharge, a small zone in a free jet of fuel-air mixture. This approximately spherically shaped burning zone, called a flame "globule," was shadowgraphed, using a high-speed motion picture camera, as it passed downstream with the mixture. Measurements taken from the photographs resulted in the flame speed data.

1 The experimental technique appears to have considerable value for the study of the propagation of laminar and turbulent flames. The data are quite consistent and reproducible, and are adaptable to the study of the transient phase of the turbulence effect. 2 The measured laminar flame speeds are in good agreement with those obtained by other investigators. 3 An encouraging quantitative correlation between an empirical equation and the experimental data is shown, but the relation to the scale of the turbulence was satisfactory for only one of the two screens used. The correlation was unsuccessful for very lean and rich mixtures. This was due to the fact that the rate of turbulent flame growth, for these cases, was lower than the laminar values.

Introduction

THE influence of coarse-body turbulence on the rate of propagation of a flame in a flowing gas stream has been the subject of considerable experimental and analytical study. Numerous experiments as well as experience with jet engine and other combustion chambers show that the rate of combustion is increased in the presence of turbulence. Analytical expressions that relate the turbulent flame propagation rate with the characteristic parameters of the turbulence have been formulated and revised but with only partial success from the standpoint of correlation with experimental results. See (1 through 11).[4]

Almost all analytical formulations have been based upon a model which assumes that the coarse-body turbulence wrinkles or roughens the flame front without influencing the local value of the laminar flame speed. The increased flame surface then results in an over-all rate of flame propagation greater than the laminar value. Recently von Kármán (7) stated his belief that the widely accepted theory of a turbulent flame being simply a wrinkled laminar flame cannot be altogether correct, and Summerfield (10), in agreement, states that "a turbulent flame is a zone of distributed reactions, similar to a laminar flame except that the reaction rate laws and transport processes are modified by the presence of turbulence."

Presented at the ARS Ninth National Convention New York, N. Y., December 2, 1954.

[1] Research conducted at Case Institute of Technology under sponsorship of the National Advisory Committee for Aeronautics, Contract no. NAw-6239.

[2] Professor of Aeronautical Engineering.

[3] Assistant Professor of Aeronautical Engineering. Mem. ARS.

[4] Numbers in parentheses indicate References at end of paper.

The work presented in this paper is an attempt to investigate the problem experimentally from a point of view which differs from that of the previous investigators, although it is recognized that concurrent experiments of a similar nature have been in progress by H. L. Olsen and collaborators at the Applied Physics Laboratory, The Johns Hopkins University. The technique consists of observing the growth of an approximately spherically shaped free-flame zone or "globule" isolated within a homogeneous, turbulent, flowing fuel-air mixture. The method eliminates certain of the disadvantages of the Bunsen burner type experiments, as well as of those employing flames stabilized on bluff bodies. These disadvantages include divergence of streamlines of the unburned gas as they approach the flame front, large velocity gradients between burned and unburned gas streams, and, where used, the influence of pilot flames. It has certain of the advantages of the experimental method used by Leason (11) without the severe restriction of very low flow rates and turbulence levels. The method of this paper yields data which differ from the usual in that they represent a time history of the influence of the turbulence on the reaction rate.

Description of the Apparatus

Primary Equipment

The primary apparatus consisted of an air supply, fuel supply, and a turbulence control system. A schematic of the arrangement is shown in Fig. 1. The air compressor was a centrifugal machine, from a type B turbosupercharger, driven by a d-c motor through an appropriate gear box. Air flow

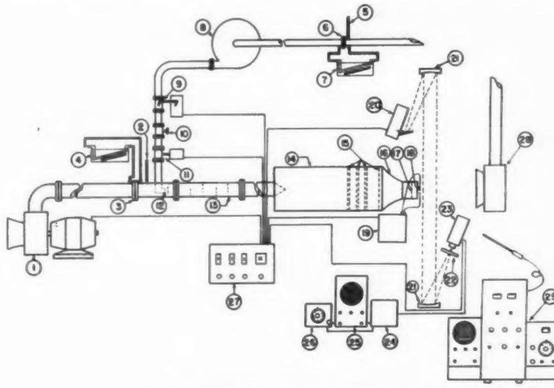

Fig. 1 Schematic of apparatus

1, Centrifugal compressor; 2, air thermometer; 3, air orifice; 4, air micromanometer; 5, gas thermometer; 6, gas orifice; 7, gas micromanometer; 8, booster pump; 9, motor-operated valve; 10, manual valve; 11, solenoid valve; 12, fuel injection assembly; 13, mixer section; 14, settling tank; 15, quieting screens; 16, nozzle; 17, turbulence grid; 18, electrodes; 19, high voltage supply; 20, light source; 21, parabolic mirrors; 22, filter; 23, Fastax camera; 24, amplifier; 25, oscilloscope; 26, oscillator; 27, control panel; 28, exhaust fan; 29 hot-wire anemometer.

was adjusted by varying compressor speeds. The compressor drive motor speed was controlled by a variable voltage generator system, giving excellent speed stability and enabling rather precise speed adjustments to be made. An orifice and micromanometer were used to measure air flow rate.

Natural gas was used as the fuel and after being metered by an appropriate orifice, used in conjunction with a micromanometer, it was admitted into a centrifugal-type gas booster pump. Flow control was achieved by throttling at the outlet of the pump. The fuel flow was stopped and started by a solenoid valve actuated from a master control panel.

The fuel was injected into the air stream at the center line of the air duct and was forced to flow radially, due to a plate placed directly in front of the fuel discharge nozzle. A series of baffles in the duct provided a forced mixing zone.

About 20 diameters downstream of the mixer, the fuel-air mixture passed through a cone-shaped screen into a settling tank. Near the outlet of the tank were seven 200-mesh screens spaced about 3 inches apart. A nozzle with a contraction ratio of about 20 and a diameter of 4 inches followed the last screen. The flow leaving the nozzle was at the minimum attainable turbulence for this apparatus, and the laminar flame data were taken using this stream.

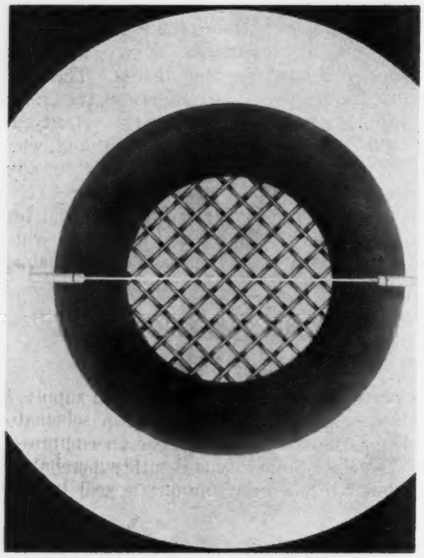

Fig. 2 Turbulence screen and nozzle

To provide turbulence, of variable scale and intensity, in the air stream, two geometrically similar screens of different mesh and wire sizes, and operated at different flow velocities, were in turn placed at the nozzle outlet. A tube was placed between the screen and the igniting electrodes. This established the point of ignition at the desired location, relative to the turbulence decay pattern, in the flow. A sketch of the arrangement is shown in Fig. 2.

Auxiliary Apparatus

Ignition System

The high-energy spark was produced by a capacitor discharge system consisting of a transformer, a high-voltage half-wave rectifier, and a capacitor. Sparking frequency was controlled by varying the electrode spacing.

The electrodes were steel needles 0.035 in. in diam and 2 in. long. Leaving a round shank for chucking, the rest of the needle was ground flat to a thickness of 0.017 in., at the end near the shank, down to 0.005 near the tip. They were chucked in holders which provided micrometric adjustment of the gap spacing as well as radial location of the gap in the stream (Fig. 3). The holders were so designed that electrode rotation was not possible. The electrodes were placed in the stream with the flat sides parallel to the flow in order to reduce the electrode-induced turbulence to a minimum. No whip or oscillation of the tip was observed under any of the operating conditions.

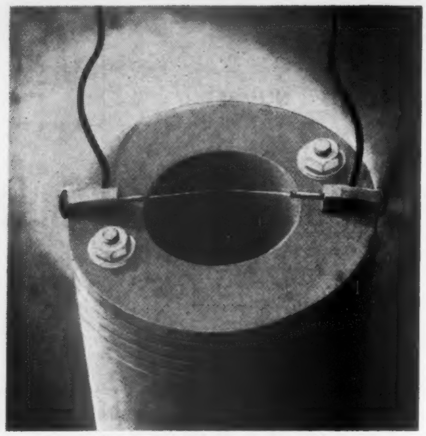

Fig. 3 Electrode assembly

Photographic Recording System

Records of the flame behavior were made by high-speed shadowgraphy. The system consisted of a carbon arc light, arranged to provide a "point" source, two 6-in. spherical mirrors, and a Fastax camera. The light source was placed off axis at the focal point of one mirror such that the resulting parallel light passed through the flame zone. The camera, which was located off axis behind the focal point of the second mirror, was so placed that the 16-mm frame was filled with the desired portion of the image. A reference scale was included in the field of vision for use in determining the magnitude of the images. A light blue filter was placed in the light path, before the camera, to provide improved contrast of the flame image.

Operation of the camera was automatic. An appropriate control circuit provided synchronized operation of the burning and recording, initiated at the operator's will.

Timing System

Since the camera speed was not constant, it was necessary to impose timing marks on the film in order to provide accurate rate measurements. The Fastax camera was originally equipped with an internal neon timing light actuated from an external voltage source of known frequency. This was changed to an argon bulb in order to provide light of better actinic value. A 1000-cycle tuning fork oscillator was used to synchronize the sweep rate of an oscilloscope, and the saw-tooth sweep signal was fed to an appropriate amplifier which provided the voltage for the bulb. Thus the density of the timing mark on the exposed film increased to a maximum and then stopped, making it possible to establish the time intervals quite accurately.

Hot-Wire Anemometer

To establish the spectrum and intensity of the stream turbulence, a constant-current hot-wire anemometer, basically of NACA design (12), was used in conjunction with a General Radio type 736-A wave analyzer and an r.m.s. computer, of the Laurence-Landes type (12). Minor modifications in circuitry and in operating procedure were made to improve convenience and to adapt the instrument to the particular application.

The turbulence measurements were made under operating conditions which were similar to those under which flame

Table 1 Fuel composition analysis of Cleveland natural gas

Date of sample →	3-19-53	4-18-53	5-20-53	10-6-53	12-15-53	2-4-54
Constituent			Percentage by volume			
Methane	90.0	89.7	85.5	85.9	89.5	91.2
Ethane	3.9	4.2	6.2	5.2	4.2	3.8
Ethylene	trace	trace	0.1	0.1	..	..
Propane	1.1	1.0	2.3	1.4	0.7	0.7
Butylene	0.1	0.4	0.1	0.1	trace	trace
Normal butane	..	0.2	0.2	0.4	0.2	0.3
Isobutane	0.2	0.1	0.4	0.2	0.1	0.1
Carbon dioxide	0.6	0.5	0.3	0.5	0.7	0.7
Nitrogen	3.9	3.7	4.8	4.7	3.2	1.5
Oxygen	0.2	0.2	0.1	0.1	0.1	0.1
Carbon monoxide[a]	..	..	..	1.2	0.9	1.4
Miscellaneous[b]	trace	trace	trace	0.2	0.4	0.3

[a] This analysis, in the presence of methane, is subject to some error.
[b] Includes hydrogen, propylene, and isopropane.

data were taken. No attempt was made to take turbulence and flame data simultaneously.

Fuel-Air Mixture Analysis

Fuel-air mixture distribution in the stream, discharged from the nozzle, was surveyed. A total head tube, 0.042-in. ID, mounted on a transversing rig, was placed at the nozzle discharge and mixture samples were drawn into the analysis apparatus through the probe. The analyzer was basically an Orsat type employing absorption materials to determine composition.

Fuel Composition Analysis

Because natural gas, supplied from city gas mains, was used as the fuel, analyses of the gas composition were made periodically during the course of the experiments in order to determine variation in constituents, if any. The fuel analyses were made using a mass spectrometer in conjunction with an IBM computer. Table 1 shows the results of these analyses.

Reduction, Interpretation of Combustion Data

Film Timing

For a typical data run, the spark gap was adjusted to achieve a sparking rate of 7 to 15 per sec, producing 10 to 20 combustion sequences on the 100-ft roll of film. Each sequence consists of 10 to 40 frames, depending upon the fuel-air flow velocity and upon camera speed at that particular section along the film. Since the film speed in the Fastax camera undergoes continuous acceleration during a run (maximum of 5000 frames per sec), only those photographs appearing on the last half of the film roll where the greater film speeds exist were used. The spacing of the 1000-cps timing marks were carefully measured for each combustion sequence to determine the film velocity. The variation of film speed over a 40-frame interval, which the average flame sequence occupied, was negligible and therefore a constant time factor (frames per sec) was measured for each individual sequence.

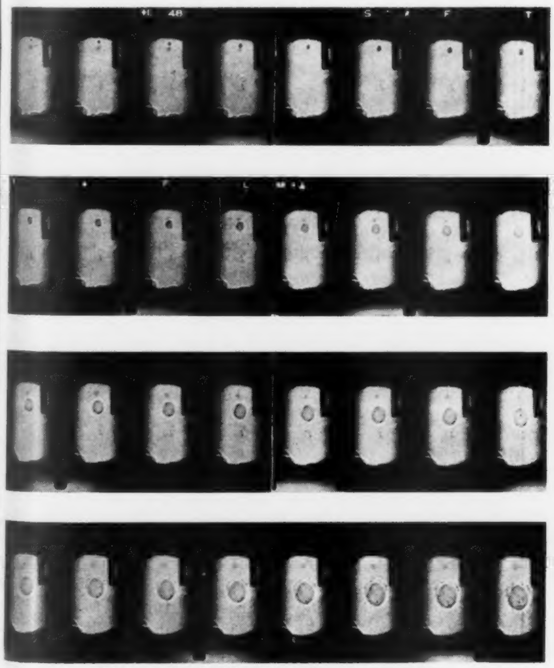

Fig. 4 Typical laminar flame sequence

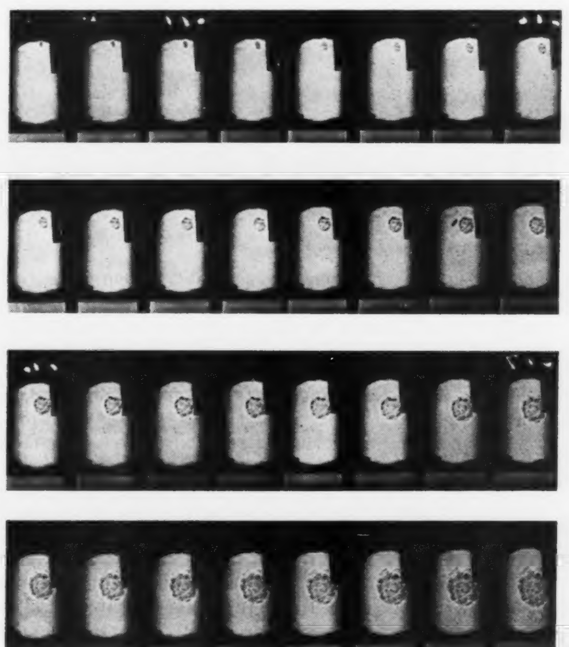

Fig. 5 Typical turbulent flame sequence

Flame Speed

Photographs of two typical combustion sequences, taken at approximately the same mixture flow velocities, one at very low turbulence, hereafter called laminar, and one under fairly high turbulence intensity conditions, are shown in Figs. 4 and 5. The object in the corner of the photographs is a scale marker which was 1 in. in length between the two razor-blade edges. The conversion of the negative film images to numerical data was accomplished as follows:

1 The film sequence was placed in an enlarger and one frame of the sequence was projected on a section of a roll of graph paper. The projection was such that the scale image was full size, thereby bringing the flame images to actual size.

2 A careful tracing of a flame globule (Fig. 6) was made on the roll of graph paper such that a fixed reference line in each frame of the film strip was equally spaced along the

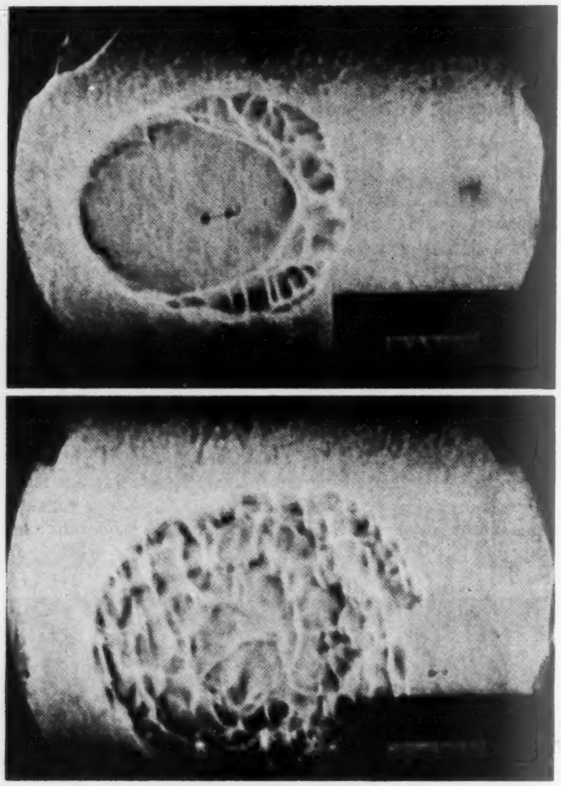

Fig. 6 Top: typical laminar flame globule; bottom: typical turbulent flame globule

paper. The film was then advanced and the procedure repeated for each frame in the sequence. For each case, care was taken to eliminate the distinguishable zone due to electrode turbulence (see Fig. 6). The method was arbitrary in that the evident flame outline, on either side of the electrode turbulence zone, was continued through the zone by an appropriate arc.

3 Each tracing was planimetered and the resulting area was used to determine the radius of an equivalent sphere for that frame.

4 The geometric center of each tracing was determined and the location of this center from the reference line measured.

5 The results of step 3 were tabulated and a fit of the data to a straight line, which gave the best statistical fit, was performed by the method of least squares for the laminar data. The least-squares fitting process resulted in an optimum value for the slope of the fitted line and, from the film speed data, the apparent laminar flame speed (change of flame globule radius per second) was calculated. The least squares calculation also gave the standard error associated with each line and this value served as a basis for confidence in the linear fit to the data.

6 The values determined in step 3 were also plotted against time and, for the laminar cases, a straight line was drawn to fit the plotted points. The slope of this line, which represents apparent laminar flame speed, was measured and provided a check on the least squares results of step 5. For

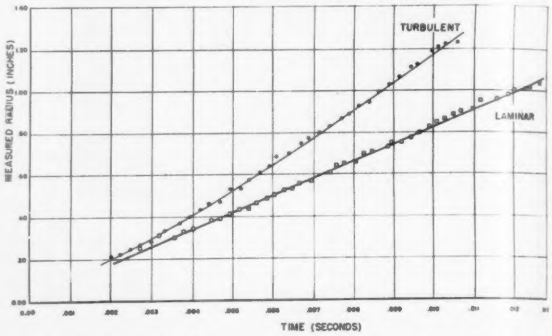

Fig. 7 Typical data of measured radius of flame globule in laminar and turbulent flow

the turbulent case, the linear fitting process was not applicable, since the flame speed is a function of time during the interval in which the data occur. Typical curves of measured globule radius vs. time for the laminar and turbulent cases, shown in Figs. 4 and 5, are given in Fig. 7.

7 The results of step 4 were plotted vs. time, and the slope of the line connecting the points represents the value used for the flow velocity of the fuel-air mixture over that interval of time. Typical results, for the cases shown in Figs. 4 and 5, are given in Fig. 8. It was always true that no noticeable change in flow velocity was apparent over the 6-in. length

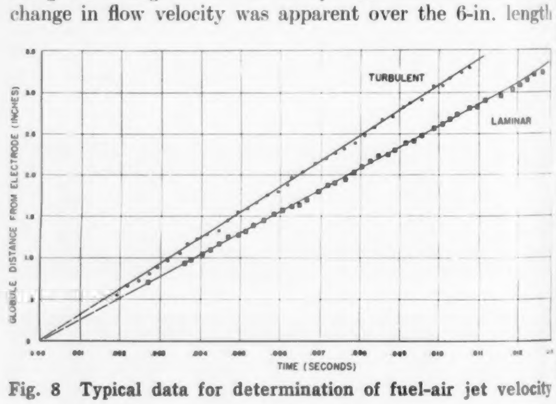

Fig. 8 Typical data for determination of fuel-air jet velocity

of free jet photographed. This indicates that no serious divergence of the free jet took place, which is in agreement with the surveys of the jet made with a pitot tube. Comparison of this flow velocity with the fuel and air-flow orifice measurements provides an independent check of the measurements.

8 Determination of actual flame speed from the apparent values of step 5 were calculated for a constant pressure process by

$$\frac{S_{\text{actual}}}{S_{\text{apparent}}} = \frac{R_u T_u}{R_b T_b}$$

where

S ≡ flame speed
R_u ≡ gas constant for the unburned mixture
R_b ≡ gas constant for the burned products
T_u ≡ temperature of the unburned gas stream
T_b ≡ adiabatic flame temperature of the fuel mixture

Fuel-air ratio, per cent	Temperature, °R
7	3552
8	3772
9	3912
10	3842
11	3692

Table 2 **Measured values of adiabatic flame temperatures of natural gas**

Values of T_b (from Ref. 13, page 690) are given in Table 2. The calculated value for R_u is 55.1, and for R_b is 55.6.

An investigation of sources of error in data and data reduction was made in an attempt to establish the accuracy of the results. Among the sources of error, which were deemed significant, were elimination of electrode turbulence, scale factor, optical resolution, timing, errors in adjusting projected image to give one-to-one correspondence with actual size, and errors in tracing and planimetering. By far, the most important of these are the errors associated with tracing the projected film image. Experiments in data reduction technique indicated a maximum relative error of about 10 per cent.

Results and Discussion

No Burning

Fuel-Air Jet Velocity Distribution

Rather complete surveys of the velocity distribution in the flowing fuel-air mixture at the nozzle exit were made, using a pitot tube 0.125-in. OD. The surveys encompassed the range of velocities to be used in the combustion runs and included data with and without turbulence generating screens. Further, for the runs with screens, the distance from screen to nozzle exit was varied as well as the screen wire size and mesh. Fig. 9 shows typical distributions across one particular diameter of the nozzle. Exclusive of the boundaries, the distribution without screens showed a deviation from the average velocity of no more than 1 per cent.

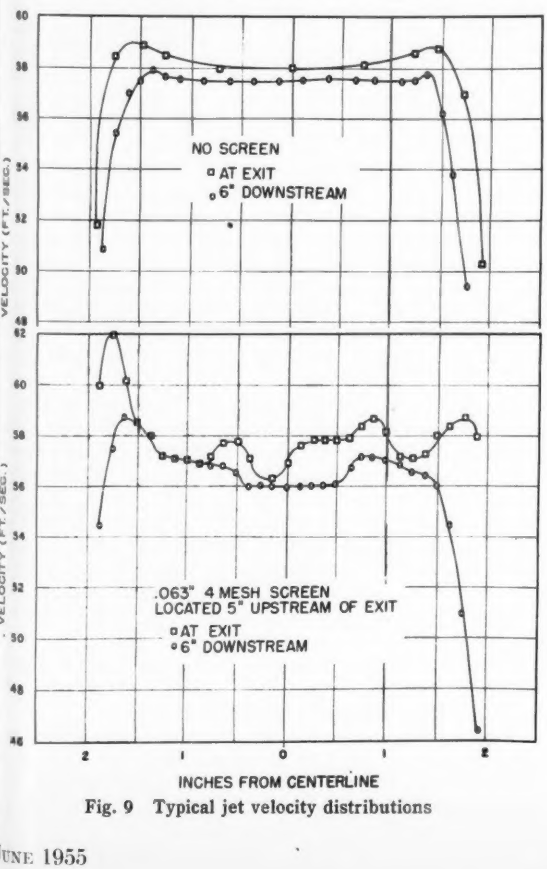

Fig. 9 **Typical jet velocity distributions**

With screens the deviation was more pronounced. Since burning was always initiated 24 mesh lengths (95 wire diameters) downstream of the screen, the surveys were made at 80 wire diameters and more. The deviation from the average was generally of the order of 5 per cent, being less as the distance was increased. An interesting feature of the profiles was that the deviations were not random across a diameter, but as shown in Fig. 9.

At distances of only 20 wire diameters from the screen, the profiles were generally quite uniform, exhibiting a saw-tooth characteristic with the low velocities directly behind and the highs between the wires. The magnitude of the deviation was about 10 per cent.

Fuel-Air Ratio and Distribution

In order to obtain an independent check on the fuel-air ratios calculated from the fuel and air orifice data, and to establish the distribution of fuel in the jet, mixture samples were taken at various locations in the flow stream. The area of the jet was divided into a center circle and four annuli, all of equal area. The sampling probe was traversed across a diameter of the jet and a sample withdrawn at each station corresponding to the center of an area. This procedure was carried out at various mixture flow velocities as well as various fuel-air ratios.

A comparison of the average fuel-air value obtained by the Orsat analysis of the samples taken during a traverse, and the value computed from the orifice data showed good agreement. This agreement provided confidence in the Orsat sample data.

The mixture profiles showed essentially uniform distribution throughout the stream. At the lowest flow velocities used, the deviation from the average fuel-air ratio did not exceed 7 per cent, while at the high velocities it did not exceed 5 per cent. In all cases the deviation was random, no stratification of mixture in a particular zone of the jet being indicated.

Turbulence Spectrum

For the experimental study of the influence of turbulence on the flame propagation rates, the turbulence was created by cylindrical wire screens placed in the fuel-air flow stream. Two different screens were used, a 0.063-in. wire diam, 4 mesh, and a 0.125-in. wire diam, 2 mesh. The screens were located sufficiently far upstream of the spark electrodes to insure isotropic turbulence where ignition was initiated.

Extensive measurements of the energy spectra of the turbulence behind these screens at different velocities were made using a single wire probe and the constant-current hot-wire anemometer equipment. A typical spectral curve is shown in Fig. 10. The r.m.s. turbulence energy level measured by the wave analyzer over a narrow frequency band width is represented by $\sqrt{\overline{E_0^2}}$, and the total r.m.s. energy level is

$$\overline{E_T^2} = \int_0^\infty \overline{E_0^2}\, df/f$$

where f is the frequency.

The energy spectra data, such as are shown in Fig. 10, were fitted by the most similar analytical curve for $\overline{E_0^2}/\overline{E_T^2}$ vs. frequency, which was calculated using the equation for isotropic turbulence given in (14). The typical spectrum shown in Fig. 10 indicates that the spectra obtained were those associated with isotropic turbulence. Comparison with data by other experimenters also substantiates this conclusion. Further, the spectra indicated that no high energy peaks at particular frequencies existed, due to compressor and duct geometry characteristics.

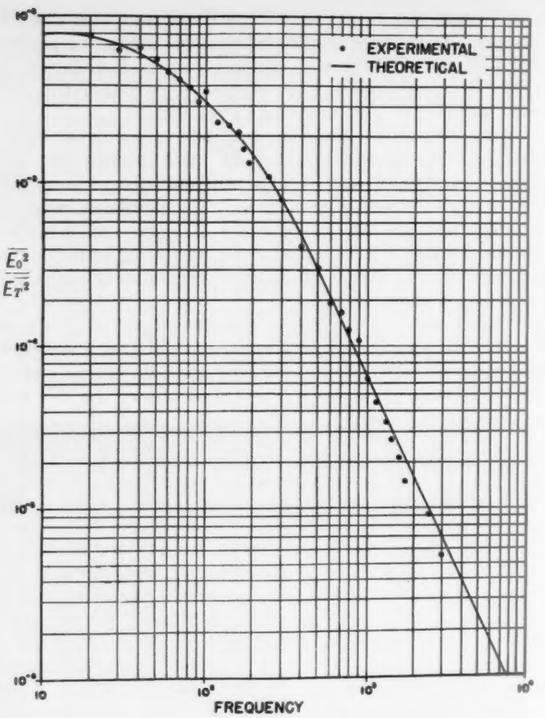

Fig. 10 Typical turbulence energy distribution

Turbulence Intensity and Decay

To determine the turbulence environment to which the flame globule was subjected as it grew and was swept downstream, the intensity and decay of turbulence with flow distance were investigated. The intensity of the turbulence $\sqrt{\overline{u^2}}$, which is the r.m.s. value of the velocity fluctuations in the free stream direction, was calculated using the equation for the hot-wire anemometer derived from King's equation and given in (15). The decay curve is a plot of the measured percentage turbulence $\sqrt{\overline{u^2}}/U$, where U is the free stream velocity, vs. the number of mesh lengths downstream of the screen x/M. The distance downstream is x, and M is the size of the screen mesh. The data for the 0.125-in. wire diam, 2-mesh screen are shown in Fig. 11 along with comparison curves of the results of data for similar screens at nearly the same Reynolds number conditions taken from (16). Since reasonably good agreement was indicated, it was felt that the turbulence velocity and decay patterns were being properly evaluated. Fig. 12 shows the decay curves for the 0.063-in. wire diam, 4-mesh screen.

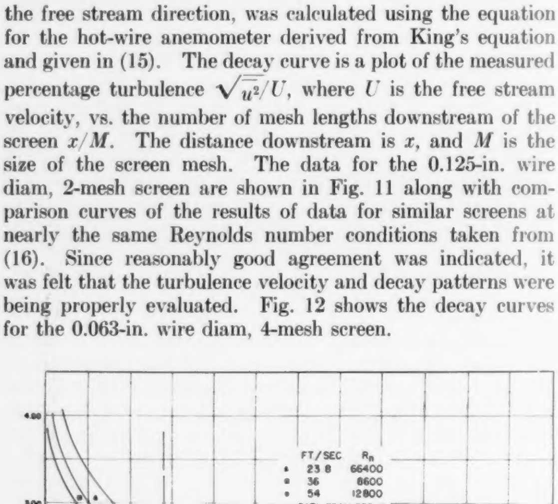

Fig. 11 Turbulence decay for 0.125-in. wire diameter, 2-mesh screen

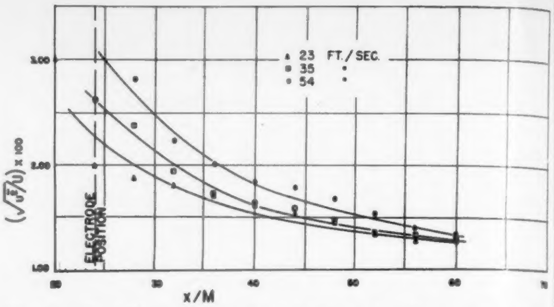

Fig. 12 Turbulence decay for 0.063-in. wire diameter, 4-mesh screen

Nonturbulent Burning

Considerable care was taken in an attempt to produce an air-fuel mixture flow at the spark electrodes that was essentially turbulence free (see under "Auxiliary Apparatus"). Hot-wire anemometer readings were taken to determine the intensity of the residual pipe turbulence that existed for the so-called "laminar" flame speed measurement experiments. These values appear in Table 3. It was noted that the per cent turbulence intensity, $(\sqrt{\overline{u^2}}\cdot 100)/U$, was of the order of 0.1 per cent.

Reproducibility

Many runs at the low turbulence conditions were made at various intervals over a period of a year to (*a*) determine the "laminar" flame speed of the natural gas-air mixtures at various values of fuel-air ratio, and (*b*) determine the reproducibility of the data. The specific purpose of the tests was to properly calibrate the technique to determine if it would be a useful experimental tool for the study of the flame propagation phenomenon.

The results of the laminar flame speed measurements, taken during the year, are given in Table 3. The runs were made over a range of flow velocities from 21 to 54 ft/sec, with fuel that varied slightly in composition as previously noted in Table 1. For the 42 determinations made at a fuel-air ratio of 0.100 to 0.102, the flame speed values of 39 of the evaluations were within ±10 per cent of the average of 0.98 ft/sec, which is within the probable error of the data reduction technique. The remaining 3 runs were within ±17 per cent of the average. The quality of the least-squares fit of the straight line, the slope of which represents the laminar flame speed, to the radius-time data is represented by the value of the linear correlation coefficient. The value of this coefficient varied from 0.990 to 0.999, indicating that a straight line is not only in excellent agreement with the data but is probably the best possible curve to fit the data.

As a criterion of the reproducibility, the standard error of estimate of the regression equation, Z, is also given in Table 3. With certain assumptions of normality, randomness, and independence, an error of not more than $2Z$ can be expected for approximately 95 per cent of the time. It should be noted that the magnitude of Z never exceeds 0.002 ft for flame globules whose size reached a maximum of 0.12 ft during the observational period. This results in an expected deviation of the data from the fitted line of about ±4 per cent for the larger globule sizes and higher percentages for the smaller sizes.

The data in Table 3 lend considerable confidence to the experimental technique as a useful and dependable tool for study of flame propagation phenomena.

The average value for the experimentally determined laminar flame speed, 0.98 ft/sec at 0.100 F/A, is about 10 per cent lower than the value reported for pure methane (17) by Bunsen burner methods. Several possible reasons for

Table 3 Laminar flame speed data

Date	Run	U	F/A	u'	Rate of globule growth by least-squares fit (ft/sec) — Flame sequence no. I	II	III	IV	V	VI	VII	VIII	IX	X	Avg.	Z_{max}	C	S_L
4-53	17	51.04	0.102	0.03	6.25	6.79	7.24	6.96	7.19	6.91	6.99	6.89	6.82	..	6.88	0.00068	7.10	0.97
4-53	18	49.57	0.101	0.03	7.24	6.90	6.04	6.81	6.88	8.14	7.09	7.38	6.74	7.50	7.07	0.00061	7.10	1.00
5-53	20	51.84	0.102	0.03	7.14	7.27	6.45	6.55	6.04	7.52	6.84	7.39	7.60	7.33	7.01	0.00067	7.06	0.99
5-53	27	50.37	0.101	0.04	7.32	7.41	7.09	..	..	..	..	..	..	..	7.27	0.0010	7.06	1.03
7-53	28	23.56	0.101	0.02	7.02	6.96	6.43	6.93	7.00	..	..	..	..	..	6.87	0.0011	7.16	0.96
7-53	29	21.90	0.100	0.02	7.00	7.01	6.99	6.99	6.90	..	..	..	..	..	6.98	0.00083	7.16	0.98
10-53	30	22.06	0.077	0.02	6.28	5.97	6.05	6.37	6.76	..	..	..	..	..	6.28	0.00125	6.93	0.91
10-53	31	22.44	0.090	0.02	6.95	6.77	7.45	7.35	7.19	..	..	..	..	..	7.14	0.00125	7.25	0.98
10-53	32	22.24	0.098	0.02	7.48	7.18	7.30	7.15	..	..	..	..	..	..	7.28	0.00167	7.07	1.03
10-53	33	21.60	0.107	0.02	6.44	6.71	6.09	6.81	..	..	..	..	..	..	6.51	0.00133	6.92	0.95
10-53	34	22.30	0.105	0.02	7.41	7.09	..	..	..	..	..	..	..	..	7.25	0.0014	7.01	1.03
10-53	35	21.20	0.112	0.02	5.54	5.80	7.23	4.56	..	..	..	..	..	..	5.79	0.00083	6.80	0.85
10-53	36	21.30	0.109	0.02	6.60	6.22	5.74	6.22	6.40	..	..	..	..	..	6.24	0.00083	6.87	0.91
12-53	39	23.86	0.090	0.02	7.81	8.10	7.84	7.55	7.60	..	..	..	..	..	7.78	0.0015	7.34	1.06
4-54	70	25.50	0.091	0.02	7.66	7.55	7.31	7.81	7.28	..	..	..	..	..	7.52	0.0020	7.45	1.01

U = flow velocity (ft/sec); F/A = fuel-air ratio (volumetric); u' = measured turbulence intensity (ft/sec); Z_{max} = maximum standard error of estimate of the regression equation occurring in the run (ft); C = expansion constant; S_L = average actual laminar flame propagation rate (ft/sec).

this discrepancy can be advanced: 1 The influence of the constituents of natural gas mixture as negative catalysts. 2 An actual flame temperature lower than that predicted.

It has been fairly conclusively shown that none of the gases occurring in the natural gas mixture (see Table 1) could act as a negative catalyst for the reaction. Experiments by Lewis (13) using Pittsburgh natural gas (similar in composition to the fuel used in these experiments) substantiated the conclusion that the mixture should behave nearly as methane.

The values of flame temperatures used to reduce the apparent to the actual flame speed are the constant-pressure temperatures measured for approximately the combination of ethane and methane used. These measurements (13) are in excellent agreement with the calculated adiabatic temperatures. The rate of heat transfer by radiation out from the burning sphere was estimated using emissivity values predicted from (18). The results of the calculation, which also includes an allowance for soot luminosity (19), indicate a maximum of about 4 per cent of the energy liberated by the combustion is lost by radiation. However, since the temperature is dissociation limited, this heat loss would have small effect on the equilibrium temperature and was, consequently, neglected.

Finally, measurements of flame speed by the soap-bubble technique (20) confirm the theoretically calculated flame temperatures and appear to further discredit the possibility of incomplete combustion or the influence of heat transfer.

Influence of Fuel-Air Ratio

As a further calibration of the experimental technique, runs were made over the range of fuel-air ratios which were ignitable. Fig. 13 presents the measured influence of fuel-air ratio on laminar flame velocity. The results are in general agreement with those of other experimenters.

Because of the rather scanty fuel-air ratio data, it should be pointed out that the shape of the laminar flame speed curve in Fig. 13 is based upon Fig. 5 of (17), but it was dis-

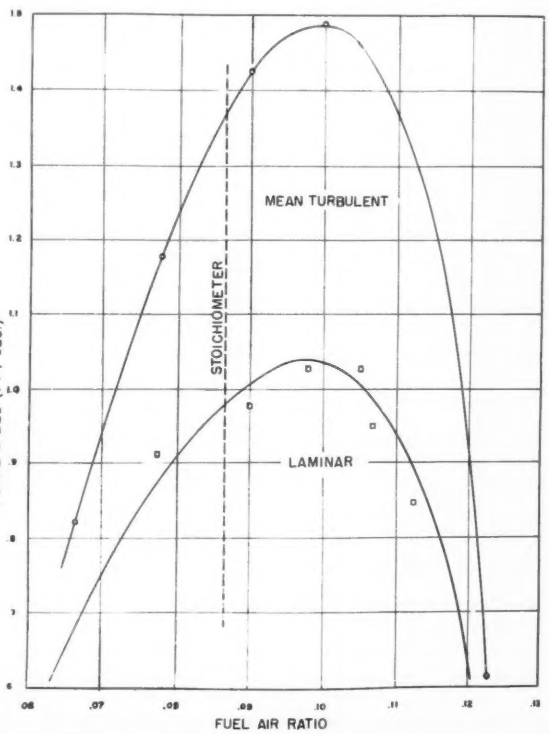

Fig. 13 Flame speed vs. fuel-air ratio for laminar and turbulent flames

placed to fit the data of runs 30 to 36. The data shown in Fig. 13 were taken in one afternoon and give a maximum value of laminar flame speed of about 1.03 ft/sec. All the data, taken over a period of a year, give an average of 0.98 ft/sec for the maximum.

Turbulent Burning

Experimental Considerations

It is significant, for the subsequent discussion, to consider the important characteristics of the experimental method for the determination of turbulent flame propagation discussed in this paper. The first factor to consider is that the flame globule was photographed as it traveled downstream with the flowing gases, and the field of observation was limited, by the mirrors of the shadowgraph system, to a maximum length of 6 in. The corresponding elapsed time for the observations was therefore not constant but depended upon the velocity of the fuel-air mixture, which was intentionally varied during the experiments. The elapsed time was also limited by the fact that only those flame globules that were present in the photographs in their entirety were measured. In some cases, the center of the last one measured was only 4 or 5 in. downstream from the electrodes, depending upon the globule diameter at that time. The important consequence was that the length of the time periods over which measurements were made (0.006 to 0.012 sec) were of the *same magnitude* as the characteristic time of the turbulence, defined in Equation [1], and *therefore the influence of turbulence on the flame propagation was a transient one.*

The second important factor to consider is that the turbulence intensity (and scale) was a variable with respect to the location downstream from the spark electrodes as shown by the decay curves in Figs. 11 and 12. This also means that the flame front was continuously exposed to a different intensity and scale of turbulence with respect to its position or, from a Lagrangian viewpoint, with respect to time.

As a result of the experimental environment the flame velocity, as determined from the rate of change in the measured size of a sequence of flame globules, is a continuously varying quantity with time (see Fig. 7). To determine the slope of the resulting curve at any instant of time is rather difficult, and subject to errors, because of the nature of the curve. Further, since a reliable theoretical equation has not been established, there is little possibility of fitting the data to such an equation by a least-squares procedure in order to evaluate the slope at any point. However, each group of repetitive sequences in Figs. 14, 15 and 16 plots out an average curve (not drawn in the figures) which can be used as a comparative curve to show the influence of the turbulence environment on flame propagation. Flame speeds can be estimated by an approximate calculation of the slope of such an average curve at any particular time.

Analytical Formulation

The measurements of the globule radius as a function of time offer an opportunity to explore the possibilities of an analytical correlation. The first impulse is to adapt a suitable theory from the literature (see, e.g., 7 and 8) to the experimental environment of these tests and then to explore the agreement between the theory and the data. Such a procedure may shed some light on the weaknesses or strengths of the theory. However, since the details of the mechanism by which the turbulence influences the flame propagation are not well understood, the existing theories are necessarily based upon certain arbitrary considerations. It was therefore thought advisable at this time to attempt correlation by means of an equation constructed upon intuition as well as on observed trends in the data.

Since the experiments discussed here result in measure-

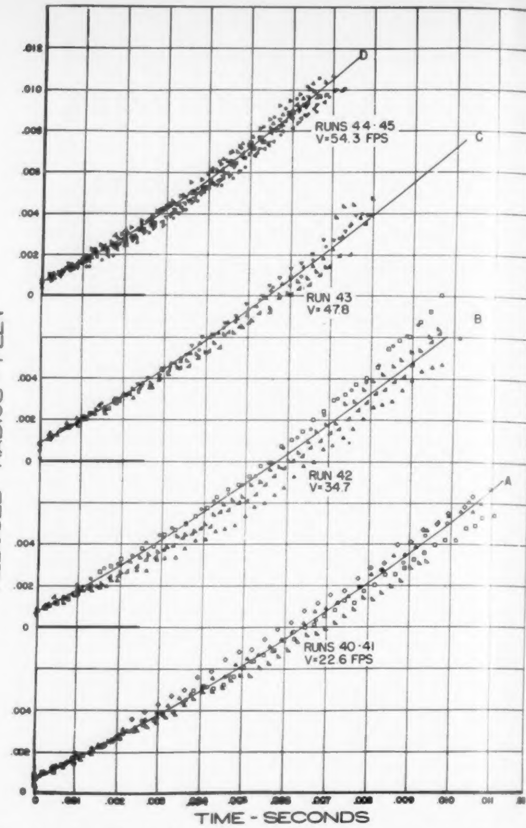

Fig. 14 The effect of turbulence on the temporal growth of a flame globule compared with analytical results for the 0.063-in., 4-mesh screen, $F/A = 0.090$ (see Tables 4 and 5)

ments of the growth of a flame globule and therefore of the turbulent flame speed as a function of time, an equation involving this time influence is necessary. An intuitive necessity of a turbulent flame propagation model based upon a wrinkled flame surface concept is that, at zero time, the flame speed should be laminar and at subsequent times should build up to a maximum steady-state value, provided the turbulence intensity level remains constant. Furthermore, if the wrinkling of the flame front is not a result of a flame instability phenomenon, one would expect that in a field of turbulence decay—such as existed in the experiments—the turbulent flame speed associated with the globule would pass through a maximum value and then decrease again with time toward the limiting laminar value.

An equation which incorporates the ideas expressed above may be written as follows:

$$r = \int_0^t S_L\,dt + B\int_0^t \frac{u'\int_0^t R_\xi\,d\xi}{T_0}\,dt \qquad [1]$$

where

$S_L \equiv$ laminar flame speed
$B \equiv$ const
$u' \equiv \sqrt{\overline{u^2}}$, root mean square turbulent velocity fluctuation
$R_\xi \equiv$ Lagrangian correlation coefficient
$T_0 \equiv$ characteristic time of turbulence $T_0 = \int_0^\infty R_\xi\,d\xi$
$l_1 \equiv$ Lagrangian scale of turbulence

In our experiments, u' is the root mean square velocity fluctuation associated with an isotropic field of turbulence behind a screen and therefore is subject to normal decay. If the

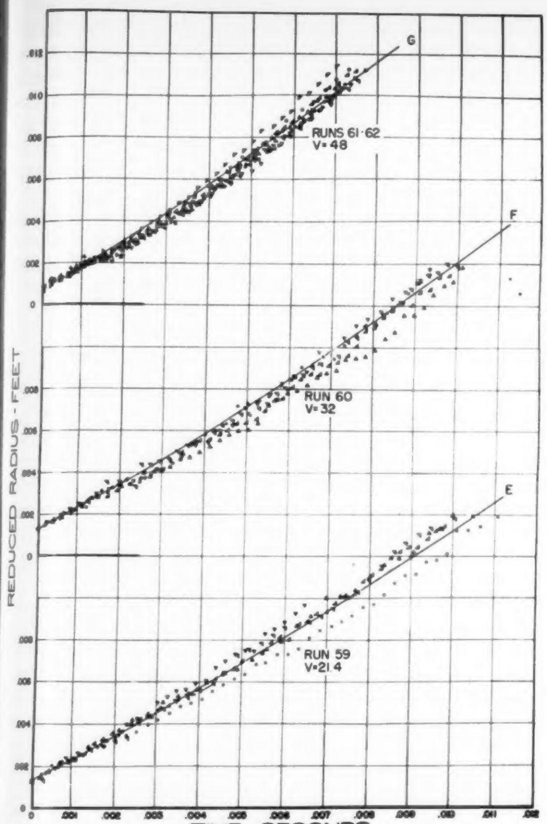

Fig. 15 **The effect of turbulence on the temporal growth of a flame globule compared with analytical results for the 0.125-in., 2-mesh screen, $F/A = 0.090$ (see Tables 4 and 5)**

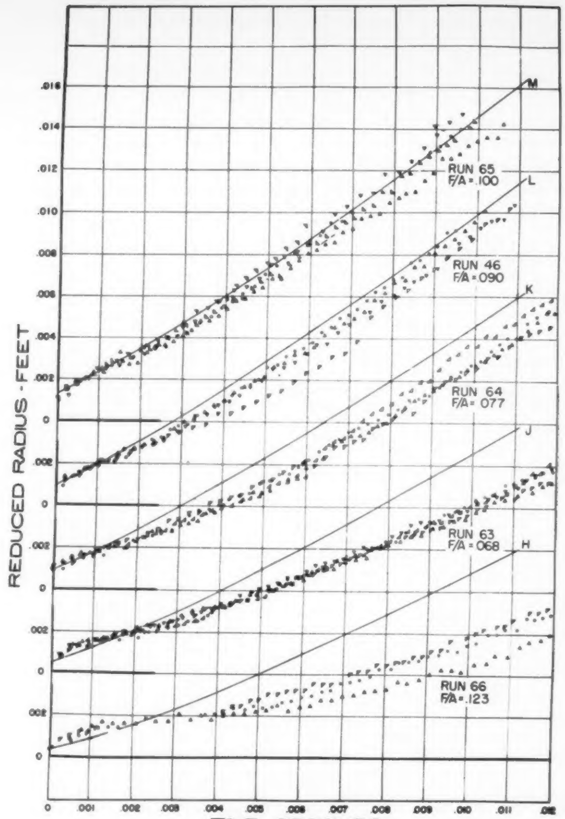

Fig. 16 The effect of fuel-air ratio on the temporal growth of a flame globule compared with analytical results for the 0.125-in., 2-mesh screen, flow velocity of 27 ft/sec (see Tables 4 and 5)

turbulence decay curve, as measured by a hot wire, is fitted by an equation

$$u' = u'_{t=0}\, e^{-\alpha t}$$

where $u'_{t=0}$ is the value of u' at the instant of ignition, $t = 0$, 24-mesh lengths downstream from the screen, and if Dryden's approximation for R_ξ

$$R_\xi = e^{-\xi/T_0}$$

is taken, Equation [1] becomes

$$r = S_L t + Bu'_{t=0} \int_0^t \frac{1}{T_0} e^{-\alpha t} \left(1 - e^{-t/T_0}\right) dt$$

where T_0, for convenience, has been taken as a constant average value. Integrating again

$$r = S_L t + Bu'_{t=0}\left[\frac{1}{\alpha}\left(1 - e^{-\alpha t}\right) + \frac{1}{\alpha + (1/T_0)}\left(e^{-[\alpha + 1/T_0]t} - 1\right)\right] + r_0 \quad \text{[2]}$$

and

$$\frac{dr}{dt} = S_T = S_L + Bu'_{t=0}\, e^{-\alpha t}\left[1 - e^{-t/T_0}\right] \quad \text{[3]}$$

Without the influence of turbulence damping ($\alpha = 0$)

$$S_T = S_L + Bu'\left[1 - e^{-t/T_0}\right] \quad \text{[4]}$$

and for $t \gg T_0$

$$\frac{S_T}{S_L} = 1 + \frac{Bu'}{S_L} \quad \text{[5]}$$

This is in agreement with equations proposed by several investigators (Equation [13], page 622, Ref. (9), e.g.). However, in this reference, Wohl and his associates point out a weakness of Equation [5] which exists for all u' values *except* $u'/S_L \ll 1$. In the above analysis and experiments, by the time steady state is approached, this condition $u'/S_L \ll 1$ is fulfilled due to the damping of the turbulence, and possibly the equation has certain merit.

For values of $t = 0$, Equation [3] becomes $dr/dt = S_L$ which fulfills a condition which is apparently observed in Figs. 14, 15, and 16.

Using $T_0 = l_1/u'$ for the definition of T_0, the characteristic time of the turbulence, and if as in Ref. (14), $l_1 = l_2/2$ where l_2 is the Eulerian scale of the turbulence, then T_0 is given by

$$T_0 = (l_2/2u')_{\text{average}}$$

It is apparent that l_2 and u' are both functions of time, but, for simplicity, l_2 and u' are taken as average values.

The values of S_L were determined and are given in Fig. 13. The values of r_0 were measured from the first photograph in each sequence ($t = 0$). The values of l_2, however, were not measured, although l_2 values for similar screens are reported in the literature, as will be further mentioned in successive paragraphs.

Results for the 0.063-In. Wire Diam, 4-Mesh Screen

Measured values of l_2, the Eulerian scale of turbulence, for and 0.063-in. diam, 4-mesh screen are presented in Fig. 14 of (4). Since the screen used here was 0.063-in., 4-mesh, a value of $0.007 \gtreqless l_2 \gtreqless 0.010$ ft was anticipated. Accordingly a value of $l_2 = 0.009$ ft was used in conjunction with $B = 1$

and the values of r and dr/dt as a function of time were calculated from Equations [2] and [3].

The calculated values of r as a function of time were plotted for each of the experimental cases using the 0.063-in., 4-mesh screen and are shown, labeled A, B, C and D, along with the experimental data in Fig. 14. Fig. 17 is a composite of the analytical curves which show the influence of turbulence intensity (by changing flow velocity) on the globule growth.

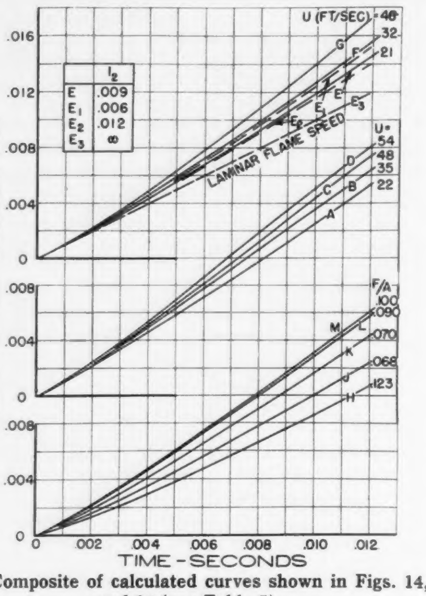

Fig. 17 Composite of calculated curves shown in Figs. 14, 15, and 16 (see Table 5)

The slopes of the radius time-curves of Fig. 17, the calculated flame speeds, are shown plotted as a function of time in Fig. 18. Fig. 18 shows the influence of the turbulence decay in the analytical solution. Unfortunately, the time periods of the observations were too small to observe whether the data begin to exhibit this property or not. It is interesting to note that when a straight line was statistically fitted to the turbulence data over the last half of the observational period, the linear correlation coefficient was of the order of 0.97 to 0.98, partially substantiating the rather flat characteristics of the last half of the curves of Fig. 18.

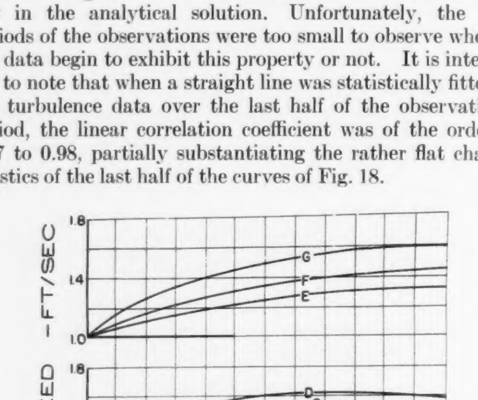

Fig. 18 Turbulent flame speed from calculated results (see Table 5)

The data show an interesting correlation with the analytical results, in the short time period involved, and in themselves exhibit fair reproducibility and consistency. It should be mentioned that the initial size of the flame globule was not quite constant but varied about ±15 per cent, probably as a result of different spark energies. The curves were arbitrarily arranged and plotted from a common initial size for convenience of comparisons.

It should be noted that the previously discussed limitations of the apparatus unfortunately resulted in relatively small differences in the turbulence intensity for the four velocity conditions studied and in small values for the over all time period of the observed growth.

Results for the 0.125-In. Wire Diam, 2-Mesh Screen

In order to obtain correspondence between Equation [2] and the flame data obtained with this screen, a single test run, No. 59, was chosen and the value of l_2 was varied until the theoretical curve was in approximate agreement with the data for this run, again using a value of $B = 1$. A value of $l_2 = 0.009$ ft resulted from this fitting procedure. Using this value for l_2 for all of the turbulence runs with the 0.125-in. screen, good correspondence was obtained between the calculated and measured values of the globule radii (see Fig. 15).

A value of 0.009 ft for l_2 is not to be anticipated, however, for this screen. On the basis of (14) and (22), it would appear that l_2/M should remain constant for geometrically similar screens such as were used. This should result in an l_2 of about 0.018 ft. It was noticed that the scanty data of (23) do not agree with the above l_2/M relation and that the reference further indicated that l_2 remained equal for two nearly geometrically similar screens of different wire diameter. The actual value for the scale will be determined experimentally in the course of future experiments in order to resolve this dilemma.

To indicate the influence of the choice of l_2 on the analytical curves, several calculations were made for the data of run 59, curve E, in Fig. 17, using values of l_2 of 0.006, 0.012, and infinity. These results are shown as the dashed lines in the figure (labeled E_1, E_2, and E_3) and they stress the fact that the results of Equation [2] deviate considerably from the measured results unless the actual characteristic length l_2 is of the order of 0.008–0.010, or unless the assumed relation $l_1 = l_2/2$ is in serious error. It should be noted that $l_2 = \infty$ produces the plot of radius as a function of time which represents the "laminar" flame speed.

The analytical curves shown in Fig. 15 are replotted from a common origin in Fig. 17 for comparison, and the slopes of these curves, the turbulent flame speeds, are given in Fig. 18.

Fuel-Air Ratio Effect on Turbulent Flame Speed

Using the 0.125-in., 2-mesh screen and a flow velocity of 27 ft/sec, the fuel-air ratio was varied over the combustible range. The resulting data are shown plotted in Fig. 16 along with the analytical curves calculated, using $l_2 = 0.009$ and $B = 1$ as before.

For the two lean and one rich fuel-air ratio runs, significant discrepancy was noted between the analytical curves and the data. However, it is apparent that the growth of the globule during the early time periods was at a rate much *less* than the *laminar* flame speed and that the experimental results are not really significant. This peculiar early growth condition that existed for both the highest and lowest fuel-air ratio experiments is shown in Fig. 16. The fact that several of the spark discharges during these sequences did not even ignite the mixture indicates that the fuel-air ratios chosen were on the threshold of ignition for the spark energies and flow velocities used.

As a matter of interest, a flame-speed fuel-air ratio curve was plotted, using a mean turbulent flame speed calculated by fitting a straight line to the last third of each radius time

Table 4 Turbulent flame speed data

Run	U	F/A	$u' = u'_{t_0}e^{-\alpha t}$ u'_{t_0}	α	C	S_T Sub-runs I	II	III	IV	V	Avg.	t
					(*A*) 0.063-in. wire diam, 4-mesh screen							
40	20.4	0.090	0.748	42.9	7.34	1.36	..	..	..	..	1.36	0.011
41	22.6	0.090	0.748	42.9	7.34	1.31	1.34	1.24	1.36	1.33	1.32	0.011
42	34.7	0.090	0.945	56.0	7.34	1.65	1.71	1.57	1.69	1.63	1.65	0.010
43	47.8	0.090	1.057	48.0	7.34	1.65	1.59	1.50	1.54	1.42	1.54	0.008
44	54.1	0.090	1.188	54.0	7.34	1.60	1.59	1.68	1.69	1.50	1.61	0.007
45	55.5	0.091	1.188	54.0	7.34	1.80	1.60	1.73	1.75	..	1.72	0.0066
					(*B*) 0.125-in. wire diam, 2-mesh screen							
46	27.0	0.090	0.688	17.9	7.47	1.62	1.35	1.44	1.49	..	1.48	0.011
59	21.4	0.090	0.535	13.9	7.45	1.26	1.35	1.22	1.33	1.37	1.31	0.010
60	32.0	0.090	0.672	16.0	7.45	1.52	1.42	1.35	1.40	1.42	1.42	0.010
61	46.3	0.090	0.875	20.7	7.38	1.62	1.59	1.55	1.51	1.60	1.57	0.0076
62	50.1	0.090	0.825	20.7	7.34	1.56	1.57	1.75	1.53	1.53	1.59	0.0071
63	27.3	0.068	0.688	17.9	6.75	0.75	0.87	0.83	0.78	0.87	0.81	0.013
64	27.5	0.077	0.688	17.9	7.11	1.13	1.24	1.40	1.23	0.89	1.18	0.012
65	27.3	0.100	0.688	17.9	7.27	1.53	1.50	1.60	1.28	1.52	1.49	0.010
66	29.2	0.123	0.688	17.9	6.65	0.57	0.63	0.64	..	..	0.61	0.013

U = flow velocity (ft/sec); F/A = fuel-air ratio (volumetric); $u' = \sqrt{\overline{u^2}}$ (root mean square fluctuating velocity, ft/sec); u'_{t_0} = value of u' at time zero; C = expansion const; S_T = mean value of the actual turbulent flame propagation rate (ft/sec) obtained by dividing the mean value of the measured rate of globule growth by C; t = observational time period (sec).

Table 5 Conditions used for calculating theoretical turbulent flow characteristics

Theory curve no.	Corresponding experimental run no.	F/A	U	Screen In.	Mesh	l_2	S_L
A	40–41	0.090	22.0	0.063	4	0.009	1.00
B	42	0.090	35.0	0.063	4	0.009	1.00
C	43	0.090	48.0	0.063	4	0.009	1.00
D	44–45	0.090	54.0	0.063	4	0.009	1.00
E	59	0.090	21.4	0.125	2	0.009	1.00
E_1	59	0.090	21.4	0.125	2	0.006	1.00
E_2	59	0.090	21.4	0.125	2	0.012	1.00
E_3	59	0.090	21.4	0.125	2	∞	1.00
F	60	0.090	32.0	0.125	2	0.009	1.00
G	61–62	0.090	46.0	0.125	2	0.009	1.00
H	66	0.123	27.3	0.125	2	0.009	0.58
J	63	0.068	27.3	0.125	2	0.009	0.72
K	64	0.077	27.5	0.125	2	0.009	0.88
L	46	0.090	27.0	0.125	2	0.009	1.00
M	65	0.100	27.3	0.125	2	0.009	1.03

F/A = fuel-air ratio (volumetric); U = flow velocity (ft/sec); l_2 = Eulerian scale of turbulence used in the calculation (ft); S_L = laminar flame speed used in the calculation (ft/sec).

curve using a least-squares procedure. These "mean" values are shown in Fig. 13 as a function of F/A ratio and are not the steady-state values, and the magnitudes have importance only as relative values.

Consistency of Turbulent Data

The consistency of the turbulent runs is not easily perceived from the plotted data (see Figs. 14, 15, and 16). In order to show this, the method discussed above was again used. That is, a straight line was fitted to the more linear later portion of each curve by a least-squares procedure and the slope of this line determined. This linear fitting process included the range of time from about 0.0035 sec to the upper end of each curve. These *mean* turbulent flame velocities are presented in Table 4 merely to show the reproducibility of the turbulent data. The results show that for any one run the maximum deviation of the slope of the fitted line (mean flame speed) is 11 per cent from the mean slope of all the sequences in that run. Values from run to run *are not comparable* since the averages are over *different time intervals.*

An interesting result of the least-squares linear fit to the later time portion of the turbulent curves mentioned above showed a linear correlation coefficient almost as high as that for the laminar cases, as was mentioned before, and appear to support the flat characteristic of the analytical curves of Fig. 18. It is of further interest to spot the values of the mean turbulent flame velocities from Table 4 on Fig. 18 and to observe the rather close numerical agreement.

Conclusions

1 The experimental technique appears to have considerable value for the study of the propagation of laminar and turbulent flames. The data appear to be quite consistent and reproducible, and particularly adaptable to the study of the transient phase of the turbulence effect.

2 The measured laminar flame speeds are in good agreement with those obtained by other investigators.

(*Continued on page 283*)

Incipient Flame Propagation in a Turbulent Stream[1]

H. L. OLSEN[2] and E. L. GAYHART[3]

Applied Physics Laboratory, The Johns Hopkins University, Silver Spring, Md.

In order to extend present knowledge about turbulent flames, and eventually to adapt that knowledge to the design of ramjet engines and high-output propulsive systems dependent on combustion, a series of experiments on turbulent flame propagation has been conducted at the Applied Physics Laboratory. The experiments provide a study of flame kernels propagating outward from a spark source of ignition in a free jet of combustible gas mixture; grids induce a turbulent flow in the free jet. The growth of the flame and the degree to which it is influenced by the turbulent flow field are measured by means of high-speed flash schlieren photography. Inasmuch as the flame kernel is carried along at the average velocity of the gas stream, the flame front must respond only to the turbulent velocity fluctuations. This constitutes an effective and simple experimental situation in which the interaction of flames and turbulent flow fields may be observed. Some of the major conclusions, based upon this experimental work, indicate that isotropic turbulent flow fields attainable with present equipment do not enhance the rate of flame propagation appreciably within the times observable, while nonisotropic turbulent flow fields immediately downstream from grids of sufficient size do increase the rate considerably. The flow property, thought to be responsible for producing the increased flame-propagation rate, is the magnitude of the velocity gradients encountered by the flame, these being greatest in the nonisotropic flow fields mentioned. Quenching of the flame kernels by excessive turbulence has been demonstrated.

Introduction

THIS paper presents a study of discrete spark-ignited flames propagating in laminar and in turbulent streams, and reports an attempt to determine, without extraneous disturbing effects, the interaction of flames and turbulent flow fields. The work was undertaken with the expectation of augmenting the background of understanding of the turbulent flame, thus aiding indirectly in the design of ramjet engines and other high-output propulsive devices depending on combustion.

On the basis of extensive and varied work reported in the literature to date on turbulent flame propagation, it seems fairly well established that flames propagate more rapidly in turbulent than in laminar flow. But as yet there is no real agreement about the reason for the effect of turbulence, or about the nature of the turbulent flame. This lack of agreement is hardly surprising in view of the nature of the phenomena involved. Laminar flame propagation is itself a most complex phenomenon not fully understood, and the turbulent flame problem must await further research in both turbulence and combustion.

This report is preliminary, discussing the initial observations made in setting up the turbulent flame research project and in working out appropriate experimental techniques. The experimental method is similar to that used extensively at the Applied Physics Laboratory for the study of spark-ignition phenomena and incipient laminar flame propagation (1).[4] An ignition spark in a combustible mixture of gas produces a flame kernel propagating outward from the source of ignition. This simple flame, which is bounded on all sides by unburned gas, is sufficiently localized to allow observation of its behavior while entirely within a gas jet of reasonable size. The apparatus has been adapted to the study of flame kernels propagating in turbulent flow induced in the free jet by grids. The growth of the flame in the turbulent stream and the influence of the turbulent flow field on the rate of growth are observed by means of high-speed flash schlieren photography.

The method, employing flame kernels, has the advantage of making possible observation of the interaction of flame and turbulent flow without disturbing influences such as walls, flameholders, boundary layers, and uncontrolled mixing. Since the flame kernel is carried along at the average velocity of the gas stream, the flame fronts are obliged to respond only to the turbulent velocity fluctuations. The experimental situation is thus reduced to the simplest one possible in which the effect of turbulence of predictable properties on flame propagation is observable. The disadvantages of the method are twofold: (a) the characteristic properties of the turbulent flow alter while the flame is propagating, making the interpretation of the interaction more difficult; (b) incipient spark-ignited flames are known to propagate more slowly and be cooler than "normal" (i.e., Bunsen) flames (1). The latter disadvantage adds further uncertainty in the interpretation of observed results. The necessity of working close to the grids because of the small size of presently available free jets makes the second difficulty impossible to avoid. The first difficulty is basic and must be tolerated.

Apparatus and Procedure

The apparatus used in this work consists of equipment to produce and control a free jet of combustible gas (either laminar or turbulent), to ignite this jet at discrete points, and to observe the ensuing flame propagation. The free laminar jet is produced by a precision Mach-Hebra nozzle 1 inch square at the exit, having a 16-to-1 area reduction from approach section to nozzle. The approach section is equipped with a square inlet diffuser followed by screens, which reduce the approach turbulence at the nozzle. The flow distribution is an accurately flat velocity profile, and the residual turbulence is at a very low level. The gas supply (air and commercial propane) is controlled by precision pressure regulators (Moore Nullmatic) and critical-flow orifices so that mass flow may be held constant at any desired value. Linear-flow velocities obtainable at the nozzle may be varied from zero to a maximum of 65 meters/sec. Any desired propane-air ratio may be obtained for the entire range of flows. Turbulent flow is produced by placing screens or grids over the nozzle. One of these grids, subsequently referred to as the precision 10-mesh grid, is rectangular, and is made up of cylindrical rods (diameter = 0.024 inch) spaced four rod-diameters apart, the two sets of rods at right angles being tangent to the same plane. Other grids were com-

Presented at the ARS Ninth Annual Convention, New York, N. Y., November 30, 1954.

[1] This work is supported under Contract NOrd 7386 with the Bureau of Ordnance U. S. Navy.

[2] Physicist.

[3] Physicist.

[4] Numbers in parentheses indicate References at end of paper.

mercial woven-wire screens of various mesh sizes and of approximately the same blockage as the precision 10-mesh screen.

Ignition of flame in the jet was accomplished by short-duration condenser sparks between slender (0.010-in. diam) electrodes immersed in the stream. The spark-gap length, relative electrode positions, and placement of the entire spark gap are readily adjustable by means of a dual three-way manipulator. This allows a gap of any desired length or orientation to be set at any position within the jet. The spark-gap energy is controllable so that appropriate ignition sparks can be produced for all flow conditions and equivalence ratios of the gas jet.

The flame kernels ignited in the gas jet are observed by means of a dioptric, low-sensitivity schlieren system, arranged to produce a schlieren field of radical symmetry. The light source is a Libessart spark of 0.25 μ sec effective duration. The time of the flash relative to the time of firing of the ignition spark is controlled by precision electronic timers (varitimer) whose ranges are zero to 1000 μ sec and zero to 10,000 μ sec. The details of development of the spark-ignited flame are thus rendered visible during any phase of its growth within the range of the varitimers and within the limits of the schlieren field.

There are several methods of recording the photographic data on the film, three of which are used in this preliminary work. Method 1—a series of single exposures is recorded on separate films, one independent exposure per film. This method produces results of best photographic quality, but makes comparison of adjacent exposures inconvenient. Method 2—for flames in successive positions in a moving stream, multiple exposures are recorded on a single film with the flashes so timed that the successive exposures show images of flames in various stages of development and positions in the stream. This method diminishes the contrast of the images and thus diminishes the photographic quality, but it presents an entire series of flame pictures on a single film for convenient over-all scrutiny. Method 3—multiple exposure of independent flames of the same age are obtained on single film to produce a composite picture when statistical variations are in question, or when it is desired to see how closely the phenomena reproduce. These three methods are used in this report to demonstrate the experimental results and to illustrate the combustion and aerodynamic phenomena involved. All the photographs so recorded are subject to accurate geometric measurement and will yield quantitative geometrical data.

Photographic Results

The behavior of turbulent flame kernels as compared with laminar kernels is shown qualitatively in the following series of schlieren photographs. As a preliminary to the flame study, the effect of isotropic turbulence on a spark-induced hot-air kernel is shown in Fig. 1. The single exposure photographs (Method 1) show independent hot-air kernels induced in still air, a laminar flow, and in isotropic turbulent flow by the ignition spark. The pictures along the bottom of Fig. 1 show development of the hot-air kernel in still air at delay times of 50, 200, and 500 μ sec. They are taken with the spark gap axis perpendicular to the plane of the film. The development shows the characteristic toroidal kernel geometry discussed in a previous report (2). The kernel maintains its toroidal shape for over 500 μ sec, but disintegrates into a turbulent mass by the time it is 1000 μ sec old, with some distortion of the toroid already in evidence at 500 μ sec. When the hot-air kernel is induced in a laminar stream of 50 meters per sec jet velocity, the development is as shown in the left-hand vertical series of pictures of Fig. 1. The toroidal development is the same as that for still air, except that the kernel is swept clear of the electrodes to

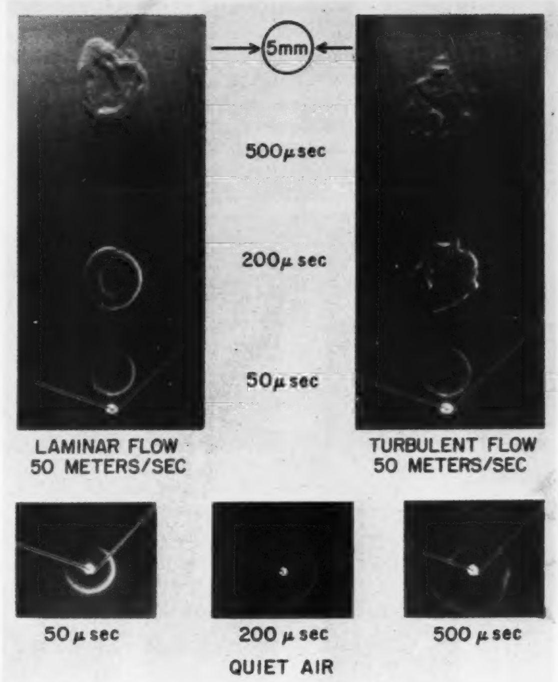

Fig. 1 Effect of turbulent flow on spark kernels in air

The turbulence is assumed to be isotropic. The delay time is indicated in microseconds.

grow in the free jet and that an effect of the wake of the electrodes is evident. The effect of the wake is discernible in the earlier photographs, but the turbulent appearance of the laminar kernel at 500 μ sec indicates clearly that the wake hastens the breakdown of the toroidal motion into random motion. When the precision 10-mesh grid was placed over the nozzle and the spark was passed 10 mesh-lengths downstream from the grid (where the turbulence is assumed to be isotropic), the turbulent kernels shown in the right-hand vertical series of Fig. 1 resulted. No appreciable effect of the turbulence on the 50 μ sec kernel is observed; however, the effect of the turbulence on the kernel at 200 μ sec is clearly evident; by 500 μ sec, the isotropic turbulence is seen to have obliterated all traces of the toroidal shape. The granular structure of the 500 μ sec kernel reveals the nature of the flow field in which we expect to study flame propagation. The "size" of the granules accords generally with the turbulence scale expected from the grid.

A comparison of laminar and turbulent flames is shown in Fig. 2. The photographs are multiple exposures showing a series of flame kernels on the same film (Method 2). The jet velocity was set successively at 25, 50, and 65 meters/sec, with turbulence induced for each speed by the same precision 10-mesh grid. For all jet velocities the laminar flame kernels show a disturbance produced by the electrode wake. The undisturbed portion of the laminar flame front progresses into the unburnt gas with no tendency to develop irregularities or discontinuities. When the flames are ignited in isotropic turbulent flow, the interaction of the turbulence and the flame front becomes apparent. The turbulence distorts the smooth laminar flame into a complex wrinkled surface, the outlines of which show soft curves for the lowest flow velocity, but which grow progressively more angular and discontinuous as the flow rate increases. Apparent discontinuities in the outline cannot be interpreted with certainty as discontinuities in the flame fronts. However, the flame is certainly shown to be highly irregular, as is to be expected from the

fluctuating velocities encountered in the turbulent flow. As in the case of the hot-air kernel, the effect of the turbulence does not show during the early life of the flame. In order to compare the rate of flame propagation for the laminar and turbulent flames, the multiple exposures along the top of Fig. 2 were obtained. These pictures are a composite (Method 3) of independent flame kernels of the same age, and otherwise of conditions identical with the series immediately below them. The "average" or "statistical" outline of these multiple exposures is sufficiently regular for purposes of comparison. When the corresponding laminar and turbulent flame kernels are so compared, they are found to be nearly identical in size. This comparison shows that the turbulent flow field involved in these flames has not affected, within the time of observation, the flame propagation rate appreciably.

To find an increase in the rate of flame propagation, one

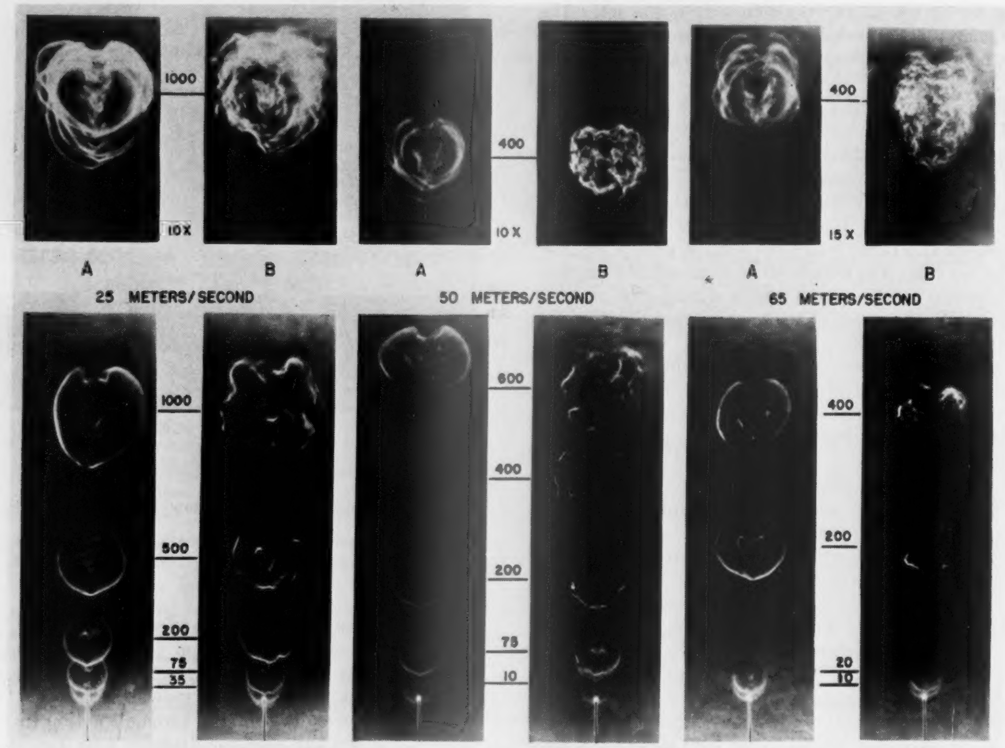

Fig. 2 Flame propagation in high-speed stream

A represents laminar flow, and B represents isotropic turbulent flow. The delay times are indicated in microseconds. The multiple exposures in the top row compare the rate of flame propagation for laminar and turbulent flames.

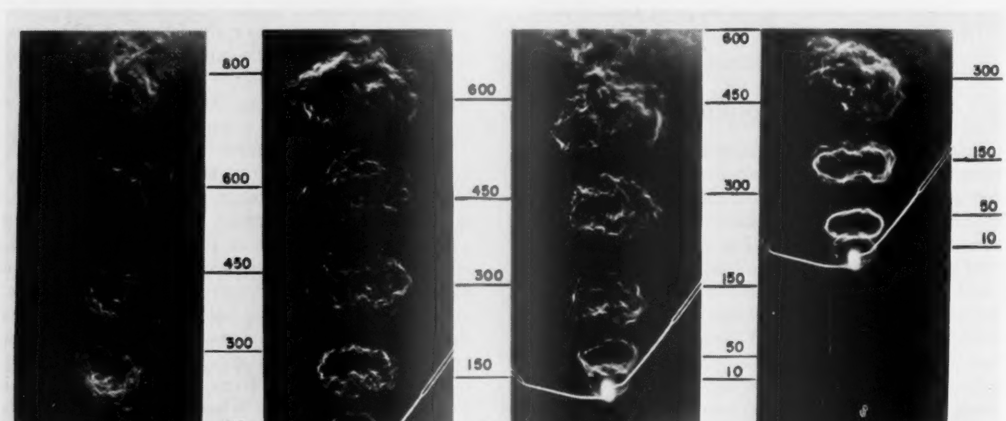

Fig. 3 Flame propagation in turbulent flow

The flame is initiated at the indicated height above the turbulence-inducing grid. M represents a mesh space of 0.1 in. The flow velocity is 50 meters/sec. The fuel-air ratio is stoichiometric. Delays are in microseconds, as indicated. The spark is centered over the mesh square.

must evidently examine flames in flow conditions other than those existing for Fig. 2. Moving the ignition source closer to the grid results in flames propagating in turbulence of greater intensity. The effect is not simple, however, since approaching the grid also changes the turbulent scale and brings one into a region of nonisotropic turbulence. Without attempting to determine the changed flow conditions exactly, and on the assumption that the principal change would be an increase in intensity, the ignition spark was moved progressively closer to the 10-mesh screen and the resulting turbulent flame propagation was observed. The results of this progression are shown in Fig. 3. As the ignition source approaches the grid, the power of the turbulence to wrinkle the flame front becomes progressively greater, and the warping of the flame front is seen to occur earlier in the life of the flame. The sizes of the flames of the same age for the different ignition positions are observed to be substantially the same, except for the flame ignited one mesh length downstream, which appears smaller than the others. More will be said of this later. Once again, the turbulence produced by the 10-mesh screen has not been effective in increasing the rate of flame propagation even when the flame is ignited close to the grid. Igniting flames in the laminar flow upstream from the grid, and observing the flames as they flow through the grid into the turbulent region also fails to show an enhanced flame propagation rate in the turbulent region. This experiment is illustrated by Fig. 4 in which the unchanged flame propagation rate is demonstrated by laying a straight edge along the boundaries of the flames above and below the grid. The flame boundaries all lie along a straight line when proper allowance is made for the rapid kernel expansion in its earliest history.

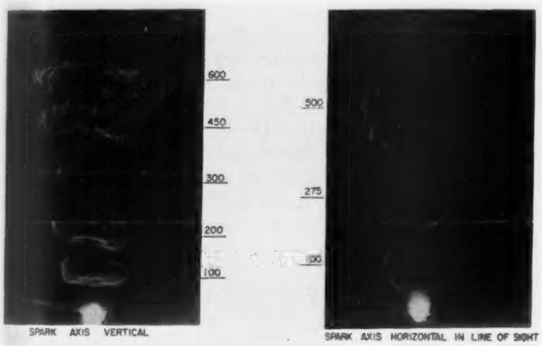

Fig. 4 Flame propagation in high-speed stream

The turbulence-inducing grid has wires 0.010 in. in diameter, spaced 0.040 in. apart. The plane of the grid is at the upper edge of the horizontal silhouette. Propane air in stoichiometric proportion is flowing at 50 meters/sec. Delay times are indicated in microseconds.

One method of altering turbulent flow conditions remains, namely, variation of the grid spacing. This leads to an increased apparent flame propagation rate as shown in Fig. 5. The first two pictures of the middle row of Fig. 5 compare a stoichiometric laminar flame with a stoichiometric turbulent flame ignited $^1/_4$ in. above the precision 10-mesh screen. Consistent with the above observations, no appreciable change in flame propagation rate is observable. However, when the 10-mesh screen is replaced by a four-mesh screen of similar blockage and no other changes made, the resulting flame appears as shown in the third picture of the middle row. This flame shows a considerable increase in the apparent rate of propagation produced by the larger screen, as is manifest by its greater area on the photograph. The effect of altering fuel-air ratio is shown in the upper and lower rows of Fig. 5, in which the equivalence ratio is 1.2 and 0.8, respectively.

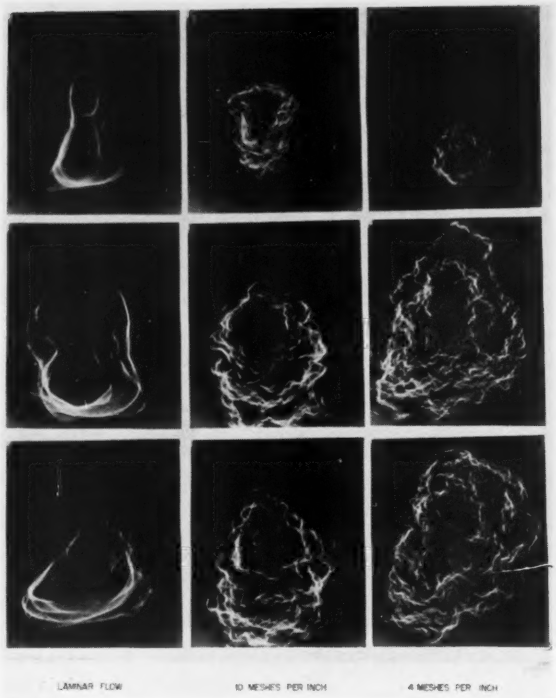

Fig. 5 Flame propagation as affected by various turbulence-inducing grids

The propane-air stream is flowing at 25 meters/sec, and the equivalence ratios are as follows: for the top row, 1.2; for the middle row, 1.0; for the bottom row, 0.8. The grid spacing, in meshes per inch, is indicated under each column.

The lean-mixture flames behave substantially the same as the stoichiometric flames, but the rich-mixture flames apparently propagate more slowly in the turbulent flow than in the laminar. The four-mesh screen seems to have partially quenched the flame propagation in the rich mixture.

Additional comparisons are provided in the series of pictures shown in Fig. 6. A photograph of a laminar flame at 290 μ sec is shown in the lower left-hand picture: the picture immediately above is a hot-air kernel, also at 290 μ sec, produced by an ignition spark of increased energy. The spark energy was so adjusted that the flame kernel and hot-air kernel were the same size at this time. The subsequent development of these kernels at 1000 μ sec is shown for various flow conditions in the remainder of the pictures. In the laminar flow the air kernel maintains nearly the same size as it had at 290 μ sec but shows some tendency to decay into a turbulent mass, whereas the flame kernel has increased in size materially though the flame fronts remain laminar in character. When the laminar flow is replaced by turbulent flow induced by a four-mesh screen, the air kernel is somewhat altered in shape and shows a granular appearance, but maintains approximately the same size as the kernel in laminar flow. The corresponding flame shows the same granular appearance as the air kernel, but apparently propagates at an increased rate. When a two-mesh screen is substituted for the four-mesh screen, the air kernel is dispersed over a considerable volume and is barely visible to the schlieren camera. The corresponding flame is likewise dispersed over a much larger volume than the flame associated with the four-mesh screen. The granularity of the two turbulent flames is strikingly similar even though the turbulent scales are different, but the flame associated with the two-mesh screen has an apparent propagation rate much greater than that of the flame from the four-mesh screens. The schlieren optical

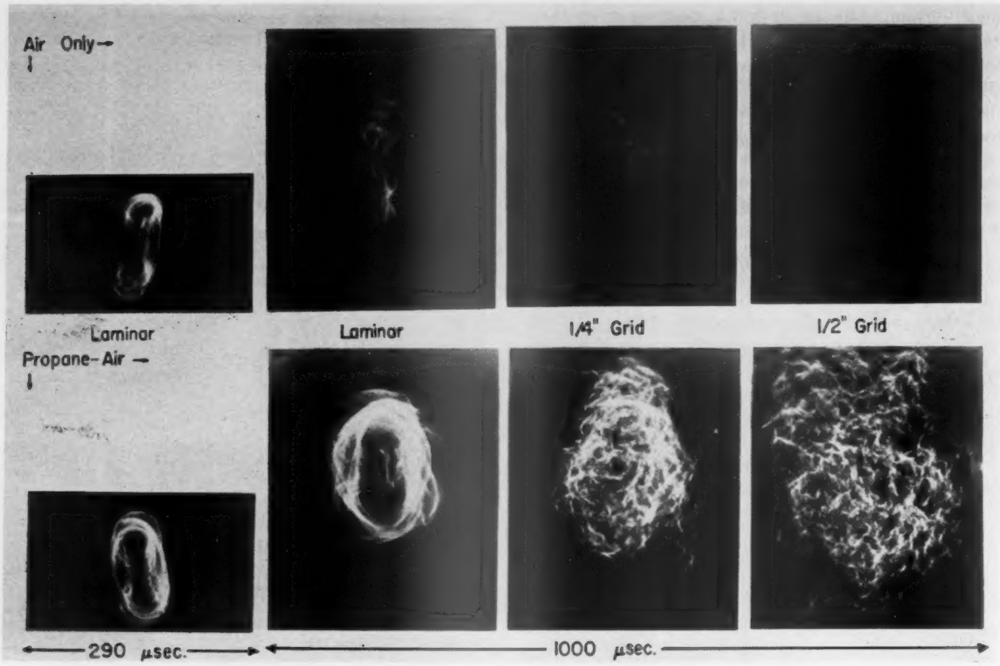

Fig. 6 Spark-ignited kernels in laminar and turbulent flow with and without fuel

The first row shows air moving at 25 meters/sec, ignition at 8000 volts and 0.05 mfd; the second row shows stoichiometric propane air at 25 meters/sec, ignition at 5500 volts and 0.02 mfd.

gradients are weaker, as is evidenced by the lessened contrast in the last photograph.

Measurements from the Photographs

The photographs presented in the previous section make possible the determination of the dimensions of the flames under specified conditions. Since the rate of change of volume of the flame is a measure of the rate of flame propagation, we are most interested in volumetric measurement. There is a simple way to approximate the relative volume by means of area measurements obtained directly from the photographs. The area of the flame, as exhibited on the negative, is measured by tracing the edges with a planimeter. This area, raised to the 3/2 power, is taken as a rough measure of the volume of the flame. Such measurements have been made for a variety of photographs showing the development of flame as affected by various grids, flow velocities, time of propagation, etc. The dependence of this virtual volume upon the several variables is shown in Figs. 7 to 9.

Effect of mesh size of turbulence-promoting screen on inflamed volume of the stoichiometric propane-air flame at various delay times is shown in Fig. 7 for a jet velocity of 12.5 meters/sec. The points at extreme left of the graph are those obtained in a laminar stream. For identical approach flow conditions, screens of various grid spacing were placed successively in the jet. A photograph of the resulting flame kernels was obtained at several heights of the ignition spark above the screen and at several delay times. The volumes were plotted on logarithmic paper, and successive points were connected by straight lines for easy identification. Fig. 8 is a representation of a similar graph obtained for a jet velocity of 25 meters/sec; the remarks pertaining to Fig. 7 also apply to Fig. 8. The figures show that the inflamed volumes increased as the size of the grid spacing increases and, therefore, the larger grid spacings produce the more rapidly propagating flames. The dependence of the inflamed volume upon the height of the ignition spark is not so clearly shown, but in general the inflamed volumes are greater when the ignition occurs close to the grid. Since no very clear-cut dependence of inflamed volume on the height of the ignition source is shown, the inflamed volumes obtained for each grid spacing were averaged without regard to the height of the ignition source. The averaged points are shown in the graph of Fig. 9. The curves for the 1000 µsec delay also indicate that the increase in inflamed volume is greater for the 25 meters/sec flow than for the $12^1/_2$ meters/sec flow. It should be remembered in examining the curves of Figs. 7, 8, and 9 that the characteristics of the turbulent flow at the same point in the jet differ for the different grid spacings.

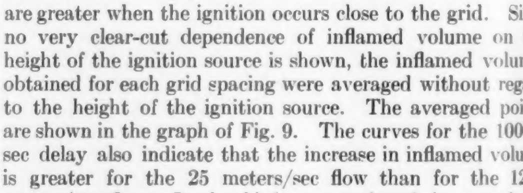

Fig. 7 Effect of grid spacing on inflamed volume at 12.5 meters sec

The ratio of spacing to wire diameter is constant at 4 to 1.

Discussion

If one is to gain understanding of the effect of turbulent flow on the rate of flame propagation, consideration of the complexity of the subject makes it seem wise to limit observation to the simplest flame system interacting with the simplest and best known types of turbulent flow. The simplest and probably best understood turbulent flow field is the isotropic turbulence induced in laminar flow by grids of a particular construction. At the outset the principal objective of this work was to observe such flame propagation in turbulent flow in the absence of extraneous disturbances, and to determine the effects of isotropic turbulent velocity fluctuations on the flame propagation rate. It was expected that the interaction of a flame front with an isotropic turbulence would produce perturbations in the behavior of the flame which might be correlated with measured or calculated properties of the isotropic turbulence (scale and intensity). This approach was expected to yield a quantitative study of turbulent flame propagation and perhaps an isolation of the mechanism responsible for the effect from turbulence. These expectations were put to the test in carrying out the previously described preliminary survey of the effect of the precision 10-mesh screen on flame kernels. The results of this survey are shown in Figs. 1 to 4. The effect of the turbulence on the hot-air kernel (Fig. 1) is precisely as expected, since the kernel becomes granulated and the size of the "grains" is in accord with the scale of the turbulence. The effect of the turbulence on the flame is qualitatively identical with the effect of the turbulence on the hot-air kernel. Furthermore, measurement of the size of the turbulent flames as compared to laminar flames of the same age shows that the flame propagation rate is not appreciably affected by the isotropic turbulence in the time interval used.

When other grids of various mesh sizes were exchanged for the precision grid, a measurable increase in the apparent flame propagation rate was observed for a larger grid (four-mesh, two-mesh). In all cases where enhanced flame propagation rate was observed, the flame had been initiated in a region of nonisotropic turbulence. For the four-mesh screen it was possible to observe flames ignited 10-mesh lengths downstream from the grid (in the isotropic turbulent region), but here no appreciable effect of the turbulence on the flame propagation rate was observed. It thus becomes apparent that the turbulent fluctuations which produce large effect on flame propagation rate have some characteristic other than that found in our isotropic turbulent field. The effect of turbulence on flame propagation does not necessarily depend on isotropy itself. As used herein, isotropy or nonisotropy is intended to specify attainable experimental conditions. Probably the velocity gradients encountered in the isotropic flow producible for this investigation are too small in magnitude to affect appreciably the propagation rate. In nonisotropic flow, where the velocity gradients have not had time to die out, they are of such magnitude as to produce the observed effects.

This observation leads immediately to a reappraisal of the objectives. Since it was found that the isotropic turbulent flow field has no apparent effect on the flame propagation rate, it becomes impossible to correlate the properties of the isotropic turbulence with flame propagation within the times of observation available in this experiment. There remains the necessity to observe the interaction of flames and nonisotropic turbulent flow, and to determine, if possible, the causes underlying the observed effects. In view of this situation, the objectives of this work have been altered and may be restated as follows: (a) to observe the effects of fluctuating aerodynamic flow fields on the rate of flame propagation of flame kernels produced within the flow fields; (b) to seek a correlation between measurable characteristics of flow field and such effects as are observed. An apparent characteristic of the flow field near a grid or other obstruction is the existence of large velocity gradients or high-intensity shear regions. Since velocity gradients are measurable and subject to manipulation and control, a study of their effects on flame propagation rate is indicated. Eddy diffusion and mixing processes should also be considered as possible correlating factors. Subsequent work on this project is directed along these lines.

By reference to Figs. 1 through 5, one may readily observe that the granularity or the "characteristic size" of the flame surface by the turbulent flow appears substantially the same, regardless of the size of the screen. Since one expects a change in the size of the vortices produced by grids of different mesh size, one would expect that the granular pattern of the flames would alter accordingly. The fact that the granularity is approximately of the same size for all the turbulent flames observed indicates that the granularity may not

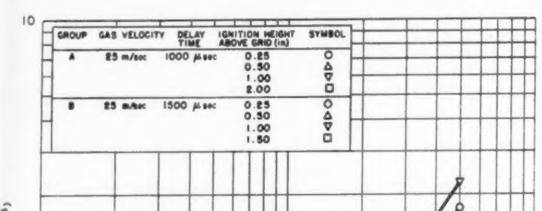

Fig. 8 Effect of grid spacing on inflamed volume at 25 meters/sec

The ratio of spacing to wire diameter is constant at 4 to 1.

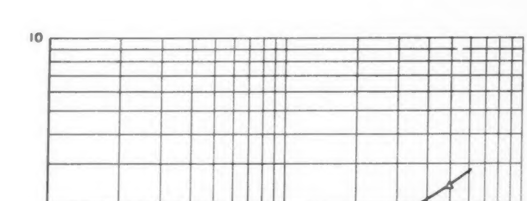

Fig. 9 Grid spacing vs. inflamed volume (averaged data)

The ratio of spacing to wire diameter is constant at 4 to 1.

be produced exclusively by the turbulent flow. By analogy with the findings of Dr. Walter G. Berl (3) in his studies of inverted stabilized flames in turbulent flow fields, it may be suggested that the effects are due to an inherent instability in the flame front initially induced by the turbulent fluctuations. Such an instability characteristic of the flame itself would be sufficient to explain the uniform granularity observed.

Reference to Fig. 6 brings out another aspect of the turbulent flame propagation with which one must deal. In that figure the effect of the 1/2-in. grid on the hot-air kernel is seen to be one of dispersal of the hot material over a considerable volume. It appears likely that a similar dispersal of the flame occurs in the turbulent field produced by the 1/2-in. grid. If this physical dispersal occurs, it projects the distinct possibility that part of the apparent growth of the flame arises from the transport of burning material by the aerodynamic flow field as well as by a steady and controlled combustion at an apparently increased flame speed. The comparisons of Fig. 6 supply strong experimental evidence for the existence of a thickened or "stirred reactor" flame front in contrast to the ordinary wrinkled flame front so commonly considered in dealing with turbulent flames. It thus appears that turbulence, depending on its properties, can produce turbulent flames propagating as thin, warped flame fronts or as thickened reaction zones in which the combustion approximates the ideal "homogeneous combustion" as visualized by Avery and Hart (4). Whether or not the dispersal occurs, cannot be finally decided by photographic observation of the flames. A question, the answer for which can be obtained only by an altered experimental technique involving additional instrumentation, has thus been raised. Should the dispersal of the flame be caused partially by turbulent diffusion, one would expect that the flame temperature in the combustion zone would be reduced by a mixture of cold gases into the flame. Such a situation would be detectable either by temperature measurements or by determination of combustion efficiency. It is clear that some such extension of the experimental techniques is required.

A further suggestion of considerable potential importance is given by the photographs of Figs. 3 and 5. In these pictures there is some evidence that the apparent flame propagation rate in certain instances has been decreased by the turbulence. This suggestion raises the possibility that flame propagation may be retarded or enhanced by turbulent flow, depending on the magnitude of the velocity gradients. The enhanced flame propagation rate has already been demonstrated. The quenching effect suggested in Figs. 3 and 5 is illustrated explicitly in Fig. 10 which shows the quenching of a flame kernel by the turbulent flow in the wake of a parallel-rod grid. The flame was ignited in the laminar flow upstream from the grid. The photographs show the flame after the passage through the grid and into the intense nonisotropic turbulent field in the wake of the rods. For a jet velocity of 18 meters/sec, the flame stabilized on the center rod and propagated strongly downstream. For higher jet velocities the flame did not stabilize on the rods but was swept downstream as a kernel. For 20 and 23 meters/sec jet velocities the flame continued to propagate after passage through the region shown in the figure, but for 25 meters/sec jet velocity, the flame was mainly quenched so that flame propagation occurred beyond this region only occasionally. For the 50 meters/sec jet velocity, the quenching was complete. Pressure or absence of flame in the jet was judged by presence or absence of blue light emitted by the flame. Quenching resulted in complete suppression of the blue light emission and also markedly reduced the sound of the flames in the jet. This quenching leads to the conclusion that there is an optimum turbulent condition in which the maximum flame propagation rate will be obtained. In addition, Fig. 5 shows that the effect of the turbulence is influenced by the mixture ratio. As a corollary, one may well find that flame propagation may be improved in some practical applications by reducing the turbulence level rather than increasing it.

Conclusions

The following summarizing statements or conclusions, based upon the preliminary work reported herein, can be made:

1 Isotropic turbulent flow fields, of the kind produced in this work, do not enhance the rate of flame propagation appreciably within the time of observation of this experiment.

2 Nonisotropic turbulent flow fields do alter the apparent rate of flame propagation. The magnitude of the change in rate depends upon the grid size (spacing and wire diameter), and upon stream velocity. (See under "Discussion" for a qualification of the words "isotropic" and "nonisotropic.")

3 The apparent rate of flame propagation may be either increased or decreased by the interaction with turbulence. This indicates the existence of an optimum turbulent condition which will result in maximum combustion rate.

4 Turbulent diffusion is partially responsible for the apparent increase in flame propagation rate. Measurement of the temperature distribution within the flame kernel would be of assistance in assessing this effect.

5 The effect of the turbulence on flame propagation depends upon the equivalence ratio of the combustible gas.

6 It is probable that if flame kernels produced in such isotropic fields as used in Fig. 1 could be observed at considerably later times, an increase in flame propagation rate might be found. Experiments are in progress to test these possibilities.

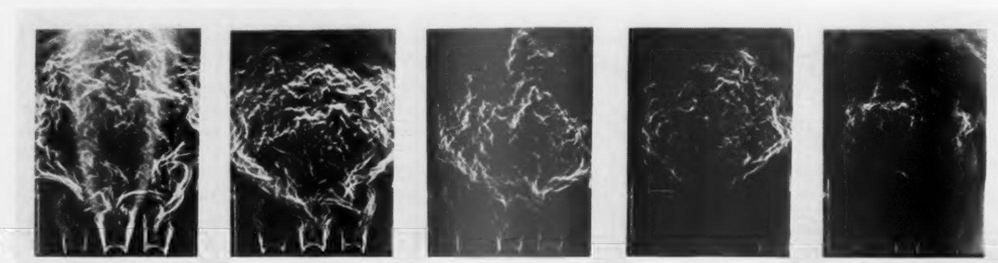

Fig. 10 Quenching of flame by turbulence

Spark gap is below grid. Numbers under pictures indicate velocity (meters/sec) of stoichiometric air-propane mixture in nozzle before placement of grid. Grid changes flow distribution and causes high velocity gradients in jet. In first picture the gradients are so low that flame is stabilized on center rod. Note progressive change in flame granularity and decrease in schlieren contrast with increase in jet velocity. At 50 meters/sec, flame is quenched such that it is no longer visible to unaided eye.

Acknowledgment

The authors are indebted to Professor Stanley Corrsin, of The Johns Hopkins University, for specification of the precision 10-mesh grid and for a discussion of the characteristics of the turbulent flow produced by it. The authors also wish to acknowledge their gratitude to W. H. Avery, W. G. Berl, and A. A. Westenberg, for their contributions to this work.

References

1 "Propagation of Incipient Spark-Ignited Flames in Hydrogen-Air and Propane-Air Mixtures," by H. L. Olsen, E. L. Gayhart, and R. B. Edmonson, in Fourth Symposium (International) on Combustion (Combustion and Detonation Waves), Baltimore, The Williams and Wilkins Company, 1953, p. 145.

2 "Microchronometric Schlieren Study of Gaseous Expansion from an Electric Spark," by H. L. Olson, R. B. Edmonson, and E. L. Gayhart, *Journal of Applied Physics*, vol. 23, October 1952, pp. 1157–1162.

3 Private communication with Dr. Berl, APL/JHU.

4 "Combustor Performance with Instantaneous Mixing," by W. H. Avery and R. W. Hart, *Industrial Engineering Chemistry*, vol. 45, 1953, p. 1634.

Influence of Turbulence on Flame Propagation Rates

(*Continued from page 275*)

3 An encouraging quantitative correlation between an empirical equation and the experimental data is shown, but the relation to the scale of the turbulence was satisfactory for only one of the two screens used. The correlation was unsuccessful for very lean and rich mixtures. This was due to the fact that the rate of turbulent flame growth, for these cases, was lower than the laminar values.

Acknowledgments

The authors gratefully acknowledge the assistance by Karl Faymon for the turbulence measurements and by Ruth Strahosky for aid in reducing data. Appreciation is also expressed to Dr. W. T. Olson, W. R. Mickelson, and other members of the staff of Lewis Flight Propulsion Laboratory, NACA, Cleveland, Ohio, for their assistance in obtaining and lending some of the instrumentation required for the turbulence measurements.

References

1 "The Effect of Turbulence on the Flame Velocity in Gas Mixtures," by G. Damkohler, *NACA TM* 1112, 1947.

2 "On Combustion in a Turbulent Flow," by K. I. Shelkin, *NACA TM* 1110, 1947.

3 "The Effect of Reynolds Number in the Turbulent Flow Range of Flame Speed of Bunsen Burner Flames," by L. M. Bollinger and E. P. Williams, *NACA TN* 1707, 1948.

4 "Flame Stabilization and Propagation in High Velocity Gas Streams," by A. C. Scurlock, Meteor Report no. 19, Fuels Research Laboratory, Massachusetts Institute of Technology, July 1948.

5 "Flame Stabilization and Propagation in High Velocity Gas Streams," by G. C. Williams, H. C. Hottell, and A. C. Scurlock, Third Symposium on Combustion, Flame and Explosion Phenomena, Williams & Wilkins, Baltimore, 1949.

6 "Investigation of Turbulent Flames," by B. Karlovitz, D. W. Denniston, Jr., and F. F. Wells, *Journal of Chemical Physics*, vol. 19, no. 5, May 1951, and "A Turbulent Flame Theory Derived from Experiments," by B. Karlovitz, Selected Combustion Problems, AGARD, Butterworths Scientific Publications, 1954.

7 "Combustion in Turbulent Flames," by Th. von Kármán, Fourth Symposium on Combustion, 1953, p. 924.

8 "Propagation of Turbulent Flames," by A. C. Scurlock and J. H. Grover, Project SQUID Contract NOnr-485(01), 1952, Fourth Symposium on Combustion, 1953.

9 "The Burning Velocity of Turbulent Flames," by Wohl, Shore, von Rosenberg, and Weil, Project SQUID Contract N6-ori-105, Fourth Symposium on Combustion, 1953, p. 620.

10 "The Physical Structure of Turbulent Flames," by M. Summerfield, S. H. Reiter, V. Kebely, and R. W. Mascolo, Jet Propulsion, vol. 24, July-August 1954, pp. 254–255.

11 "Turbulence and Flame Propagation in Pre-Mixed Gases," by D. B. Leason, *Fuel*, vol. 30, October 1951.

12 "Auxiliary Equipment and Techniques for Adopting the Constant-Temperature Hot-Wire Anemometer to Specific Problems in Airflow Measurements," by J. C. Laurence and L. G. Landes, *NACA TN* 2843, November 1952.

13 "Combustion, Flames and Explosion of Gases," by B. Lewis and G. Von Elbe, Academic Press, New York, 1951.

14 "A Review of the Statistical Theory of Turbulence," by H. L. Dryden, *Quarterly J. of Applied Mathematics*, vol. 1, 1943.

15 "Effect of Turbulence in Wind Tunnel Measurements," by H. L. Dryden and A. M. Kuethe, *NACA Report* 342, 1929.

16 "Measurements of Turbulence Level Behind a Set of Square Mesh Grids and Correlation with Grid Pressure Loss," by L. Davis, Progress Report no. 3-22, Jet Propulsion Laboratory, California Institute of Technology, November 1950.

17 "Effect of Initial Mixture Temperature on Flame Speed of Methane-Air, Propane-Air and Ethylene-Air Mixtures," by G. L. Dugger, *NACA Report* 1061, 1952.

18 "Heat Transmission," by W. H. McAdams, McGraw-Hill, Book Co., Inc., New York, 1942, pp. 65–67, 83.

19 "Explosion and Combustion Processes in Gases," by W. Jost, McGraw-Hill Book Co., Inc., New York, 1946, p. 370.

20 "An Evaluation of the Soap-Bubble Method for Burning Velocity Measurements Using Ethylene-Oxygen-Nitrogen and Methane-Oxygen-Nitrogen Mixtures," by Dorothy M. Simon and Edgar L. Wong, *NACA TN* 3106, 1954.

21 "Diffusion by Continuous Movements," by G. I. Taylor, *Proc. London Math. Soc.*, series 2, vol. 20, p. 196.

22. "Measurements of Intensity and Scale of Wind Tunnel Turbulence and Their Relation to the Critical Reynolds Number of Spheres," by Dryden, Schubauer, Mock, and Skramstad, *NACA Report* no. 581, 1937.

23 "Some Recent Researches in Turbulence," by J. Kampé de Fériét, Fifth International Congress for Applied Mechanics, 1938, p. 354.

August 1 is deadline for Student Award entries

Latest date for submission of entries in the ARS Student Award competition is August 1. Papers in the general field of rocket and jet propulsion are invited. There are no special requirements as to length, form, or content. The award, a bronze medal, will be presented at the Annual Convention in Chicago, November 16.

Entries should be submitted to

Robert C. Truax
Chairman, ARS Awards Committee
2924 N. Oxford Street
Arlington, Va.

The Effect of an Opposing Jet on Flame Stability

ALLAN SCHAFFER[1] **and ALI BULENT CAMBEL**[2]

Gas Dynamics Laboratory, Northwestern University, Evanston, Ill.

Past investigations of flame stabilization in high velocity combustion have dealt primarily with the effects of physical flameholders such as bluff bodies. In this paper a different technique of stabilization consisting of an opposing gaseous jet rather than a bluff physical body is proposed. The performance of this system is described as a possible research tool and brief mention is made of its possible applications to aircraft. Blowoff data are presented for several conditions and configurations. Direct and schlieren photographs of the flames are included and an attempt is made to interpret the mechanism of the stabilization of the flame.

Introduction

In high-velocity turbulent combustion of air-fuel mixtures, a flame cannot be anchored in a flow chamber unless some type of flameholder is employed. Physical flameholders in the form of bluff bodies of various shapes are commonly employed.

There has been much effort to formulate a theory as to why a flame attaches itself behind a bluff body. The problem is complicated by the interaction of the effects of fluid dynamics, heat transfer, and diffusion of active species. The question as to which of these transport phenomena predominates is of great importance in the scientific field.

Existing hypotheses explain stabilization in terms of a zone of recirculation in which heat and active species are transported from the burned gases to the incipient region of the flame. Although this explanation appears to be valid, details of the mechanism are lacking because it has been difficult to control the variables involved.

In an attempt to gain perspective on the problem, a different technique of flame stabilization is described in this paper. (For comparison with other methods of stabilizing flames in high-speed flow, the reader's attention is directed to references 1, 2, and 3 at the end of the paper.) The proposed approach consists of stabilizing the flame by the use of an opposing gaseous jet, rather than by the presence of a physical holder.[3] Quantitative blowoff data are presented, and the combustion process is observed by direct and schlieren photography. Analysis of the mechanism of stabilization is in agreement with the recirculation hypothesis.

This paper is a preliminary report of investigations in progress at the Gas Dynamics Laboratory, Department of Mechanical Engineering, Northwestern University.

Apparatus

The apparatus which was used in the experimentation described in this paper is shown in Figs. 1 and 2. As may be seen in these figures, the apparatus consists of a mixing chamber, a Vycor test section, and an opposing jet tube as well as control, measuring, and ignition devices. Instrumentation was provided for determining the velocity of unburned mixture, the fuel-air ratio, and the mass rate of flow of jet media. The quantitative data were obtained using a cylindrical Vycor test section having 1.77-in. ID. However, for certain schlieren photographs a rectangular test section 9 in. long, $2^1/_2$ in. high, and 1 in. wide, having Vycor sidewalls, was employed. In both test sections the stabilizing jet was introduced along the axis of the main flow (but in the opposite direction) through an 18-in. long, $^1/_8$-in. stainless-steel tube having an ID of about $^1/_{16}$ in. A conical-shaped physical flameholder, which was used in additional tests for purposes of comparison, was anchored from the upstream side. It had a $^3/_8$-in. base and a 60-deg apex angle. In all quantitative tests discussed here the flames originated 9 in. from the open end of the Vycor tube. The fuel employed was commercial propane. The unburned mixture was premixed but not preheated.

Fig. 1 Schematic view of apparatus

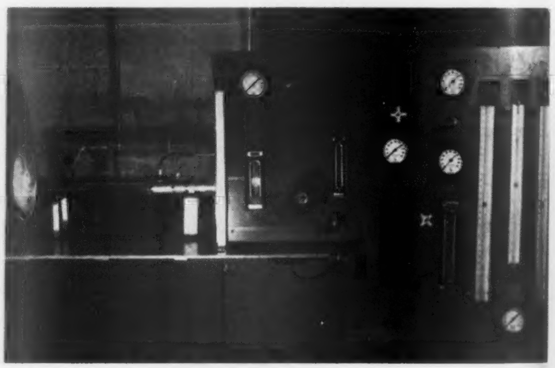

Fig. 2 External view of apparatus

Presented at the Ninth Annual Convention of the American Rocket Society, New York, N. Y., November 30, 1954.

[1] Research Fellow, General Motors Company. Stud. Mem. ARS.

[2] Associate Professor of Mechanical Engineering. Mem. ARS.

[3] At the time of checking proofs of this paper, the authors encountered a report entitled "Flame Stabilization in a Hot Gas Stream by the Upstream Blast Injection of Kerosene Fuel," by N. Golitzine, *National Aeron. Establ. Lab. Rep.* 102 (Canada), May 1954.

Procedure

The experimental study consisted of two parts: first, a quantitative study in which blowout data were obtained for opposing jets, for the $^{3}/_{8}$-in. physical flameholder, and for no flameholder; second, a qualitative study consisting of direct and schlieren photographs of confined and unconfined flames.

Blowout of a stabilized flame was achieved, in effect, by making the supply mixture either too rich or too lean. A blowout point could be obtained by setting the air flow to a desired value and varying the fuel flow, or by setting the fuel flow and varying the air flow. Although both methods were used to check points, it was less tedious to obtain data by varying the fuel flow, since changes in the air-control valve were more likely to result in surges. At any blowout point, instantaneous readings were taken to enable computation of the approach velocity and of the fuel-air ratio. For the quantitative tests employing the opposing jet, three jet media were studied, namely, air, oxygen, and nitrogen. In all quantitative tests the jet supply pressure was held constant at 100 psig and only one size jet tube was employed.

Operating Characteristics

Direct photographs of flames stabilized by the physical holder and by the air jet are shown in Figs. 3 and 4, respectively. In these particular pictures the approach velocity of the unburned gas was 140 fps. In Fig. 4 it is observed that the flame originates about 2 in. in front of the tip of the metallic jet tube, and therefore it may be concluded that the flame is stabilized by the gaseous jet itself rather than by any physical body. Furthermore, it is seen that the flame length necessary to cover the cross section of the Vycor tube is considerably less in the case of the air jet than in the case of the physical holder.

Qualitative experiments indicated that the value of the jet pressure was not critical. However, the flame did recede

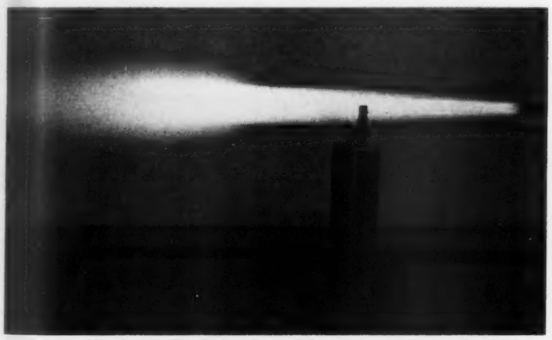

Fig. 3 Photograph of flame anchored on a conical holder

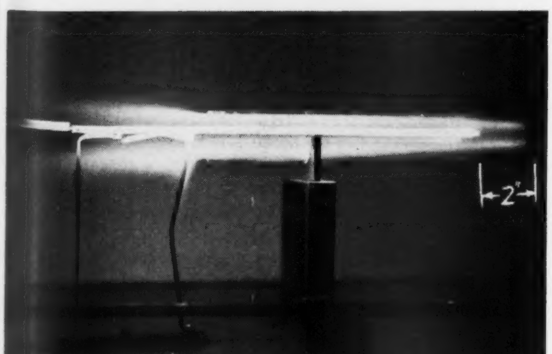

Fig. 4 Photograph of flame stabilized by an opposing air jet when velocity of mixture is 140 fps

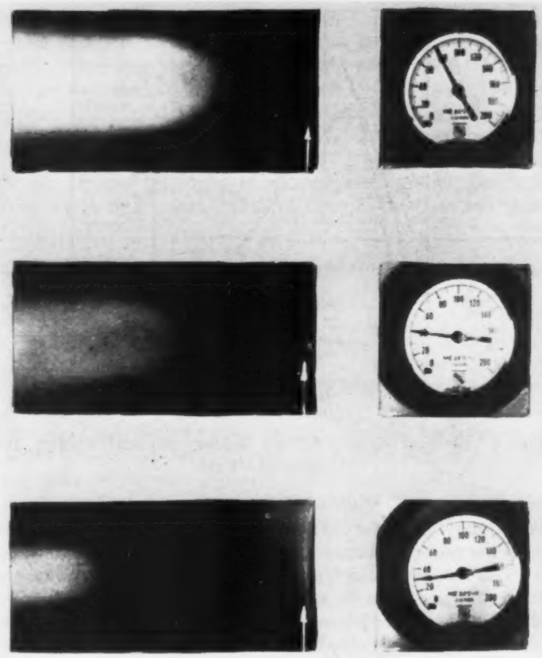

Fig. 5 Effect of decreasing jet supply pressure. Top: 80 psig; middle: 40 psig; bottom: 30 psig. Velocity of mixture is 140 fps

with appreciable decreases in pressure and, finally, there was some minimum pressure below which the opposing jet was ineffective as a stabilizer. In Fig. 5 this sequence of events is shown when the velocity of the unburned mixture was maintained at 140 fps. The photographs were taken at jet pressures of 80, 40, and 30 psig, as shown on the gages. The arrow to the right of the flame points out the reference mark on the circumference of the glass. Blowout in this series of tests occurred at 26 psig. It was observed that, in general, raising the velocity of the unburned mixture tended to shrink the flame for any particular jet pressure. This phenomenon might indicate that higher velocities are possible with an air jet simply by increasing the jet pressure, and thus the air jet shows potentialities as a flameholder which can be adjusted for optimum conditions during flight. Another advantage of the air jet in practical applications will be the simulation of a removable flameholder, thus presenting the possibility of eliminating the undesirable pressure drop associated with a physical flameholder when the afterburner is not in use.

Generally, a flame could be anchored initially more easily with the air jet than with the physical holder. On the other hand, it was found that, as a rule, richer mixtures were needed for this anchoring process with the air jet. These richer mixtures often resulted in a more explosive ignition. During operation, approach velocities could be raised more readily with the opposing jet than with the physical holder. This flexibility is due to the increased range of operation of the air jet, a characteristic which will be discussed in some detail later. Furthermore, the physical holder was much more sensitive to rich blowout than was the air jet, as will be shown by the performance curves.

Performance

Curves of blowout velocity vs. equivalence ratio for the air jet, for the physical holder, and for no flameholder are shown in Fig. 6. (The equivalence ratio is defined as the actual fuel-air ratio divided by the stoichiometric fuel-air ratio.) In Fig. 6 it may be seen that for any equivalence ratio a higher velocity

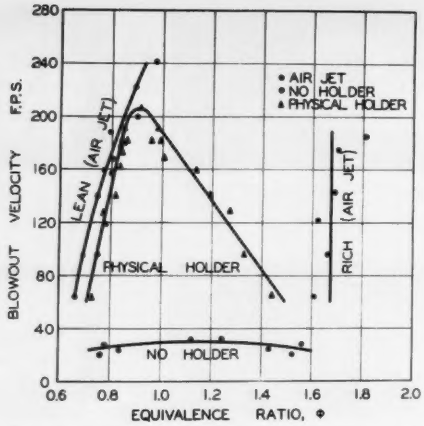

Fig. 6 Blowout curves for no holder, physical holder, and opposing air jet

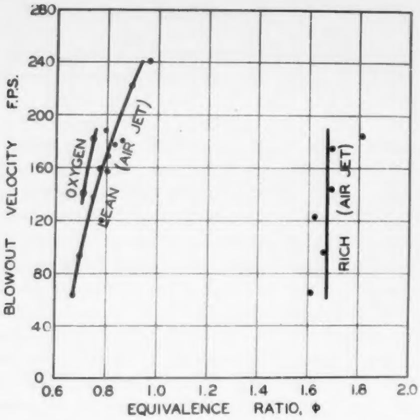

Fig. 7 Blowout curves for opposing jet using air and oxygen

is attained with the air jet than with the physical holder. Also the range of operation of the air jet is wider; that is, for a given velocity the rich and the lean limits of the equivalence ratio show a greater span. On the lean side the air jet curve lies slightly to the left of the curve for the physical holder, whereas on the rich side it is far to the right.

In these experiments the maximum velocity attained with the air jet was 241 fps compared to 207 fps for the physical holder and 32 fps for no flameholder. It should be noted that in the figure complete curves for the physical holder and for no flameholder are shown, while for the air jet only parts of the curve are given. The peak of the air jet curve could not be attained because the air supply was limited, but it is likely that values of velocity considerably greater than 241 fps can be attained with expanded facilities. The peak of the curve for the physical holder occurs on the lean side, whereas it appears that the peak of the air jet curve, if it were complete, would fall on the rich side. This shifting of the air jet curve toward the right is believed to be due to the dilution of a "critical" zone in the flame by the jet media, as will be explained in the next section.

The Mechanism of Stabilization

It is suggested that there exists in the flame a small critical zone and that conditions in this zone determine the stabilization. With a physical holder this critical zone occurs in the shedding boundary, or "ears," and is made up of unburned and recirculated gases. With an opposing jet the critical zone occurs at the nose of the flame and consists of unburned gases, recirculated gases, and the jet gas.

Recirculation occurs in a jet-stabilized flame due to entrainment of the burned gases along the boundary of the free jet. The performance curves indicate that, for the flameholders tested, the recirculation is greater for the air jet than for the physical holder. This would account for the greater range of operation and the higher velocity at any equivalence ratio yielded by the air jet. The same effect might be produced by employing a larger physical holder.

The shifting of the air jet curve to the right can be explained by considering the effect of jet media on the critical zone. For stabilization with an air jet, this critical zone is probably diluted by the jet so that it may be considerably leaner than the approaching mixture. Thus the recorded equivalence ratio is probably much higher than the equivalence ratio in the critical zone. If blowout is determined by conditions in the critical zone, the result should be a shifting to the right of the air jet curve as compared to the curve for the physical holder. The phenomenon is evident for the blowoff curves in Fig. 6.

The introduction of gases other than air in the opposing jet appears to verify the idea of a critical zone, at least for stabilization with a jet. The mass flow through the jet had a maximum of 1.6% of the primary air mass flow but in most cases was less than 1%. The results obtained with air and oxygen are shown in Fig. 7.

Because of the high jet velocities it might be suspected that the flow pattern ahead of the jet would be considerably altered but that the chemistry of the stabilizing area would be unchanged because of the apparently insignificant relative mass flow through the jet. However, when nitrogen was used as a medium in the jet it was impossible to stabilize the flame, although it was possible to ignite the mixture as before. Since the flow patterns for the air jet and for the nitrogen jet can be assumed to be the same, it follows that the 1 per cent nitrogen so diluted the critical zone that stabilization became impossible. Furthermore, it follows that the critical zone must occur in the part of the flame upstream from the end of the jet tube in a region where the concentration of the jet is significant. In view of this apparent importance of the composition of the critical zone, it is conceivable that the blowout curve for an air jet may be translated to the left by introducing a small quantity of fuel into the jet air, thus enriching the critical zone.

In Fig. 7 two points on the lean side of the curve for an oxygen jet are shown. Oxygen stabilized flames appear to burn much hotter than air stabilized flames, and this fact probably accounts for the improved performance with the oxygen jet. It should be noted that no points on the rich side of the oxygen curve are given. Experiments for rich blowout with an oxygen jet were found to be beyond the limits of the apparatus.

Schlieren Photographs

Schlieren photographs of the flames studied in this paper were taken in a two-dimensional test section as well as outside of the Vycor tube used in the quantitative tests.

In Fig. 8 is seen the schlieren photograph of a flame stabilized by the air jet inside the two-dimensional section. The velocity of the unburned gas was 95 fps and the mixture was lean. The photograph indicates the existence of a recirculation zone immediately upstream from the tip of the jet tube. The image of the flame has the shape of the letter U placed on its side. In all schlieren photographs of a flame stabilized by an air jet this U-shaped region of intense density gradient is seen. It is apparently a flame front between the unburned gases and the recirculation zone and is probably analogous to the "ears" seen in photographs of flames stabilized by physical holders. Furthermore, the photographs indicate a region of intense burning just at the upstream tip of the U.

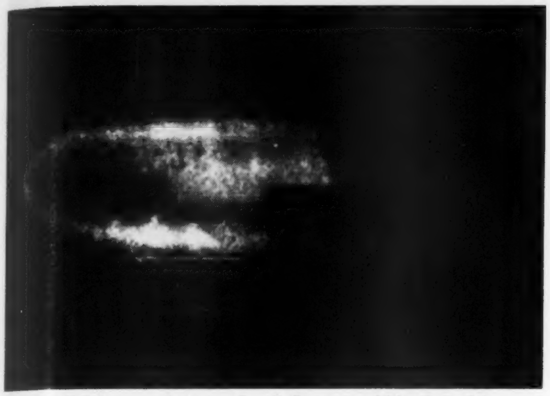

Fig. 8 **Schlieren photograph of flame stabilized inside two-dimensional test section by opposing air jet. Mixture velocity is 95 fps**

It has already been suggested that this region is the critical zone.

It should be mentioned in all fairness that while interpreting flame structure between glass walls, optical factors may be very misleading. Because of the greater sensitivity of the refractive index of the glass in comparison with that of the gas, deflections of the light in the Vycor plates predominate. This difficulty was obviated superficially by stabilizing flames outside the test section, and these unconfined flames

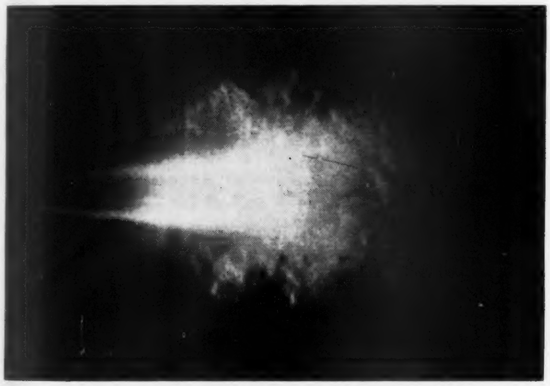

Fig. 9 **Schlieren photograph of flame stabilized outside tube by conical flameholder**

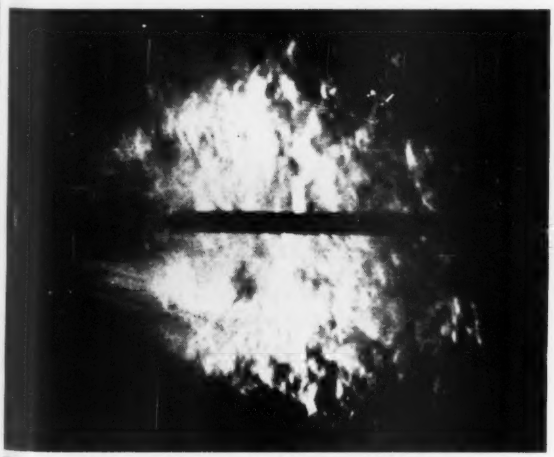

Fig. 10 **Schlieren photograph of flame stabilized outside tube by an opposing air jet**

are shown in Figs. 9 and 10. In both Fig. 9 for the physical holder and Fig. 10 for the air jet may be seen recirculation zones. The zone for the air jet has a larger area. It is of interest to observe that the flame front for the physical holder appears to be more vividly defined than the flame front for the air jet. As was noted for the confined flame, a bright spot is apparent at the upstream tip of the flame front for the air jet. It can be noted, in general, that the jet stabilized flame seems to be more turbulent throughout than the flame stabilized by the physical holder.

Conclusions

The conclusions of this paper may be summarized as follows:

1 A turbulent flame may be stabilized by means of an opposing gaseous jet.

2 For the flameholders tested, higher velocities and greater span of operation could be attained with the air jet than with the physical holder.

3 Operating characteristics of the air jet were superior in that, when it was employed, starting could be accomplished more easily and changes in the velocity of the approaching mixture could be effected more readily without blowout.

4 Certain phenomena observed with the stabilization of flames by gaseous jets are readily explained by the hypothesis that there exists in the flame a small critical zone.

5 A nitrogen jet will not stabilize a flame, probably because of dilution of the critical zone; but on the other hand, an oxygen jet will stabilize a flame considerably better than will an air jet.

6 Schlieren pictures indicate that a recirculation zone seems to exist for both the jet stabilized and the physically stabilized flames.

7 Indications are that to obtain a desirable flame geometry for stabilization the jet pressure should be increased with increasing approach velocity, although there is a wide range of jet pressure over which stabilization can be accomplished.

8 An opposing jet presents the possibility in practical applications to afterburners of eliminating the undesirable pressure drops associated with V-gutters when the afterburner is not in use.

Acknowledgments

The senior author (A. B. Cambel) expresses his gratitude to his former student and collaborator, Howard N. McManus, Jr., now of the University of Minnesota, for many stimulating discussions leading to the initiation of this study. This paper is based on the M.S. thesis of the junior author (A. Schaffer), the investigations being financed by Northwestern University through Faculty Research Project 103-53. The authors acknowledge the generous help extended them by the faculty, administration, and staff of the Technological Institute. The constructive criticisms by the members of the Gas Dynamics Laboratory, in particular the many suggestions of Edward Pohlmann, are greatly appreciated.

References

1 "The Variation of Flame Holding Characteristics of Open Vee-Gutters with Apex Angle," by Howard N. McManus, Jr., and Ali Bulent Cambel, Proc. Iowa Thermodynamics Symposium, 1953, pp. 84–93.

2 "Stabilisation des Flammes par des Obstacles," by M. Barrere and M. Mestre; Selected Combustion Problems, NATO-AGARD Symposium, 1954, pp. 426–446.

3 "Problems on Ramjet Combustion," by John P. Longwell; Fifth Symposium (International) on Combustion, August 30–September 3, 1954, The University of Pittsburgh.

Boundary Layer Flame Stabilization

ROBERT A. GROSS[1]

Fairchild Engine and Airplane Corporation, Farmingdale, N. Y.

An initial experimental investigation of boundary layer flame interaction has been carried out. Homogeneous propane-air gas mixtures with laminar free stream flow were studied. The flames were essentially two-dimensional and intersected a boundary layer flowing over a flat plate or airfoil shaped plate. Two distinct types of flame stabilization were found, depending upon the nature of the boundary layer. Experimental nonsteady phenomena of blowoff, flashback, and boundary layer flame oscillation are reported and discussed.

Introduction

THE interaction of fluid motions and chemical reactions is complicated. Because of the lack of physical understanding of the behavior of flames near walls, the author undertook an introductory experimental study of the role of the fluid boundary layer on flame stabilization. The reactants were homogeneous propane-air gas mixtures with a laminar free stream flow. Flames stabilized by thin flat plates and symmetrical airfoil shaped plates were studied. Particular attention was paid to the nature of the boundary layer. Two distinct types of flames stabilization were found. Nonsteady phenomena of blowoff, flashback, and boundary layer flame oscillation were studied.

Experimental Setup

To obtain a better fundamental understanding of flames in the neighborhood of a solid surface, it was decided to study the relatively simple condition of a flame stabilized or attached to a flat plate. The plate is aligned with the direction of the flow and the gas is a premixed homogeneous mixture of propane and air. This arrangement made possible the observation of the details of the flame in the fluid boundary layer. The experiments were carried out in the Harvard University Combustion Aerodynamics Tunnel. A picture of the tunnel test section showing a flat plate acting as a flameholder is shown in Fig. 1. The flat plate is above the primary nozzle from which flows the combustible mixture. Secondary air, whose velocity matches the primary jet mixture, surrounds the nozzle and keeps the jet stable. The stream velocity was varied from about 5 ft/sec to 100 ft/sec.

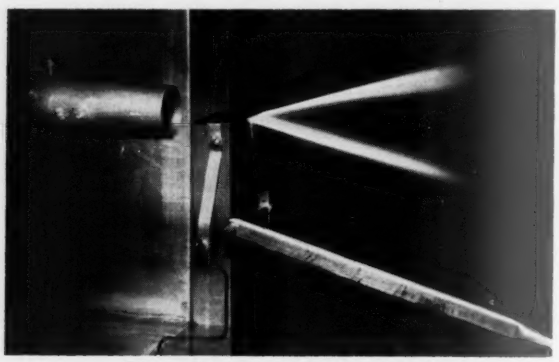

Fig. 1 Harvard combustion tunnel

An initial experimental survey showed that a thin flat plate would act as a flameholder but that, under certain operating conditions, thermal warping destroyed the desired aerodynamic characteristics. Somewhat thicker airfoil shaped plates were then used with satisfactory results. However, this introduced the effect of the curvature of the plate and the associated pressure gradients. Both types of plates (flat thin plates and airfoil shaped plates) have been studied. The treatment of the results will be divided into two sections: (a) steady state phenomena, i.e., the flame stays fixed relative to the plate; and (b) nonsteady phenomena, i.e., blowoff, flashback, oscillations, etc.

Steady State Phenomena

Aerodynamics in the Neighborhood of a Thin Flat Plate

The fluid flow in the immediate neighborhood of a surface, where viscous effects become important, is called the boundary layer flow. For a flat plate in longitudinal flow, an exact analytical solution to the laminar boundary layer equations exists for the case of zero pressure gradient in the free stream. This solution by Blasius (1)[2] has been confirmed by numerous experiments. The problem of heat transfer through the boundary layer is treated by Chapman and Rubesin (2). The flow in the neighborhood of the trailing edge of the flat plate (the wake) has been studied in detail by Goldstein (3). Therefore, there are solutions for the flow (without combustion) over the entire region of interest in the present study.

Thin flat plates made from stainless steel were studied as flameholders. Their thickness was 0.020 inch, their lengths (flow direction) were from $^3/_8$ to 3 inches, and their widths (across the tunnel nozzle) were all 3 inches.

The aerodynamics of the boundary layer flow was first examined experimentally without combustion. A thin flat plate was aligned over the tunnel nozzle and parallel to the flow so that no pressure gradient existed along the plate. A small flattened total head tube was attached to the tunnel traversing mechanism. The tube has a wall thickness of 0.009 inch and an opening 0.010 inch wide. This total head tube was used in traversing the boundary layer and wake immediately behind the plate. The readings were converted to velocities and compared with the solutions of Blasius and Goldstein. The experimental and analytical solutions are in reasonable agreement.

Types of Flame Holding

The flat plates were used as flameholders. Conditions were maintained so that the flame did not move down along the plate (and hence cause thermal warping).

From schlieren photographs it appears that the flame has stabilized itself in the boundary layer or in the wake just behind the plate. No eddy or boundary layer separation is evident nor did pitot tube boundary layer traverses ahead of the combustion region indicate very appreciable changes from the former cold laminar flow condition. This is physically possible since there exists in the boundary layer region very slowly moving fluid. The question naturally arises as to why the flame does not propagate down through the entire boundary layer, since this layer exists along the entire plate. The solid

Received November 2, 1954.

The work reported here was performed by the author at the Combustion Aerodynamics Laboratory, Harvard University, Cambridge, Mass.

[1] Research Engineer, Engine Division.

[2] Numbers in parentheses indicate References at end of paper.

surface acts as a heat sink and an absorber of active particles from the flame front and, therefore, acts as a type of flame-quenching device. The flame can only survive at a certain distance from the wall. Attempts to measure this "quenching" distance have been carried out by several investigators. There is considerable difference in the results so that this quenching distance is still in an unsatisfactory state of understanding. The quenching distance appears to be a combined aerodynamic, heat transfer, and chemical problem.

Let us define the flame as a very thin sheet in which the thermodynamic properties change rapidly and that this sheet has a unique rate of propagation, the flame speed. The flame may be thought of as attempting to find a position along the plate where the fluid velocity is equal to the flame speed and the distance from the plate is greater than or equal to the quenching distance. If no such position can be found, then the flame cannot stabilize itself in a laminar boundary layer. The quenching distance appears to decrease with increased plate temperature. The fact that the flame can stabilize itself along the plate when the boundary layer is laminar indicates that turbulent eddies are *not* a necessary condition for flame holding. In fact, a flame front penetrating a boundary layer should help prevent separation. Across a flame front there is a small pressure drop and an acceleration of the flow. This helps delay the occurrence of boundary layer separation. An enlargement of a schlieren photograph of boundary layer flame interaction is shown in Fig. 2. The bright line is the flame front and the way in which it penetrates the boundary layer is clearly seen.

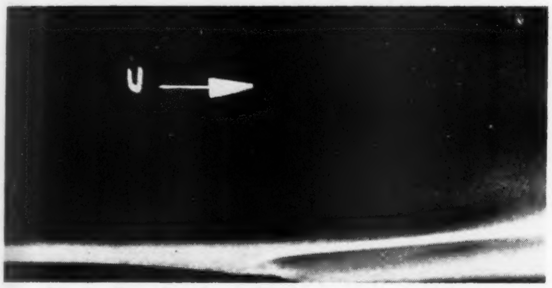

Fig. 2 Boundary layer flame interaction—schlieren

The streamlined airfoil plates were also tested as flame-holders. They are of the same width and length as the thin flat plates, but their thickness follows a symmetrical airfoil contour. All the airfoil plates have geometrically similar profiles and these can be seen in schlieren photographs; e.g., Fig. 3. With no combustion present, hot wire tests indicated a laminar boundary layer over the entire plate length. With combustion present, flow separation just behind the flame front is clearly seen in schlieren photographs such as Fig. 3.

Fig. 3 Airfoil plate as a flame holder—schlieren

This appears to be the result of the positive pressure gradient and the heating effect of the flame. The flame appears stabilized by this turbulent eddy. Hot gases remain in this eddy and feed active particles and thermal energy to the incoming stream. The blowoff characteristics of these two different types of flame-holding mechanism were found to be different.

Two classes of steady flame stabilization are thus found to exist: stabilization in a laminar boundary layer, and stabilization by an eddy.

Plate and Gas Temperature

Two of the airfoil plates were built with surface thermocouples located along the width and length of the plate. The surface temperatures were then measured as functions of the product gas temperature and the free stream velocity. The trailing edge temperature was of the order of 700 F, and a gradient existed to the leading edge which was of the order of 200 F.

Temperature gradients in the plate wake were found and are probably the result of the presence of unburnt boundary layer material. The existence of this unburnt boundary layer flow was found by making thermocouple temperature traverses in the wake of the flat plate. This was done in the center of the combustible core so that diffusion from the secondary tunnel air stream was negligible. For a distance up to one fourth of a plate length behind the plate, the temperatures were below the final temperature of the burnt gas elsewhere. The effect is apparently due to unburnt or partially burnt fluid flowing through the boundary layer, passing the flame front, and then burning further downstream.

The Schmidt Shadowgraph technique was used to determine the heat transfer coefficients between plate surface and free stream. These were found to be of the order of 2 to 10 Btu/hr ft^2 °R. An attempt to analytically compute the equilibrium flame position along the plate and the flame stand-off distance, using energy conservation for steady state conditions, was made. The model was too crude to permit better than order of magnitude values for the stand-off distance.

Nonsteady Phenomena

Blowoff

Experimental blowoff data for the flat plates and the airfoil plates were compiled. The blowoff correlation curve for the thin flat plates is shown in Fig. 4. For a fixed air-fuel ratio, the longer the plate length, the higher the free stream velocity necessary to cause blowoff. Curves of a similar shape have been found for blowoff from burner tubes. Since correlation was found for tubes by plotting the wall velocity gradient vs. the air-fuel ratio, the same technique was employed here. The velocity gradient was taken from the Blasius solution and is equivalent to the assumptions made by Lewis and von Elbe (5) in their tube blowoff correlation.

The blowoff gradients are about six times larger than those found by Lewis and von Elbe. This difference may be caused by the use of tunnel secondary air and the different aerodynamic situation in the present experiments. Just before blowoff, the flame would lift off the plate for distances up to one-quarter of an inch. It was thus semistabilized in the trailing wake. This condition was nearly always followed by blowoff. Occasional reseating of the flame occurred and this may be due to small velocity changes in the stream. The correlation becomes poor in the rich regions of air-fuel mixture. This is caused by the diffusive mixing between the primary and secondary jet. For very rich mixtures, the flame will actually leave the plate in the center section, but will "hang on" at the core edges. This is the result of a somewhat leaner mixture that exists in this outer section of the core because of diffusion.

The streamlined airfoil plates were tested for blowoff and the compiled data are shown in Fig. 5. The trend is quite different than that shown by the thin flat plates. The shorter the plate, the greater the free stream velocity necessary for blowoff. No simple correlation for blowoff was found. This is no doubt because of the complicated nature of the eddy which is thought to be the essential feature for flame stabilization in this case. No flames were found to stabilize in the

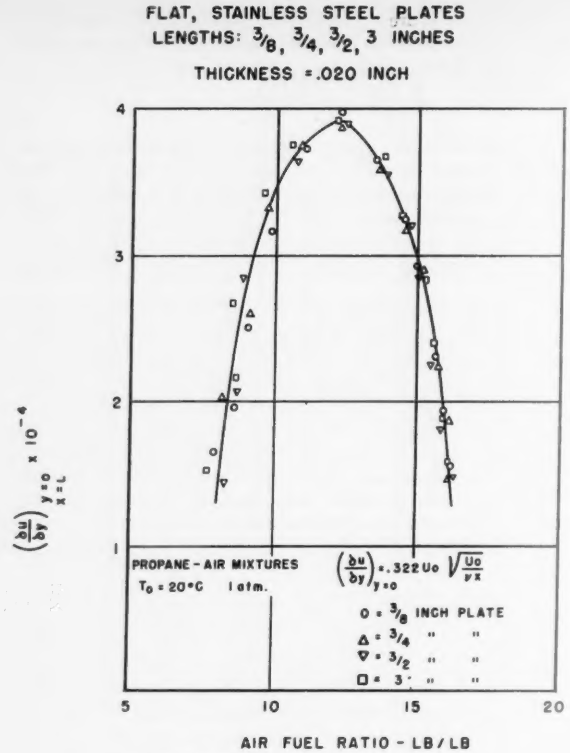

Fig. 4 Flat plate blowoff correlation

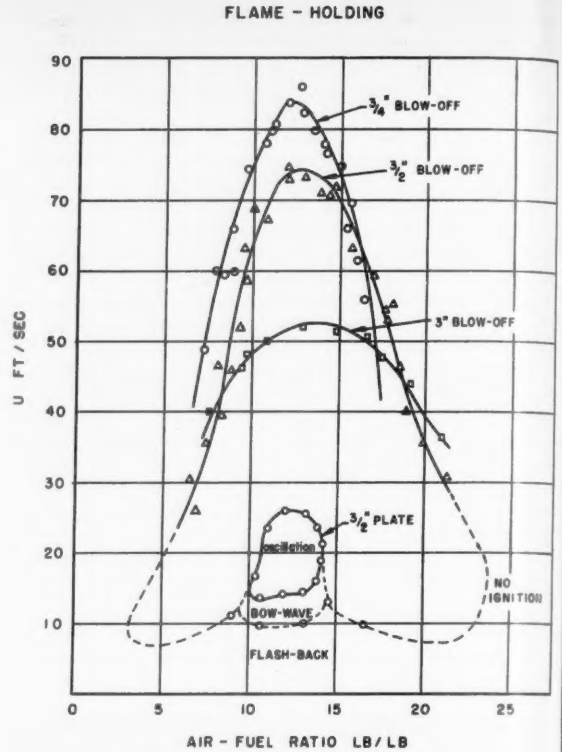

Fig. 5 Airfoil plate performance

wake of the trailing edge. The flames stabilized along the eddy and then blew directly off. There was no intermediate step, as in the case of flat thin plates.

An interesting result of the flat and streamlined plates that were studied was in the opposite characteristics of flame holding. Thus, for the flat plates, the longer the plates the higher the free stream velocity necessary for blowoff (at a fixed air-fuel ratio), while just the opposite trend is noted for the streamlined plates. Similar blowoff characteristics are found for plate lengths of about $1^1/_2$ inches.

Flashback and Bow Wave

Using the airfoil shaped plates, the flame could be allowed to move down along the plate side without causing serious thermal warping. Upon reaching the vertical section, flame oscillation took place. By keeping the air-fuel ratio the same and lowering the free stream velocity, the flame front could move all the way to the plate leading edge. A stable region exists there and the flame front forms a bow wave. The region in which the bow wave exists is shown in Fig. 5.

A slight decrease in the free stream velocity, when a bow wave existed, resulted in flashback. That is, the flame left the bow and flashed upstream and usually passed right down the primary laboratory tank, causing an explosion. This termined the experiment! The region for flashback is indicated in Fig. 5. Only a few points were obtained because of the strain of such experiments upon both the equipment and the personnel.

A bow wave exists as the result of a stagnation point along the leading edge of the airfoil. The flame can stabilize itself in this region. Flashback no doubt originates in the boundary layer coming off the primary tunnel nozzle.

Flame Oscillation

There is an operating condition where the flame front is unstable and oscillates along the plate length. The length of oscillation along the plate can be partially controlled by the free stream velocity. The oscillation region for the $1^1/_2$-inch plate is indicated in Fig. 5. The oscillations can be made to occur by using a slightly rich mixture and then lowering the free stream velocity. The flame front moves down along the plate until it reaches a vertical section. Oscillations then begin. They are rapid and appear as a blur to the eye. Their amplitude can be made to cover the entire plate.

To obtain some understanding of this interesting phenomenon, high-speed motion pictures were taken with a Fastax camera. These schlieren pictures indicate a periodic phenomenon. The frequency is about 25 ± 5 cps. The movement down the plate (about 15 fps) is about four times as fast as the movement toward the trailing edge. The phenomenon is clearly initiated in the boundary layer. The flame front appears to dart down through the boundary layer, dragging the rest of the flame with it. It then stops near the leading edge and washes back toward the trailing edge. Upon arriving somewhere along the rear section of the plate, the flame stops and again plunges down through the boundary layer for another cycle.

The plate temperature is important for the existence of the oscillation. A water-cooled plate was built. The oscillations were allowed to begin and then the water-cooling system was turned on. The oscillations rapidly stopped and the flame stabilized itself along the rear edge of the plate. An average plate temperature of about 600 F was sufficient for the oscillations to take place.

No adequate explanation yet exists for this phenomenon. Pressure fluctuations in the test section do not account for the oscillations since the tunnel test doors have been left open with no apparent change. The idea of the boundary layer periodically going turbulent may account for part of the phenomenon, but not for all of it. This appears to be an extremely complicated problem for which no very simple explanation is yet known.

(*Continued on page 293*)

Technical Notes

The Importance of Mixture Ratio Control for Large Rocket Vehicles

RUDOLF H. REICHEL[1]

Bell Aircraft Corporation, Buffalo, N. Y.

THE importance of adjustment procedures and automatic control for rocket power plants will increase in the future when more powerful rocket engines and larger rocket missiles are developed and optimum working conditions during the flight path are of determining influence.

On principle, the different methods as used within the power plant have in view the control of mixture ratio, thrust (1)[2], combustion stability (2), or a combination of them. For large rocket vehicles the control of the mixture ratio is of special importance. Until the present time, not much attention has been paid to the whole control problem.

Why mixture ratio control?

In order to obtain maximum missile performance by completely emptying the propellant tanks simultaneously. Herewith the full burning time can be realized and an increase of the total rocket mass at cutoff by a remainder of either fuel or oxidizer, is avoided.

By what can a predetermined mixture ratio be influenced?

1 By density variations of the propellants as a consequence of different temperatures. Let us consider some rocket propellant combinations, Fig. 1. Within a usual operational temperature range of the propellants between −40 F and +120 F, the characteristics of most fuels as well as oxidizers run approximately parallel. However, the slope of the characteristics of these two propellant groups is a different one. Therefore a change in propellant temperatures can lead to a noticeable deviation from the desired mixture ratio.

2 By incorrect propellant weight flow rates resulting from incorrect pump characteristics or production tolerances of the various components.

3 By the effect of the rocket acceleration on the propellant feed system.

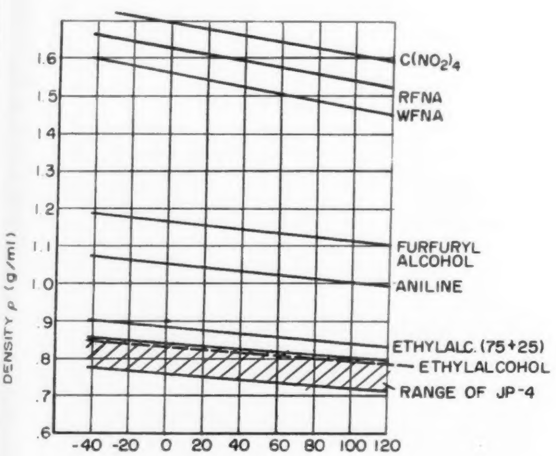

Fig. 1 Specific gravity of some typical rocket propellant components due to the temperature

How can control be performed?

1 By adjustment methods

(*a*) Calibration of the entire propellant feed system, Fig. 2. This method considers only one working condition, and cannot compensate for any variation of an assumed set value such as acceleration influence or changing temperature

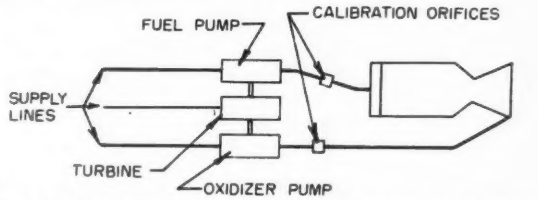

Fig. 2 Rocket engine adjustment by means of calibration orifices

(*b*) Special design of propellant pumps with such characteristics that the acceleration influence on the injection system will be diminished

(*c*) Special propellant tank arrangement. It can be seen that, by means of an alteration of the propellant tank installation height with respect to the injector and by means of an alteration of the tank configuration, it is possible to compensate for the acceleration influence and to keep constant the injection nozzle pressure in such a manner that almost a constant propellant consumption and a constant mixture ratio are guaranteed.[3] More details can be found in a paper which is to be published (3).

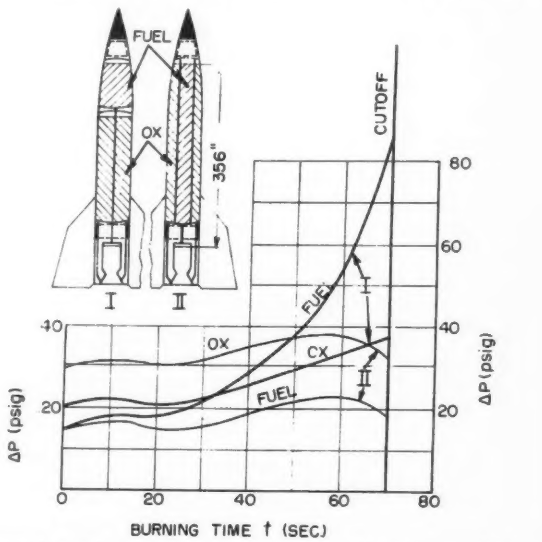

Fig. 3 Injection pressure augmentation ΔP due to the acceleration influence for two different tank arrangements

A very instructive example of such a compensating arrangement is given in Fig. 3. This example is only considered as a comparison without any consideration of a controlled turbine pump unit. Missile type I represents the conventional con-

Presented at the 9th ARS National Convention, New York, N. Y., Dec. 2, 1954.

[1] Rocket Development Engineer. Mem. ARS.

[2] Numbers in parentheses indicate References at end of paper.

[3] This concerns only the accelerated trajectory.

EDITOR'S NOTE: This section of JET PROPULSION is open to short manuscripts describing new developments or offering comments on papers previously published. Such manuscripts are published without editorial review, usually within two months of the date of receipt. Requirements as to style are the same as for regular contributions (see first page of this issue).

figuration with tanks one behind the other. The shape of the rocket is similar to the well-known V-2. Propellants are common jet fuel, and tetranitromethane $C(NO_2)_4$ as the oxidizer.[4] The disproportionate injection pressure variation ΔP due to the acceleration shows the corresponding curves I for oxidizer and fuel. Nevertheless, when a design with concentric propellant tanks is used corresponding to missile type II, an undesirable ΔP tendency can be compensated (see curves II). In this case the tanks are to be arranged in an optimum height with respect to the injector level.

This compensating tank arrangement considers only fixed values such as thrust and propellant density, and is not useful for controlling any disturbances.

2 By automatic control

We saw that a part of the influences which cause any alteration of the mixture ratio can be compensated by means of different adjustment methods. Nevertheless, in order to attain optimum conditions, automatic control can hardly be avoided if we want to solve this whole problem.

Taking the weight flow rate as a control basis, we compensate all possible influences automatically, such as alteration of propellant density, of ΔP, and of manufacturing tolerances. A corresponding control arrangement is shown in Fig. 4. Both of the propellant components are measured by flowmeters and then compared. When a deviation from the set ratio occurs, the control device effects an adjustment of the control valve, until this deviation disappears.

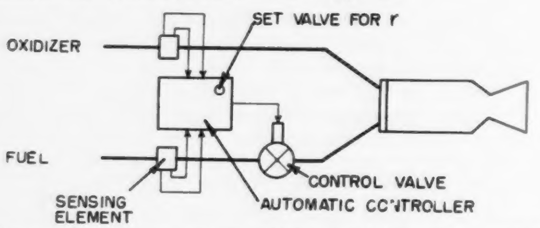

Fig. 4 Arrangement of an automatic mixture ratio control system

For our control purposes we can use continuous or discontinuous control systems similar to some methods already in use to solve industrial problems. It is possible to use devices as sensing elements which determine the propellant density, such as a throttle disk or a venturi.

The control accuracy which can be expected depends on the system used and the installation conditions. We can assume an over-all tolerance with respect to the mixture ratio set value of less than 1 per cent. This amount corresponds to technical requirements, as will be seen later.

Mixture ratio control for a large rocket vehicle

In order to demonstrate the importance of the mixture ratio control, we can take for comparison purposes the one-step long-range rocket corresponding to Fig. 3, type I. At first we assume a controlled mixture ratio; this means that all design parameters are to be maintained. Because the cutoff velocity v_e represents the performance criterion, we can write the basic equation

$$v_e = I_{sp} g \ln \frac{W_0}{W_e} - gt$$

when W_0 and W_e mean the initial and the end mass, respectively, and t means the burning time. For our comparison of performance we can assume a vertical drag-free flight. Thus the following values are given:

Initial weight, lb	53,600
Empty weight, lb	9,500
Mass ratio	5.65
Propellant weight, lb	44,100
Set value for mixture ratio	4.52
Combustion chamber pressure, psig	250
Thrust, lb	132,500
Specific impulse, sec	210
Cutoff velocity, ft/sec	9,460
Peak altitude, miles	303

Now we assume that there is no control arrangement, and no disturbance will be compensated. Under consideration of the foregoing equation we can see that three parameters change if the mixture ratio does not correspond to the set value, namely:

1 The specific impulse I_{sp}. The characteristics of some typical propellant combinations are shown in Fig. 5. The range of a ± 10 per cent mixture ratio deviation is plotted in by means of hatching. Each alteration of the set value means always a decrease of the specific impulse.

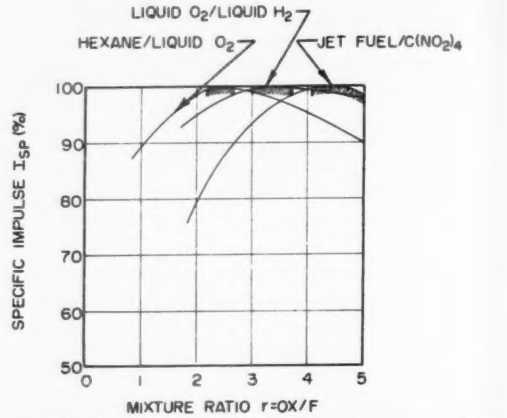

Fig. 5 Specific impulse I_{sp} vs. mixture ratio r for some propellant combinations, with P_c = 285 psig as parameter

2 The mass ratio W_0/W_e. The reason is that for any deviation from the correct mixture ratio (determined by design), a remainder of one propellant component will result, i.e., fuel or oxidizer. This causes an increase of the end mass of the rocket, and a decrease of the cutoff velocity.

3 The burning time, due to the remaining propellant.

For our purpose we consider the influence of a mixture ratio inaccuracy up to ± 10 per cent with respect to the set value as a consequence of change of propellant density, acceleration, and manufacturing tolerances. Thus the conditions as plotted in Fig. 6 result. It is seen that for an uncontrolled rocket the loss of performance represents a considerable amount, especially for the fuel rich combustion. With respect to the cutoff velocity we find a diminution of about 5 per cent if the mixture ratio is only 2 per cent fuel rich, which

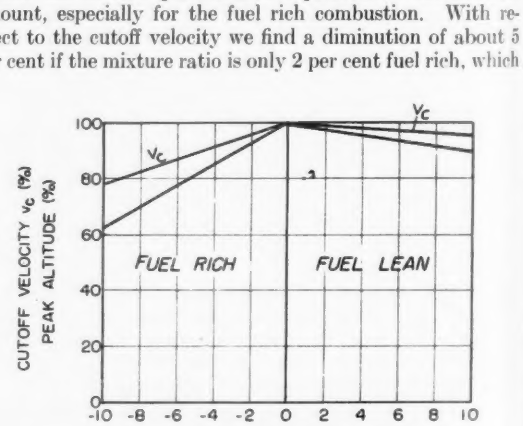

Fig. 6 Loss of cutoff velocity and peak altitude, respectively due to the inaccuracy of the mixture ratio

[4] This oxidizer has its melting point at 13 C. Nevertheless, it does not concern this special consideration.

corresponds to a loss of 8 per cent with respect to the peak altitude. For 5 per cent inaccuracy of the mixture ratio the loss values become about 11 per cent and 20 per cent, respectively.

In order to have a better idea with respect to practical values, we consider furthermore the acceleration influence on the propellant feed system. It can be found by calculation that the predetermined mixture ratio is altering from r = 4.52 to 4.9 under launching conditions, attaining r = 4.2 at cutoff. This corresponds to 9 per cent fuel lean and 7 per cent fuel rich, respectively. This statement gives only a rough idea because, for design purposes, the influence on the combustion chamber pressure as consequence of the altered propellant consumption would not be neglected.

The control of mixture ratio can be of special importance. For large rocket vehicles a very small alteration of the design parameters must be maintained in order to result in maximum flight performance. It does not make good sense only to expedite research and development for motor components and propellant systems in order to improve performance, if on the other hand the maintenance of a correct mixture ratio is not taken care of sufficiently.

References

1 "Throttling Thrust Chamber Control," by M. Meyer, *Journal of the American Rocket Society*, no. 85, 1951, pp. 68–73.

2 (*a*) "Stability of Flow in a Rocket Motor," by D. F. Gunder and D. R. Friant, *Trans. ASME*, vol. 17, 1950, pp. 327–333.

(*b*) "Aspects of Combustion Stability in Liquid Propellant Rocket Motors," by L. Crocco, *Journal of the American Rocket Society*, vol. 21, 1951, pp. 163–178; vol. 22, 1952, pp. 7–16.

(*c*) "Servo-Stabilization of Combustion in Rocket Motors," by H. S. Tsien, *Journal of the American Rocket Society*, vol. 22, 1952, pp. 256–262.

(*d*) "Servo-Stabilization of Low-Frequency Oscillations in a Liquid Bipropellant Rocket Motor," by F. E. Marble and D. W. Cox, Jr., *Journal of the American Rocket Society*, vol. 23, 1953, pp. 63–74.

(*e*) "Stability and Control of Liquid Propellant Rocket Systems," by Y. C. Lee, M. R. Gore, and C. C. Ross, *Journal of the American Rocket Society*, vol. 23, 1953, pp. 75–81.

(*f*) "Unconditional Stability of Low-Frequency Oscillations in Liquid Rockets," by Sin-I Cheng, *Journal of the American Rocket Society*, vol. 24, 1954, pp. 310–312.

3 "Adjustment and Automatic Control Possibilities for Rocket Power Plants," by R. H. Reichel, to be published.

Comment on "A Remotely Controlled Aerial Torpedo"

(attributed by this Journal to an "unknown author")

The inventor of the device described and pictured on pp. 173–174 of the April 1955 issue of Jet Propulsion is by no means unknown, as you say. What happened is that your contributor used a secondary source, namely, a German magazine published during the first World War, which, for obvious though temporary reasons, did not mention the inventor, who was a Frenchman. His name was René Lorin, and the original articles which were the source of the German condensation had been published from 1910 to 1912 in the magazine *l'Aérophile.* Most of these articles were later included in René Lorin's book, "L'Air et la Vitesse, Vues nouvelles sur l'Aviation," Paris, Librairie Aéronautique, 1919, with a preface by Georges Besançon.

Willy Ley
37–26–77th Street
Jackson Heights, N. Y.

Boundary Layer Flame Stabilization

(*Continued from page 290*)

Acknowledgments

The author would like to express his appreciation to the Office of Ordnance Research for making this work possible. Also, it is a pleasure to acknowledge many stimulating discussions with Prof. Howard W. Emmons.

References

1 "Grenzschichten in Flussigkeiten mit Kleiner Reibung," by H. Blasius, *Zeitschrift für Mathematik und Physik*, vol. 56, 1908, p. 1.

2 "Temperature and Velocity Profiles in the Compressible Laminar Boundary Layer with Arbitrary Distribution of Surface Temperature," by Chapman and Rubesin, *Journal of the Aeronautical Sciences*, vol. 16, September 1949, pp. 547–565.

3 "Concerning Some Solutions of the Boundary Layer Equations in Hydrodynamics," by S. Goldstein, *Proceedings of the Cambridge Philosophical Society*, vol. XXVI, part 1, January 1930, pp. 1–25.

4 "Schlierenaufnahmen des Temperaturfelds in der Nahe Warmeabgebender Koper," by E. Schmidt, *Forschungsarbeiten auf dem Gebiet des Ingenieurwesens*, no. 3, 1932, p. 181.

5 "Combustion Flames and Explosions of Gases," by Lewis and von Elbe, Academic Press, Inc., New York, 1951, pp. 571–578.

Meetings on Fluid and Applied Mechanics

Two 3-day meetings being held by other organizations have potential interest for ARS members.

The 1955 Heat Transfer and Fluid Mechanics Institute will meet on the Los Angeles campus of the University of California, June 23–25. Papers on shock waves, turbulence, boundary layer, combustion instability, flutter, and metal fluidity are included in the five sessions scheduled. Myron Tribus of the University of California, Los Angeles, is chairman of the meeting.

Taking place at Rensselaer Polytechnic Institute, Troy, N. Y., June 16–18, is the ASME National Applied Mechanics Conference. Seven sessions on the slate include papers on rotating beams, vibration of cylindrical and conical shells, boundary layer, thermal stress, stability of plain fluid sheets, convection flow, and aerodynamic interference of cascade blades in synchronized oscillation. Chairman of the Conference is R. H. Trathen of RPI.

Jet Propulsion News

Alfred J. Zaehringer, American Rocket Company, *Associate Editor*

Jet Aircraft, Engines

BRITAIN is building up its air strength by fitting its fighter squadrons with substantial numbers of Hawker Hunter (photo) jets which in 1953 set a 726 mph speed record. The radar-equipped Hunter is equipped with four 30-mm Aden guns. A major effort is also being made in long-range jet bombers which can deliver the H-bomb. The V-Bombers, Valiant (photo), Victor, and Vulcan are to form the backbone of this force. Other jet craft coming into production are the Gloster Javelin, all-weather delta craft, and the English Electric P-1 interceptor. Westland Aircraft has recently developed a jet thrust deflector which is used to increase the lift of jet aircraft. A jet stream can be directed downward by as much as 60 deg. In a mount in the middle of a Rolls Royce Nene turbojet, the stalling speed of a Gloster Meteor has been reduced by as much as 20 per cent. The Meteor is the first British plane to be fitted with jet deflectors. They permit the aircraft to take off and land in a confined space (photo). Although the use of the deflectors has recently been revealed, the plane has been flying successfully with them since last May.

British Information Services

Hawker Hunter

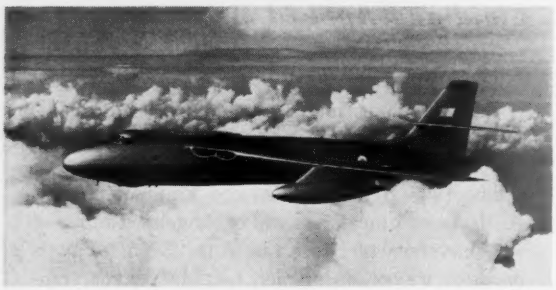

Vickers

Valiant jet bomber

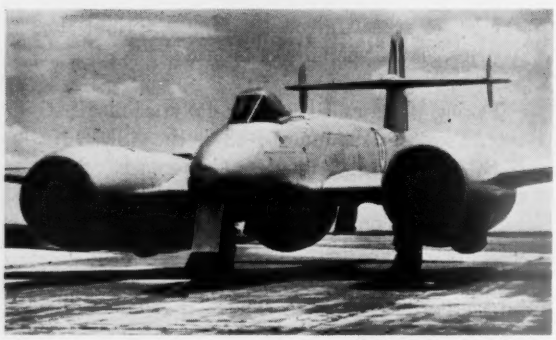

British Information Services

New jet has vertical thrust

- France is producing the jet-propelled SNCASO SO 1221 Djinn helicopter. The two-place 'copter is powered by a 240-hp Turbomeca Palouste turbojet which acts as a gas generator to supply power for the rotors.

- A new Soviet fighter, nicknamed Fresco, has been announced by our Navy Department. Fresco is a modified MiG-15, and is designed to provide increased altitude maneuverability by the use of a novel jagged wing planform and new tail section. Meanwhile, the MiG-17 is rapidly being placed into squadron service. Also shown in increasing numbers is the Il-39 ("Badger"), twin jet bomber in the B-47 class.

- High-power turbojets have been making recent news. The P&W J57 which is now rolling off the production lines has a thrust rating of 11,000 lb without afterburner. Tests of the P&W J75, delivering over 15,000 lb thrust are expected soon. Other U. S. engines in various stages of development are: Wright J67 of 15,000 lb thrust; GE J73 of 9000 lb thrust; Allison J71 of 10,000 lb thrust. The British Bristol Olympus engine—rated at 11,000 lb thrust (without afterburner)—has been service-approved after 150 hr of tests. The engine, known as the 101, weighs 3650 lb and employs a twin-spool compressor (photo). The French Snecma Vulcain turbojet

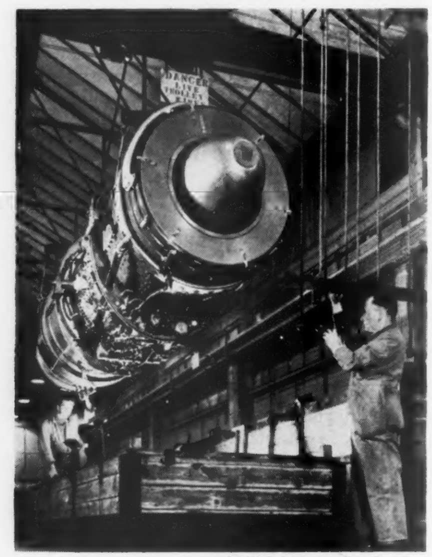

British Information Services

Olympus 101 turbojet

EDITOR'S NOTE: The information reported in this Section has been selected from approved news releases originating with the Department of Defense, private manufacturers, universities, etc., and from published news accounts in journals and newspapers. The reports are considered generally reliable, although no attempt has been made to verify them in detail.

has been tested at 13,200 lb thrust. Meanwhile, the U.S.S.R. revealed the existence of its four-jet Tu-37 "Bison" bomber, in the B-52 class, which is powered by axial flow turbojets in the 15,000 lb thrust class.

• At the other end of the propulsion spectrum, small turbojets have also been making news. Two small J44 turbojets have been mounted as integral wingtip installations on the C-123 Avitruc transport for ATO. Weighing only 330 lb each and delivering 1000 lb thrust each, the motors are sealed off to reduce drag during normal flight. Two of the J44's were recently used by Bell in their lightweight VTO aircraft. In this novel craft, the engines can be rotated 90 degrees to provide vertical thrust for take-off and sustaining thrust for horizontal flight. Meanwhile, the J44-R-20 engine, boasting higher thrust and lower fuel consumption, is being delivered for use in the Ryan Firebee target drone. An entirely new, small-size, lightweight turbojet engine for target drones and pilotless aircraft is to be produced for U.S.A.F. by Fairchild and General Electric.

• The Allison Division of General Motors has announced a new turboprop engine, the 501-D10 for use on commercial

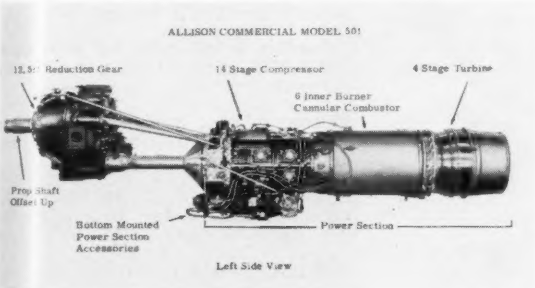

Allison

Allison turboprop

aircraft (photo). The engine is a version of the T56 engine being used on the Lockheed C-130 U.S.A.F. transport. Model 501 develops 3750 shp. Weight is 1610 lb. Fuel consumption (sea level static) is 0.54 lb fuel/hp/hr. Dimensions: 145 in. long; 27 in. wide; 6 sq. ft frontal area. In typical four engine installations, aircraft speeds of up to 450 mph are anticipated.

Materials, Instruments

A NEW technique has been employed by Marquardt engineers in producing ductile welds on titanium sheet. A fusion weld eliminates the need for weld bead grindings in the fabrication of afterburner shrouds for turbojet engines.

• Considerable progress is being made in the use of molybdenum for high temperature applications. Tests have been made with a coating of aluminum-chromium alloy on moly and have shown good thermal shock characteristics at 1800 F for 500 hr. Several companies are now rolling moly and two companies are spinning it. Big problem is still welding, because of low ductility at room temperatures.

• The first synthetic diamonds were produced by General Electric in a process involving carbon subjected to tremendous heat and pressure. The chamber in which the diamonds were made can maintain temperatures of 5000 F and pressures of 1.5 million psi. The object of the program is to prepare industrial diamonds.

• Sir Arnold Hall, Director of Britain's Royal Aircraft Establishment at Farnborough, visualizes extensive use of glass-reinforced plastic for future aircraft flying at speeds of 1300 mph and at altitudes of 45–50 thousand feet. The plastics, cheaper and lighter than aluminum, are described as "singularly free" from metal fatigue. Metal fatigue is reported as being responsible for the jet Comet crashes.

• Missile trajectories may now be traced at night by a special recording camera being produced by Gordon Enterprises of North Hollywood, Calif. Designated as the 22-GE, an f2.5 Aero Ektar 12-in. lens is used. Remote operation is possible.

• The Bristol Engineering Corp., Bristol, Pa., has developed an explosive gas accumulation detector. The electronic detector can be set at 10–100 per cent of the lower explosion limit and can respond in less than 1/2 sec.

• A complete strand burning installation is being offered to the solid propellant industry by Atlantic Research Corp., Alexandria, Va. Included are a bomb, timer, control panel, and pressure gages.

Facilities

TEST facilities at Edwards AFB, Calif., are being expanded in a $2.2 million construction program. Convair and Douglas will share the new hangars, shops, and offices.

• Nitroparaffins are to be produced at a new Commercial Solvents Corp. plant at Sterlington, La. The $5 million plant will produce volume quantities of nitromethane, nitroethane, 1-nitropropane, 2-nitropropane, and nitrobutane.

• An Armament Department is being established by Aerojet-General at its Sacramento, Calif., facility. The new addition will allow a complete carry-through from basic evaluation through mass production.

• The NACA is completing its $32.85 million supersonic wind tunnel at Cleveland, Ohio. Speeds of Mach 3.5 are possible in the test section which measures 10 ft × 10 ft. An interesting feature of the blowdown tunnel is the air-drying unit (photo). Filtered air is brought into contact with huge beds of activated alumina. Gas heaters of 256 million Btu per hr capacity then heat the air to 350 F. A butterfly valve 15 ft in diameter and weighing 38 tons controls the air flow.

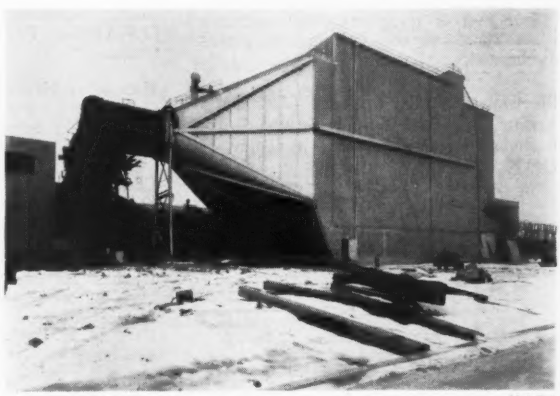

NACA

Six-story NACA air dryer for supersonic wind tunnel

• Steady speeds of Mach 15 have become routine in testing at the hypersonic research program at Forrestal Research Center's Gas Dynamics Laboratory. Plans now call for testing at Mach 20. Present techniques employ helium as the working fluid. Conditions can be simulated from sea level to altitudes of 150,000 ft and speeds of 700–17,000 mph.

New Patents

George F. McLaughlin, *Contributor*

Liquid propellant rocket (2,700,337). James M. Cumming, San Marino, Calif.

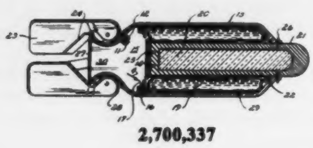

2,700,337

Retractable rocket igniter (2,674,088). Walther Riedel and Lewis J. Wessels, Los Angeles, Calif., assignors to North American Aviation, Inc.

Combustion apparatus for burning particles of solid or heavy liquid fuel in a fast moving stream (2,680,951). Ernest F. Winter, Hove and Hans Havemann, Working, England, assignors to Power Jets (Research and Development) Ltd.

A combustion chamber with two opposed coaxial side walls, one formed with a central inlet for part of the stream, and the other with a central outlet, means for admitting a further part of the stream into the chamber with a swirling motion, and means for causing ignited particles of fuel to be carried outward from a stable zone of combustion and into the peripheral part of the combustion chamber.

Tangential sheet cooling of internal combustion chambers (2,689,453). Robert H. Goddard, deceased, Esther C. Goddard, executrix, Worcester, Mass., assignor of one-half to The Daniel and Florence Guggenheim Foundation.

Gas turbine power plant (2,679,726). Veon I. Moncrieff, West Hartford, Conn., assignor to United Aircraft Corp.

A gas-turbine-driven compressor for supplying to the combustion chamber air in substantial excess over that required for driving the turbine, and an auxiliary combustion chamber connected to the discharge end of the compressor and into which part of the compressed air is discharged.

Electric control system (2,700,356). Arthur V. Hughes and Lawrence B. Rademacher, Sharon, Pa., assignors to U.S.Navy.

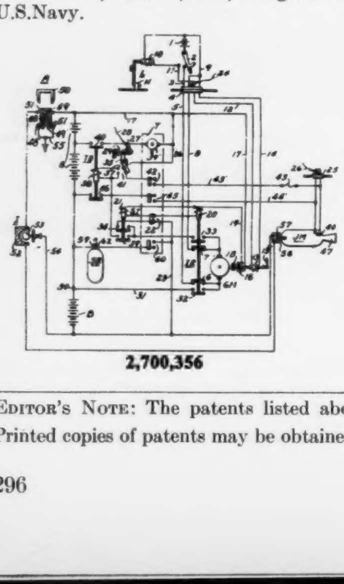

2,700,356

Rocket reactant feed system (2,687,168). Robert P. Haviland, Scotia, N. Y., assignor to General Electric Co.

A rocket with reservoirs for liquid fuel and oxidizer reactants, and pumps in series with conduits from the reservoirs to the rocket motor, and a system arranged so that when the liquid level in one reservoir is below that of the other, an electrical bridge is unbalanced, relaying a signal to an electrical motor which actuates a valve to trim the reservoir levels.

Combined rocket and jet propulsion (2,676,457). Fred S. Kramer, Prospect Park, Pa., assignor to the U. S. Navy.

High-pressure ratio gas turbine of the dual set type (2,704,434). Heinz E. Schmitt, Dayton, Ohio, assignor to U. S. Air Force.

Manual and automatic fuel feed control for gas turbines (2,700,276). Wilfred S. Bobier, Jr., Grosse Pointe Woods, Mich., assignor to George M. Holley and Earl Holley.

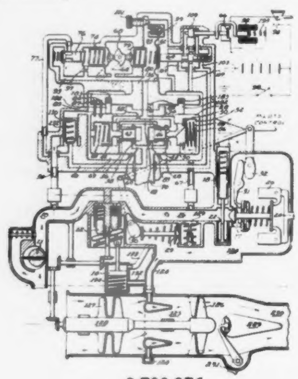

2,700,276

Multiple combustion chamber jet turbine (2,675,675). Paul R. Haueter, Navarre, Ohio.

Helicopter blade jet propulsion chamber (2,679,295). Jas. R. Parsons, Ballston Spa, N. Y., assignor to General Electric Co.

Control for gas turbine power plant (2,706,383). John W. Jacobson, Schenectady, N. Y., assignor to General Electric Co.

Devices for confinement and release of high velocity hot gases (2,706,382). Ian M. Logan and John P. Swentzel, Niagara Falls, N. Y., assignors to the Carborundum Co.

Landing bumper for decelerating the fall of an object (2,706,605). Maurice Rose and Donald M. Lawrence, Wood-Ridge, N. J., assignors to the U.S.A.F.

Pilotless aircraft design (172,170). I. Nevin Palley, Lancaster, Calif., assignor to Chance Vought Aircraft, Inc.

Fuel control apparatus for turbojet engines (2,700,275). Milton E. Chandler and Trent H. Holmes, Middletown, Conn., assignors to Niles-Bement-Pond Co.

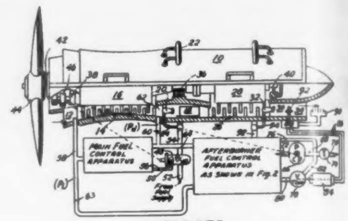

2,700,275

Means for controlling temperature of exhaust gases of jet engines (2,681,547). Robert J. MacDonald, Hicksville, N. Y., assignor to Republic Aviation Corp.

Reversible thrust nozzle for jet engines (2,681,548). Peter G. Kappus, Munich, Germany.

Exhaust effusion turbine jet propulsion unit (2,679,725). Devendra N. Sharma, London, Eng.

Explosive composition (2,704,706). Ludwig F. Andrieth, assignor to Olin Mathieson Chemical Corp.

Combination airplane and helicopter design (174,254). Chas. J. Fletcher, Franklin, N. J.

Missile (2,686,473). Wm. F. Vogel, Cross River, N. Y.

Long range timing apparatus (2,687,173). Arne Loft, Scotia, N. Y., assignor to General Electric Co.

Motor-driven cumulative and interval timers for signaling the end of preset time intervals, and means for initiating the operation cycle of a time delay relay each time the timer reaches the end of its time interval, whereby the first timer accumulates intervals equal to the sum of successive operating cycles of the time delay relay.

Subminiature potentiometer (2,687,463). John M. Riley, Smyrna, Ga., assignor to Chance Vought Aircraft, Inc.

Rocket engine (2,689,454). Hans Schneider, Chatenay-Malabry, France, assignor to Societe d'Etude de la Propulsion par Reaction.

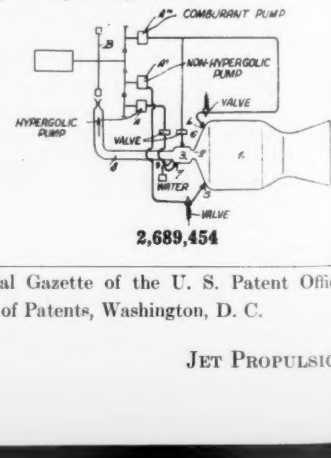

2,689,454

EDITOR'S NOTE: The patents listed above were selected from recent issues of the Official Gazette of the U. S. Patent Office. Printed copies of patents may be obtained at a cost of 25 cents each, from the Commissioner of Patents, Washington, D. C.

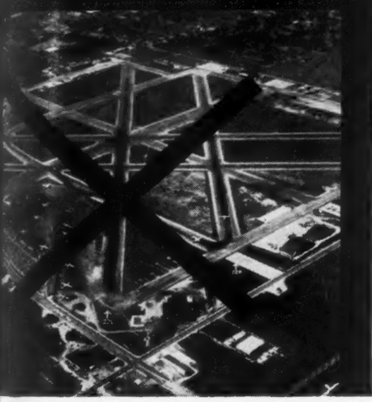

tic 'tac' toe!

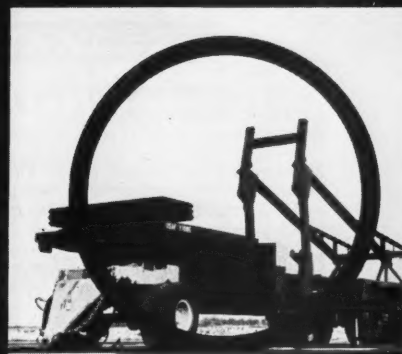

In the event of surprise attack, today's new and more powerful USAF Tactical Air Command can now carry war to the enemy anywhere in the world—around the clock and in any weather.

Here at a glance are some of the elements that might be used in such an attack and which are contributing to Tac Air's new mobility and striking power.

In modern warfare, major fixed bases are certain to become targets for initial enemy action. The Martin zero-length launcher makes possible swift mobility and advance-area operation of the TM-61 Matador tactical missile and—if need be—of piloted jet fighters.

In addition, new versions of U.S. Air Force's B-57 bomber, a major tactical weapon, are now being developed for service.

And for tomorrow's Tactical Air Command arsenal, new and more powerful Martin weapons systems are on the way.

MARTIN
BALTIMORE · MARYLAND

ARS News

ARS SECTION PRESIDENTS

Alabama: Joseph Wiggins, *Thiokol Chem. Corp.;* **Arizona:** R. H. Hansen, *Hughes Aircraft Co.;* **Central Texas:** B. S. Adelman, *Phillips Petroleum Co.;* **Chicago:** V. J. Cushing, *Armour Research Foundation;* **Cleveland-Akron:** John Sloop, *NACA;* **Detroit:** Fred Klemach, *Nat'l Research & Development Corp.;* **Florida:** R. S. Mitchell, *Pan American World Airways;* **Indiana:** A. R. Graham, *Purdue Univ.;* **Maryland:** W. G. Purdy, *Glenn L. Martin Co.;* **National Capital:** E. C. Page, *Page Communications, Inc.;* **New Mexico-West Texas:** R. C. Sherburne, *New Mexico A & M;* **New York:** C. W. Chillson, *Curtiss-Wright Corp.;* **Niagara Frontier:** T. Zannes, *Bell Aircraft Corp.;* **Northeastern New York:** Kurt Berman, *General Electric Co.;* **Northern California:** M. A. Pino, *California Research Corp.;* **Pacific Northwest:** R. M. Bridgforth, *Boeing Airplane Co.;* **Princeton Group:** Irvin Glassman, *Princeton Univ.;* **St. Louis:** Norton B. Moore, *McDonnell Aircraft Corp.;* **Southern California:** Č. M. McCloskey, *ONR;* **Southern Ohio:** W. J. Mizen, *Bendix Aviation Corp.;* **Twin Cities:** J. J. Schons, *Univ. of Minnesota.*

Sandorff to Speak on Space Flight at Boston

Full technical program, cosponsored by ASME Aviation Division, to include four sessions with nine papers

Paul Sandorff, associate professor of aeronautical engineering at Massachusetts Institute of Technology, has chosen "New Thoughts on Space Flight" as the subject of his talk at the banquet to be held during the ARS 25th Anniversary Semi-Annual Meeting, Hotel Statler, Boston, June 22–23. The meeting is being held in conjunction with the Diamond Jubilee Semi-Annual Meeting of ASME. The latter's Aviation Division will cosponsor the two ARS sessions, and vice versa.

The complete program is as follows:

WEDNESDAY, JUNE 22

2:30 p.m. ARS I
ASME Aviation II (cosponsor)

Chairman: Morton Finston, M.I.T.
Vice-Chairman: F. H. Greene, Jr., National Research Corp.

Measurement of Rocket Thrust and Internal Pressure During Static Testing with High-Frequency Response Instrumentation—Jack Buchanan, Thiokol Chemical Corp.

Combustion Time-Lag Measurements in a Liquid Bipropellant Rocket Motor—Jerry Grey, Luigi Crocco, and George Matthews, Princeton University

Rotor Speed Influence on Rotor Blade Torsional Frequencies: An Approximate Evaluation—C. E. Danforth, General Electric Co., Aviation Gas Turbine Div.

Hydrogen and Its Safe Liquefaction—Alexis Pastuhov and C. Lincoln Jewett, Arthur D. Little, Inc.

7:00 p.m. ARS Banquet

Toastmaster: F. C. Durant III, Arthur D. Little, Inc.
Speaker: Paul Sandorff, M.I.T.
Subject: New Thoughts on Space Flight

THURSDAY, JUNE 23

9:30 a.m. ASME Aviation III
ARS II (cosponsor)

Chairman: Ascher H. Shapiro, M.I.T.
Vice-Chairman: R. E. Small, General Electric Co., Aircraft Gas Turbine Div.

A Survey of Aerodynamic Excitation Problems in Turbomachines—A. Sabatiuk and F. Sisto, Wright Aeronautical Div., Curtiss-Wright Corp.

A Practical Approach to the Problem of Stall Flutter—Chi-Teh Wang, Robert J. Vaccaro, and Daniel F. DeSanto, New York University

2:30 p.m. ASME Aviation IV
ARS III (cosponsor)

Chairman: F. F. Ehrich, Westinghouse Electric Corp.
Vice-Chairman: James W. Wheeler, Sperry Gyroscope Co.

The Flow in a Vee-Gutter Cascade—William G. Cornell, General Electric Co., Aircraft Gas Turbine Div.

Determination of Mach Number from Pressure Measurements—Frank W. Barry, United Aircraft Corp.

8:00 p.m. ARS IV
ASME Aviation V (cosponsor)

Chairman: Lawrence Levy, Allied Research Assocs.
Vice-Chairman: Claude Brenner, Allied Research Assocs.

Stabilization of Low-Frequency Oscillations of Liquid Rockets and Fuel Line Stabilizers—Yao Tzu Li, M.I.T.

Films: "ROR Helicopter," Reaction Motors, Inc.; "One Man Helicopter," Kellett Aircraft

FRIDAY, JUNE 24

Inspection trip, sponsored by ASME Aviation Division, to Wyman Gordon Co., Worcester, Mass. Visitors will see a 35,000-ton press producing aluminum forgings, and a 50,000-ton press partially assembled, as well as other plant facilities.

Baltimore Beats Band for ARS

More than 200 registered at the Lord Baltimore and Southern Hotels in Baltimore during the 25th Anniversary Spring Meeting, April 20–22. The Meeting was held in conjunction with ASME's Diamond Jubilee Spring Meeting, April 18–22.

Ten papers were presented (see summary of technical sessions, next page) and a luncheon was held at which the principal speaker was G. Edward Pendray, founding Member, Fellow, and Past President of the Society, and president of Pendray & Co.

Papers at Spring Meeting ran gamut from rockets to instruments

Speakers John W. Townsend, Jr., Henry B. Riblet, and Richard B. Snodgrass convene prior to session on rocket test vehicles

Instrumentation session heard Leopold Winkler, Lawrence J. Fogel, and Howland B. Jones, Jr., put forth their views

Toastmaster of the affair was President Richard W. Porter.

On the final day of the meeting, chairman of which was Sears Williams, vice-president of the **Maryland** Section, inspection trips were made to the U. S. Naval Academy Experiment Station at Annapolis and to Aberdeen Proving Ground.

Astronautics Over a Jug of Wine

"There was nothing like a jug of red wine to stimulate our space flight discussions," was one of the comments by Dr. Pendray in his reflections on the beginnings of ARS at the 25th Anniversary luncheon on Thursday.

He told of meetings during the early 1930's in his Greenwich Village apartment during which the founding members of what was then called the "American Interplanetary Society" used to discuss ideas for expanding the public's interest in space flight. "Most of us were occupied with writing 'horse operas in space' at the time," he said, "but we were convinced that space flight was coming soon.

"In fact, I've been keeping thin all these years to go on the first rocket flight. If it isn't going to happen pretty soon, I'm going to start eating square meals," he quipped.

In introducing Sears Williams at the luncheon, Dr. Porter described the affable chairman of the meeting as "one of the few casualties of the Glenn L. Martin Company's Viking firings. He broke his leg at White Sands when he tripped over first base in a softball game."

Dr. Porter, himself, had his leg pulled facetiously earlier in the week when he was introduced by the toastmaster of ASME's banquet, Senator Ralph E. Flanders, as the president of the American "Racket" Society. Senator Flanders then, in a more serious vein, paid tribute to the tremendous advances in science which the rocket and guided missile industry have produced.

William G. Purdy, president of the host **Maryland** Section, was recruited as toastmaster for the dinner organized by The Glenn L. Martin Company. A fine pinch-hit job was done by the Viking impresario. Speaker for the evening was E. G. Uhl, vice-president—engineering at Martin, and he had some profound comments to make on such things as motivation to perform creative effort, the company's responsibility to the engineer, and vice versa.

Rocket Test Vehicles

The relative merits of existing research rockets were discussed by J. W. Townsend, Naval Research Laboratory. Research capabilities of the V-2, Viking, WAC Corporal, Aerobee, Deacon, and the Aerobee Hi were outlined. The latter is to be a high-performance (designed to carry a 150-lb payload to an altitude of 180 miles), low-cost ($^1/_{10}$ the cost of the Viking) research rocket. Twenty-two of these new rockets will be fired at Fort Churchill during the International Geophysical Year, 1957–1958.

Aspects of the Viking rocket were treated by L. Winkler and R. B. Snod-

grass, both of NRL. Winkler gave an illustrated account of photography from the Viking 11 rocket during the record-breaking flight to 158.4 miles. Snodgrass reported on aerodynamic heating on the nose cone of Viking 10 over a Mach range of 1.20–5.28. This was one of the few accounts of temperature measurements gathered from flight data.

S. F. Singer elaborated on his MOUSE orbital satellite by detailing information which would be available for geophysical and astrophysical applications. Such parameters as solar and cosmic radiation, magnetic fields, upper atmosphere studies, etc., could be investigated with satellite lifetimes of only a few days and payloads of as low as 50 lb.

Instrumentation

A new approach for the design of instruments used in the control of manned rocket vehicles was suggested by L. J. Fogel, Stavid Engineering. Fogel said that the human operator is only to be expected to program and reprogram flights and to make decisions beyond the capabilities of available control devices.

Two facets of rocket testing were presented by H. B. Riblet, Applied Physics Laboratory, and H. B. Jones, Forrestal Research Center. Riblet reviewed instrumentation techniques and requirements such as telemetry, instrument design, ground station equipment, and data reduction. Jones discussed the use of audiofrequency pressure data in combustion instability studies and gave experimental results obtained with a lox-alcohol rocket motor.

Manned Rocket Vehicles

Applications of rocket power to operational aircraft was the theme of papers by W. R. Brown, Reaction Motors, and W. F. Moore and R. C. Smith of Bell Aircraft. Rockets can provide reliable auxiliary power for rotary wing aircraft, pointed out Brown, who described the ROR (rocket-on-rotor) system for helicopters (see JET PROPULSION, January 1955, p. 38). Practical aspects of such rocket-powered aircraft as the Bell X-1, X-2, and Douglas D558 were outlined by the Bell authors. Plagues such as working with cold lox, fittings, seals, electrical components, etc., were eventually overcome, but operations still remain rather complex.

An optimum climbing technique for rocket powered aircraft was the subject of a theoretical paper by A. Miele of Polytechnic Institute of Brooklyn. Investigated was the speed-altitude relationship which minimizes time and propellant consumption from one set of conditions to another.

Good Field Trip; Nice Trip Home, Too

ON SATURDAY, April 9, about 80 members and friends of the **Alabama** Section made a field trip to the USAF Arnold Engineering Development Center at Tullahoma, Tenn.

The program included a short lecture on the background and history of the center and a two-hour guided tour of the Wind Tunnels, Gas Dynamic facilities, and Engine Test facilities.

The group examined the transonic and supersonic wind tunnels now under construction and the supersonic blow-down tunnel used by the Gas Dynamics facilities.

At the Engine Test facilities, the group observed how full-scale prototype turbojet and ramjet engines were tested in a wide range of environmental conditions.

On the return home, an interesting tour was made through the Jack Daniels Distillery at Lynchburg, Tenn.

Lauds WSPG Instrumentation Scheme

LT. COL. Bernie Luczak called White Sands Proving Ground the "best instrumented range in the world" at the

Porter speaks to Niagara Frontier Section

An April 13 dinner meeting of the Niagara Frontier Section featured ARS President Richard W. Porter as the main speaker. Shown at the head table are: Noah Davis, national vice-president; Tommie Zannes, president of the Section; Dr. Porter; John H. Van Lonkhuyzen, chief of the technical department at Bell Aircraft Corp.; Robert H. Gray, Section vice-president; and Willis Sprattling, Jr., last year's Section president.

April meeting of the **New Mexico-West Texas** Section. Col. Luczak, head of the Integrated Range at WSPG shared the program with John Titus of the proving ground's Flight Determination Laboratory, who spoke on high-speed computing machines.

"It is fortunate that the range can be kept busy since the instrumentation is expensive to install, operate and maintain, and by making full use of it the taxpayer is getting the most for his money," Luczak said.

He described the chain radar system and cameras used for tracking missiles, illustrating his talk from a large-scale relief map.

Dr. Titus pointed out that the solutions to most partial differential equations can be obtained only for specific situations. Computers, on the other hand, are equipped to perform dozens of calculations in minutes. Slides were shown on the operation of the Model 1103 Electronic Research Associates' computer operated by FDL.

280 visit Picatinny to see solid rockets

Uncles, cousins, nephews, and New York Section members numbering 280 made a tour of Picatinny Arsenal as guests of the U. S. Army on the fine Spring Saturday of May 7. Shown above at a meeting which preceded inspection of the Arsenal's museum and rocket firing areas are (left to right): Paul M. Terlizzi, Section director and chairman of the meeting; C. W. Chillson, president of the Section; Col. J. A. Barclay, commanding officer at Picatinny; and Col. I. O. Drewry, chief of the ammunition laboratory.

A luncheon was served in the Arsenal cafeteria at noon during the all-day tour. In the firing area, guests saw a T-50 JATO unit (used in launching the Matador), a smaller T-4, and a bazooka rocket on instrumented test stands.

Stehling Coins "Saloon"; Romick Picks "Monster"

A COMBINATION satellite vehicle and balloon has been dubbed, appropriately enough, a "Saloon," by Kurt Stehling, Bell Aircraft Corp., Buffalo, N. Y.

The Saloon, coupled with the "Monster," conceived by Darrell Romick, Goodyear Aircraft Corp., Akron, Ohio, furnished the subject matter for an April 21 meeting of the **Cleveland-Akron** Section before 200 people at the Lewis Flight Propulsion Laboratory, NACA, in Cleveland.

Both the Saloon and the Monster made their debuts at last winter's Ninth Annual Convention in New York, although neither had been given their names at the time. The Saloon is an orbital satellite which would be launched at an altitude of about 70,000 ft (ARS Preprint 187-54, High Altitude Launching of a Small Orbital Vehicle).

Monster, on the other hand, is a large three-stage ferry vehicle designed to carry passengers and cargo to a satelite station (ARS Preprint 186-54, Preliminary Design Study of a Three-Stage Satellite Ferry Rocket Vehicle with Piloted Recoverable Stages).

SoCal Dines on "Regenerative Cooling"

AT A dinner meeting on March 22, B. H. Sage and H. H. Reamer of CalTech's Department of Chemical Engineering

spoke to the **Southern California** Section on "A Demonstration of Some Types of Fluid Behavior Encountered in Regenerative Cooling."

Dr. Sage, a consultant at NOTS, Inyokern, is an authority on the design and manufacture of solid propellant rockets as well as on the thermodynamic, volumetric, and phase behavior of hydrocarbons.

An April 12 dinner meeting had Royal Weller, chief scientist at USNMTC, Point Mugu, speaking on "The Evaluation of Military Equipment."

Youngquist on Viking

A TALK on the Viking high-altitude rocket research program was given before the **Chicago** Section on April 27 by John R. Youngquist of The Glenn L. Martin Co.

After the showing of a film, Youngquist dealt with the design, operation, and test results of the rocket.

Klemach takes office in Detroit

THE **Detroit** Section, which recently completed its first year of operation, has elected Fred Klemach, president of the National Research and Development Corp., Detroit, as its new president. Klemach succeeds Laurence M. Ball, founding president (photo), chief laboratories engineer at the Chrysler Corporation Missile Branch, who will continue to serve the Section as a director.

Other new officers are: Charles W. Williams, vice-president, and Lovell Lawrence, Jr., treasurer, both of Chrysler; and Richard B. Morrison, chief of the Aircraft Propulsion Laboratory, University of Michigan, secretary.

In addition to Ball, the directors are: David N. Buell and Edward J. Dofter, Chrysler; and David J. Craig, Wyandotte Chemical Corp.

The Section heard Harold W. Ritchey, technical director of Thiokol Chemical Corp., Rocket Development Division, Huntsville, Ala., speak on design criteria for solid propellant rockets at an April 20 meeting held at the Engineering Society of Detroit.

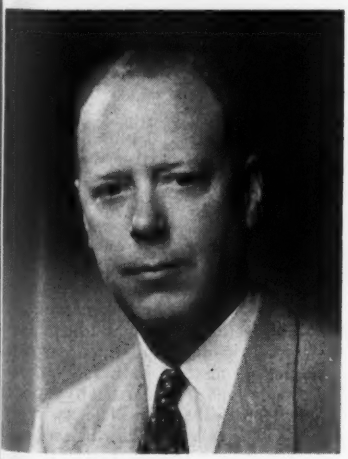

Laurence M. Ball, outgoing president of Detroit Section

Book Reviews

C. F. Warner, Purdue University, *Associate Editor*

Characteristics and Applications of Resistance Strain Gages, U. S. Department of Commerce, National Bureau of Standards Circular 528, U. S. Government Printing Office, 1954, 140 pp. $1.50.

Reviewed by R. C. Geldmacher
Purdue University

This small hard-cover book contains a miscellaneous collection of papers presented at a symposium held at the National Bureau of Standards, November 8 and 9, 1951. One or more of these papers describes work related to the following topics: strain sensitivity of conducting films, characteristics of unbonded resistance-wire strain gages, characteristics of a resistance-wire gage manufactured in Sweden, measurement of force, cementing and waterproofing resistance-wire gages, Poisson-ratio determination, properties of concrete.

The discussion of each paper has been included and is interesting and informative.

The title of the publication is somewhat misleading in that the fundamental characteristics of resistance-wire gages manufactured in the United States are not discussed in any great detail. The best source for this information is still the series of NACA Technical Notes prepared by Wm. A. Campbell.

General Theory of High Speed Aerodynamics, edited by W. R. Sears, Princeton University Press, Princeton, N. J., 1954, 758 pp. $15.

Reviewed by H. J. Goett
Ames Aeronautical Laboratory, NACA

This volume is one of a planned "Princeton Series" which promises to bear the same relationship to modern aeronautics that the "Durand Series" had with respect to aeronautics of the early 1930's. The much broader scope of the present series is in itself an impressive commentary on the growth of the field in the past thirty years. The General Editors Preface indicates that the entire work will consist of twelve volumes; earlier volumes will treat the more fundamental aspects of the properties of gases, liquids and solids, and combustion, dynamic, and viscous processes in these media; later volumes deal with applications of these fundamentals to aircraft and power plants and to experimental methods in the field.

The volume being reviewed is the sixth in the series, but one of the first to be published. It summarizes present-day knowledge in the theory of high-speed aerodynamics and consists of eight sections, prepared by different authors under the editorship of W. R. Sears. The organization of the book is well conceived, progressing from the linear theories of both subsonic and supersonic flow to the methods of higher approximation which are used to improve the first-order theories and to explain and eliminate their shortcomings. Each section includes the most recent work in this rapidly expanding field of aerodynamic theory, and the reference lists are comprehensive. To the aerodynamic analyst seeking available theories pertinent to his particular engineering application, this volume should supply a most useful reference, and to the original worker in the field it points the way to many new avenues for development of the theory.

The first section by Theodore von Kármán serves to define the relationship that exists between the subsequent sections in largely nonmathematical terms. The major features of subsonic, transonic, supersonic, and hypersonic flow are outlined, and thus the physical foundation for the mathematical treatments of these flows in the later sections is supplied.

The second section by K. O. Friedrichs is also somewhat introductory; it discusses the nature of hyperbolic flows such as are dealt with in supersonic or unsteady compressible flow theory. The material in this section is likely to be used by the research worker seeking to check the question of existence or uniqueness of his mathematical solutions.

The next two sections by W. R. Sears and by Heaslet and Lomax summarize applications of linearized theory to subsonic, transonic, and supersonic flow. In each case the various applications are unified through their relationship to the more basic and general acoustic theory. Since conventional linear analysis suffices for most engineering purposes, it is likely that these two sections will be more generally used than any others in the volume. This is particularly true of the section on supersonic and transonic small perturbation theory, since it is surely the most complete collection and unification of available results and methods. The arrangement of this section is based on an attempt to study problems of progressively increasing geometric and theoretical complexity; thus successive applications are made to steady-state profile theory, wing (planform) effects, slender bodies, lifting wings and wing-body combinations, unsteady flow, reciprocity relations, and similarity rules. In each case the end result is explicitly present in a form lending itself readily to engineering application.

The next two sections are devoted to "nonlinear" effects in subsonic and supersonic flow. The section on "Higher Approximations" by M. J. Lighthill deals with these effects by the more general method of successive approximation. The following section by Kuo and Sears treats the more rigorous but more restricted hodographic method in which the nonlinear equations are linearized by replacing space coordinates with velocity coordinates. It is believed that the section by Lighthill will be one of great interest to the original worker in the field of theo-

retical supersonic aerodynamics; it should provide the starting point for many graduate theses. As the author's introduction indicates, his approach is intentionally based on physical thinking rather than explicit mathematical method. As a result, this section is not one that lends itself to immediate engineering application but is of interest to the research worker.

The final two sections are by Antonio Ferri. They deal with the method of characteristics applied to steady two- and three-dimensional flows and flow patterns characterized by the presence of shock waves. The treatment is similar to that of Professor Ferri's book, "Elements of Aerodynamics of Supersonic Flow," which heretofore has been the most complete reference on this subject.

As can be inferred from the foregoing comments, this volume has fully contributed in all respects to its triple objective "of consolidating the literature, of presenting the more advanced problems and their solutions, and of stimulating further research." With this precedent the succeeding volumes of the series will be anticipated with great interest.

Modern Developments in Fluid Dynamics—High Speed Flow, 2 vols., edited by L. Howarth (with the assistance of H. B. Squire and the late C. N. H. Lock), Oxford University Press, New York, 1953, 875 pp. $17.

Reviewed by Lester Lees
Guggenheim Aeronautical Laboratory
California Institute of Technology

The two earlier volumes in this series edited by Dr. Sidney Goldstein have long been regarded as the "bible" for problems of real fluid flow at low speeds. These two new volumes edited by Dr. Howarth deal with the field of compressible flow, which has been developed so extensively since the publication of the earlier volumes in 1938. Vol. I treats the theoretical foundations of compressible flow, including shock waves, blast waves (strong waves produced by release of a definite amount of energy), unsteady motion, and boundary layers. Vol. II is concerned mainly with experimental methods, experimental data, and problems in applied aerodynamics of airfoils and bodies of revolution, including semiempirical methods.

Although these volumes contain certain obvious deficiencies, it must be said in all fairness that most of these shortcomings can be attributed to the long-delayed publication date and the rapid rate of development in this field. For example, Ward's article on Approximate Methods makes no mention of Lighthill's "improvement" of linearized theory, or of the extensive works by Lighthill, Whitham, Hayes, and others on second-order effects in the flow field around bodies. Transonic theory is only sketched, and no mention is made of hypersonic similarity or of the extremely useful and powerful approximate methods which have been developed for treating flows over slender bodies in the range of Mach numbers above 2.5–3.0. Meyer's article on the method of characteristics could not be expected to discuss Ferri's linearized characteristics scheme, which had not yet been invented when the article was written! A similar time lag is evident in the article on boundary layers and in the otherwise excellent chapter in Vol. II on Experimental Methods; the point of view in this last chapter seems to be that experimentation stops at a Mach number of around 4.0. Even so, shock tubes have already shown their worth in the transonic range, and deserve more than a few brief paragraphs.

In spite of these omissions (and others), the authors and editors are to be commended for covering such an enormous range of material at a generally high level and in a relatively compact space. For example, Meyer's excellent article on characteristics is not only clear and readable, but also more general in concept than most such discussions. Illingworth's chapter on shock waves and shock interactions is also very useful, and contains a brief description of Bethe and Teller's treatment of vibrational relaxation, which may introduce the reader to real gas effects. Cope's article on flow past bodies of revolution presents a considerable amount of information not readily available elsewhere, and Young's treatment of compressible boundary layers, while somewhat uncritical, contains most of the innumerable transformations that have proved to be valuable.

To summarize, one should be aware of the shortcomings of these volumes, but grateful that they are generally understandable and readable, rather than merely encyclopedic.

Technical Literature Digest

M. H. Smith, *Associate Editor*, **and M. H. Fisher**, *Contributor*
The James Forrestal Research Center, Princeton University

Jet Propulsion Engines

Before Afterburners, by Frank F. Rand, Jr., *IAS Preprint*, Jan. 24–27, 1955, 6 pp.
Tradewind Turboprops (Allison T-40 in Convair XP5Y-1 and R3Y), *Flight*, vol. 67, Feb. 4, 1955, pp. 139–141.
Dutch Ramjet 'Copter Burns Kerosene, (Sobeh H-2), *Aviation Age*, vol. 23, Feb. 1955, pp. 140–141.
Sound Abatement by North American, *Air World*, vol. 7, Nov.-Dec. 1954, p. 81.
Turbine Starting Engine Weighs 75 lbs., Develops 350 HP, *Automotive Ind.*, vol. 112, Jan. 15, 1955, p. 72.
Small Gas Turbine Progress, by Hans Kosman and Randolph Hawthorne, *Aviation Age*, vol. 23, Feb. 1955, pp. 26–58.
T56 Boosts U. S. Turboprop Airliner Bid, by Irving Stone, *Aviation Week*, vol. 62, Jan. 24, 1955, p. 80.
French Steam-cum-gas Turbine Cycles (French Mercier Engines), *Oil Engine and Gas Turbine*, vol. 22, Dec. 1954, pp. 315–318.
The Aerodynamics of Compressor Blade Vibration, by H. Pearson, *Aeronautical Conference, 4th*, London, Sept. 15–17, 1953, pp. 127–162.
The Development of the Spill Flow Burner and Its Control System for Gas Turbines, by F. H. Carey, *Shell Aviation News*, Oct. 1954, pp. 16–23.
Augmenting Helicopter Take-Off Power by Ramjets, by R. T. DeVault, *Aircr. Engng.*, vol. 27, Feb. 955, pp. 34–36.
Reheat for Gas Turbines, by J. L. Edwards, *J. Roy. Aeron. Soc.*, vol. 6, part 1, Feb. 1955, pp. 127–150.
The Rocket Helicopter, by Edward Zaehringer, *Amer. Helicopter*, vol. 36, Nov. 1954, pp. 12, 17.
Bell Builds Rocket Engine Know-How, by David A. Anderton, *Aviation Week*, vol. 62, Jan. 10, 1955, pp. 28–31.
Rocket Propulsion for Aircraft, *Flight*, vol. 67, Feb. 18, 1955, pp. 197–201.
The Armstrong Siddeley "Snarler," *J. Brit. Interplan. Soc.*, vol. 14, Jan.-Feb. 1955, pp. 13–16.

Heat Transfer and Fluid Flow

Thoughts on Boundary Layer Noise, by Alan Powell, *Gt. Brit. ARC. F. M.* 2061, April 15, 1954, 5 pp.
High-Speed Flow Through Cascades: Results Obtained at S.N.E.C.M.A., by W. Luksch (in French), *Docaero*, no. 30, Nov. 1954, pp. 39–46.
Metering Pulsating Flow; Coefficients for Sharp-Edged Orifices, by J. M. Zarek, *Engineering*, vol. 179, Jan. 7, 1955, pp. 17–19.
The Calculation of Mass Transfer Rates in Absorption, Vaporization, Condensation and Combustion Processes, by D. B. Spalding, *Proc. Instn. Mech. Engrs.*, vol. 168, no. 19, 1954, pp. 545–570.
The Mechanics of the Rijke Tube, by G. F. Carrier, *Quart. Appl. Math.*, vol. 12, Jan. 1955, pp. 383–395.
Axisymmetric Solutions of the Flow Through a Single Stage Axial Compressor, by Raymond W. Moore, Jr., and David L. Richardson. **Measurements of Flow Through a Single Stage Axial Compressor,** by Raymond W. Moore, Jr., and Kurt H. Schneider, *Mass. Inst. Tech. Gas Turbine Lab. MIT Rep.* nos. 27-5, 27-6, Dec. 1954.
Experimental Techniques for Three-Dimensional Flow Research, by Raymond W. Moore, Jr., Warren G. Nelson, Arun Prasad, et al., *Mass. Inst. Tech. Gas Turbine Lab. MIT Rep.* no. 27-8, Dec. 1954, 18 pp.
Theoretical Consideration of Secondary Flow, by George L. Mellor, Jr., *Mass. Inst. Tech. Gas Turbine Lab. MIT Rep.* no. 27-2, Dec. 1954, 18 pp.

Combustion

Office of Naval Research High Temperature Project, by J. B. Conway and Maurice S. Kirshenbaum, *Temple Univ. Res. Inst., 9th Prog. Rep.*, Jan. 1954, 31 pp.
Ignition Limits of Hydrogen Peroxide Vapor, by C. N. Satterfield, P. J. Ceccotti, and A. H. R. Feldbrugge, *Mass. Inst. Tech. Dept. Chem. Engng. Rep.* no. 47, Nov. 1954, 10 pp.
Ignition Studies. Part IV. Relation of Minimum Ignition Point to Other Ignition Phenomena, by J. W. Crellin, J. E. Johnson, and H. W. Carhart, *Naval Research Lab. Rep.* 4476, Jan. 1955, 13 pp.
Mechanism and Kinetics of the Reaction Between Fuming Nitric Acid and/or its Decomposition Products and Gaseous Hydrocarbons, *Franklin Inst. Labs. for Res. and Dev. Quart. Prog. Rep.* no. Q-2452-2, Sept. 11, 1954–Jan. 15, 1955, 8 pp.
Physical Chemical Equilibrium and Thermodynamic Data of Mixed Gases at Elevated Temperatures (in French), by G. Ribaud and N. Manson, *France Ministère de l'Air Pub. Sci. Tech.* no. 294, 1954, 111 pp.
Effect of Diluents on Burning Velocities in Hydrogen-Bromine Mixtures, by M. C. Huffstutler, Jas. A. Rode, and Robbin C. Anderson, *J. Amer. Chem. Soc.*, vol. 77, Feb. 5, 1955, pp. 809–810.
Applied Chemical Kinetics. X. Reactions in the Liquid Phase, by J. C. Jungers and F. Coussemant, *l'Inst. français du Pétrole, Rev. Ann. des Combustibles Liquides*, vol. 9, Nov. 1954, pp. 619–697.
Gaseous Detonations. VI. The Rarefaction Wave, by G. B. Kistiakowsky and P. H. Kydd, *J. Chem. Phys.*, vol. 23, Feb. 1955, pp. 271–274.
Detonation Waves and the Principle of Minimum Entropy Production, by George H. Duffey, *J. Chem. Phys.*, vol. 23, Feb. 1955, p. 401.
Mechanism of Detonation, by Melvin A. Cook, *J. Chem. Phys.*, vol. 23, Feb. 1955, pp. 409–410.
Breakdown Processes in Nitrogen, Oxygen, and Mixtures, by Elsa L. Huber, *Phys. Rev.*, vol. 97, Jan. 15, 1955, pp. 267–274.
Some Calculations on Ideal Combustion in a Parallel Duct, by A. B. P. Beeton, *Gt. Brit. Natl. Gas Turbine Estab. N.G.T.E.* M.221, July 1954, 15 pp.
The Absolute Thermal Decomposition Rates of Solids. Part II. The Vacuum Sublimation Rate of Molecular Crystals, by R. D. Schultz and A. O. Dekker, *Aerojet General Corp.* TN-3, Nov. 1954, 12 pp.
General Enthalpy - Temperature - Entropy Diagram for Ideal Gases and Gas Mixtures up to 5000 K, by W. C. Noeggerath, *NAVORD Rep.* 3341 (*NOTS* 882), June 1954, 95 pp.
A Correlation of Reaction Rates, by George S. Hammond, *J. Amer. Chem. Soc.*, vol. 77, Jan. 1955, pp. 334–338.
Experimental Determination of Rotational Temperatures and Concentrations of OH in Flame Emission Spectra, by S. S. Penner and E. K. Bjornerud, *J. Chem. Phys.*, vol. 23, Jan. 1955, pp. 143–152.
Approximation Method of Calculating Vibrational Frequencies of Polyatomic Molecules, by S. Bratoz, *J. Chem. Phys.*, vol. 23, Jan. 1955, pp. 159–161.
Organ-Pipe Oscillations in a Burner with Deep Ports, by Abbott A. Putnam and William R. Dennis, *Battelle Memorial Inst. Tech. Rep.* no. 15034-4, Sept. 1954, 59 pp.
A Survey of Organ-Pipe Oscillations in Combustion Systems, by Abbott A. Putnam and William R. Dennis, *Battelle Memorial Inst.*, Aug. 1954, 29 pp.
The Design and Testing of a Full Scale Vortex Combustion Chamber for Residual Oil Burning, by A. P. Johnstone, *Gt. Brit. Natl. Gas Turbine Estab. Memo* no. M.203, March 1954, 31 pp.
Flames Burning at Pressures up to 1500 psia, by R. Edse, L. E. Bollinger, and W. A. Strauss, *Ohio State Univ. Res. Foundation Rep.* no. 7, *Quart.* Progress Rep., Oct. 16, 1953–Jan. 15, 1954, March 5, 1954, 40 pp.

Fuels, Propellants, and Materials

High-Temperature Alloy Brazing of Thin Materials for Jet Engines, by Arnold S. Rose and William N. Lewis, *J. Welding*, vol. 34, Jan. 1955, pp. 30–39.
Magnesium in the Fabrication of Guided Missiles, by A. J. Bell, *Light Metal Age*, vol. 11, Dec. 1954, pp. 25–27.
Titanium in Jet Engines, by D. C. Goldberg, *Modern Metals*, vol. 10, Dec. 1954, pp. 42–43.
Selecting Metals for Supersonic Aircraft and Guided Missiles, by Spencer L. Shaw, *Materials and Methods*, vol. 40, Dec. 1954, pp. 89–92.
Ceramic Coating Conference, 27 and 28 May, 1952, *Wright Air Devel. Cen. Tech. Rep.* 53-37, Sept. 1954, 96 pp.
Hydrogen Peroxide, a Monograph. Part 3, by W. C. Schumb, C. N. Satterfield and R. L. Wentworth, *Mass. Inst. Tech., Dept. Chem. Chemical Engng., Rep.* no. 44, Dec. 1954, 233 pp.
Investigation of the Bonding of Silicon Carbide by Metals, by Richard A. Alliegro and James R. Tinklepaugh,

Editor's Note: This collection of references is not intended to be comprehensive, but is rather a selection of the most significant and stimulating papers which have come to the attention of the contributors. The readers will understand that a considerable body of literature is unavailable because of security restrictions. We invite contributions to this department of references which have not come to our attention, as well as comment on how the department may better serve its function of providing leads to the jet propulsion applications of many diverse fields of knowledge.

Wright Air Dev. Cent. Tech. Rep. 53-5, Jan. 1953, 28 pp.

Thermal Stability of Gas Turbine Fuels, by C. D. McLean and H. M. White, *Calif. Research Corp. Bimonthly Prog. Rep.* no. 2, July 31, 1954, 19 pp.

Investigation of Carbon (Graphite) Base Materials Suitable for Rocket and Ramjet Applications, by William S. Smiley, *Stanford Res. Inst. Bimonthly Progress Rep.* no. 6, Feb.-March 1954, 6 pp.

Titanium Alloys for Elevated Temperature Application, by W. F. Carew, F. A. Cossley, and D. J. McPherson, *Illinois Inst. Tech. Quart. Rep.* no. 11, Dec.-Feb. 1954, 18 pp.

On Study of the Microstructure of Cermets, by Thomas S. Shelvin, Herbet W. Newkirk, and E. George Stevens, *Ohio Univ. Res. Found. Bimonthly Rep.*, July-Aug. 1954, 5 pp.

Cermet Development, by Charles A. Hauck, Louis J. Trostel, and Thomas S. Shevlin, *Ohio State Univ. Res. Found. Quart. Progress Rep.* no. 4, April-July 1954, 24 pp.

Basic Research on Sintered Titanium Powder Analogous to "Sap" for High Temperature Strength, by E. P. Weber and G. F. Davies, *Brush Labs. Co. Bimonthly Rep.*, Sept.-Nov. 1953, 3 pp.

Methods of Analysis of Hydrogen Peroxide, by Wilbur A. Riehl, John R. Nunnelley, and David D. Watson, *Redstone Arsenal Rep.* no. 1R1, May 1954, 69 pp.

Volumetric and Phase Behavior in the Nitric Acid-Water System, by C. H. Duffy, W. H. Corcoran, and B. H. Sage, *Calif. Inst. Tech. Jet Prop. Lab. Progress Rep.* 20-235, July 1954, 12 pp.

Relation Between Roughness of Interface and Adherence of Porcelain Enamel to Steel, by J. C. Richmond, D. G. Moore, H. B. Kirkpatrick, and W. N. Harrison, *NACA Rep.* 1166, 1954, 9 pp.

Machining Titanium, by J. T. D. Holt and J. Purcell, *Aircr. Production*, vol. 17, Feb. 1955, pp. 60–64.

Some Fundamental Experiments on High Temperature Creep, by J. E. Dorn, *J. Mech. Phys. Solids*, vol. 3, Jan. 1955, pp. 85–116.

Prestressed Ceramic Structures, by F. R. Shanley, W. J. Knapp, J. F. Brahtz, et al., *Wright Air Dev. Center Tech. Rep.* 54-75, Jan. 1954, 65 pp.

Instrumentation and Experimental Techniques

Use of Photography in Ballistic Measurements, by George E. Merritt, *J. Soc. Mot. Pict. Tel. Engrs.*, vol. 63, Dec. 1954, pp. 240–244.

The Design and Construction of Hot Wire Anemometers for High Speed Flows, by D. L. Schultz, *Gt. Brit. A.R.C. F.M.* 2046; *T.P.* 424, March 4, 1954, 7 pp.

Adiabatic Calorimeter for Use with Condensable Gases and Gas-solid Systems Between 10 and 150°K, by E. L. Pace, Louis Pierce, and Kent S. Dennis, *Rev. Sci. Instrum.*, vol. 26, Jan. 1955, pp. 20–22.

Analog Computer for Nonlinear Coordinate Transformation, by Norman L. Fritz, *Rev. Sci. Instrum.*, vol. 26, Jan. 1955, pp. 23–27.

Measurement of Time Varying Optical Absorption, by A. V. Phelps and J. L. Pack, *Rev. Sci. Instrum.*, vol. 26, Jan. 1955, pp. 45–49.

Use of the Hot-Wire Anemometer as a Triggering and Timing Device for Wave Phenomena in a Shock Tube, by Darshan S. Dosanjh, *Rev. Sci. Instrum.*, vol. 26, Jan. 1955, p. 65.

Phototransistors and Photoelectrets, by Edward D. Padgett, *Radio Electronics*, vol. 26, Feb. 1955, pp. 61–63.

Measurement of Gun Barrel Temperatures, by T. William, J. E. Brock, W. L. Sibbitt, and G. A. Hawkins, *Instrum. and Automation*, vol. 28, Jan. 1955, pp. 106–108.

A Wider Choice of Missile Control Instrument Functional Characteristics, by B. C. Muzzey and V. J. Sims, *IAS Preprint*, Jan. 24–27, 1955, 7 pp.

What can Electronic Simulators do for the Missile Designer?, by Floyd E. Nixon, *IAS Preprint*, Jan. 24–27, 1955, 10 pp.

Space Flight, Astrophysics, Aerophysics

Tentative Absorption and Emission Spectra of the Atmosphere, by H. K. Kallman, *Calif. Univ. Inst. Geophysics Sci. Rep.* no. 2, June 1954, 29 pp.

Weather Phenomena at High Levels, by J. Durward and D. C. E. Jones, *Aeroplane*, vol. 88, Jan. 7, 1955, pp. 18–21.

A New Design for the Space Station, by Kenneth Durbin, *J. Space Flight*, vol. 7, Jan. 1955, pp. 1–6.

Stationary Rocket Trajectories, by D. F. Lawden, *Q. J. Mech. Appl. Math.*, vol. 7, Dec. 1954, pp. 488–504.

Calculation of Step-Rockets, by M. Vertregt, *J. Brit. Interplan. Soc.*, vol. 14, Jan.-Feb. 1955, pp. 20–25.

The Earth Photographed from 158 Miles Up, by R. C. Baumann and L. Winkler, *Research Reviews (Office of Naval Res.)*, Feb. 1955, pp. 16–18.

Upper-Atmosphere Wind, Temperature and Pressure Measurement, by N. W. Spencer, *Michigan Univ. Engng. Res. Inst. Rep.* no. C7-C8, *Progress Rep.*, April 1–Sept. 30, 1954, 12 pp.

Aerological Sounding Balloons, by Gordon M. Martin, John Mandel, and Robert D. Stiehler, *J. Res. Nat. Bur. Stand.*, vol. 53, Dec. 1954, pp. 383–392.

Basic Principles of Astronautics, Part I, by L. R. Shepherd, *J. Brit. Interplan. Soc.*, vol. 14, Jan.-Feb. 1955, pp. 37–44.

Aeromedical and Biological Considerations of Flight Above the Atmosphere, by Paul A. Campbell, *J. Bell. Interplan. Soc.*, vol. 14, Jan.-Feb. 1955, pp. 1–12.

The Low-Level Jet Phenomenon, by Alfred K. Blackadar, *IAS Preprint*, Jan. 24–27, 1955, 15 pp.

Reaching for the Stars, by Gaetano Arturo Crocco, *Interavia*, vol. 10, 1955, pp. 22–23.

Conference on the Physics of the Ionosphere, by A. E. Slater, *J. Brit. Interplan. Soc.*, vol. 14, Jan.-Feb. 1955, pp. 17–20.

Terrestrial Flight, Vehicle Design

Cruise Performance of Jet Aircraft, by D. C. Whittley, *Aero Digest*, vol. 70, Feb. 1955, pp. 38–48.

Swiss Guided Missile (Oerlikon 54), *Flight*, vol. 67, Jan. 7, 1955, pp. 7–9.

A Statistical Method of Specification, Testing and Evaluation of Missile Systems, by E. J. Althaus, S. C. Morrison, and W. R. Tate, *Hughes Aircraft Co. TM* 368, July 1954, 31 pp.

Atomic Energy

Measured Effective Thermal Conductivity of Uranium Oxide Powder in Various Gases and Gas Mixtures, by J. S. Boegli and R. G. Deissler, *NACA RM* E54L10, March 1955, 20 pp.

Do you think about Angular Acceleration?

DOUGLAS

does...

and uses Statham Angular Accelerometers to test

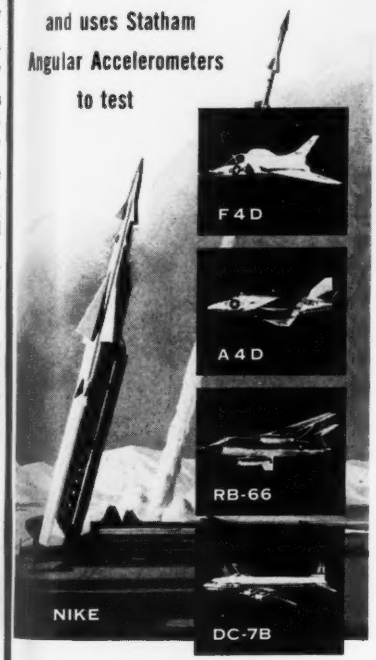

Statham unbonded strain gage liquid rotor angular accelerometers offer a simple, reliable means for the study of the rotary motion of a test body under conditions where a fixed mechanical reference is not available. For static and dynamic measurements in ranges from ± 1.5 to $\pm 3{,}000$ rad/sec^2, four standard models are offered.

Please request Bulletin AA2

Statham

LABORATORIES
LOS ANGELES 64, CALIFORNIA

TO THE FINE ENGINEERING MIND
SEEKING THE CHALLENGING PROJECTS IN

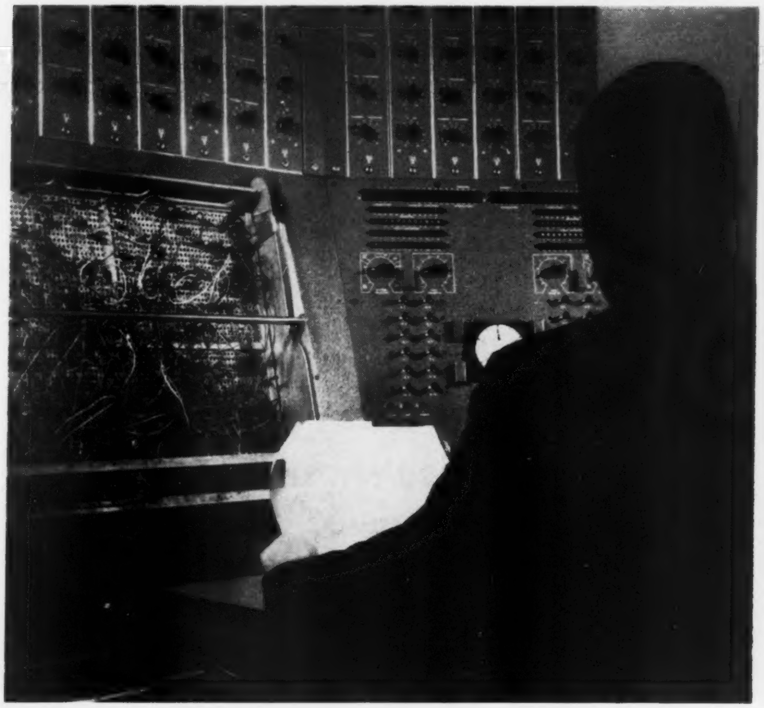

DYNAMICS

Convair, in beautiful San Diego, California, now offers exceptional career opportunities to **DYNAMICS ENGINEERS** with experience in: general flight and control dynamics for both airplane and missile design — analysis and synthesis of servomechanisms, autopilot design, controls and computers — aeroelasticity, fluid dynamics, vibration and flutter — aerodynamic, dynamic, and transient load analysis — solution of dynamic problems by analytical methods and by analog machine computations. Special opportunities for men holding advanced engineering, physics, or mathematics degrees.

At **CONVAIR** you will find an imaginative, explorative, energetic engineering department... truly the "engineer's" engineering department to challenge your mind, your skills, your abilities in solving the complex problems of vital, new, long-range programs. You will find salaries, facilities, engineering policies, educational opportunities and personal advantages excellent.

Lovely, sunny, **SMOG-FREE SAN DIEGO**, ever-growing area of three-fourths million people, offers you and your family a way of life judged by most as the Nation's finest for climate, natural beauty and easy (indoor-outdoor) living. Housing is plentiful and reasonable.

Generous travel allowances to engineers who are accepted. Write at once enclosing full resume to:

H. T. Brooks, Engineering Personnel, Dept. 1406

CONVAIR

A Division of General Dynamics Corporation

3302 PACIFIC HIGHWAY SAN DIEGO, CALIFORNIA

Index to Advertisers